The ATF3/IL6-axis as determinator between innate and adaptive immunity

Dissertation

der Mathematisch-Naturwissenschaftlichen Fakultät

der Eberhard Karls Universität Tübingen

zur Erlangung des Grades eines

Doktors der Naturwissenschaften

(Dr. rer. nat.)

vorgelegt von

Stefanie Reinknecht (geb. Müller)

aus Oberndorf am Neckar

Tübingen

2020

Gedruckt mit Genehmigung der Mathematisch-Naturwissenschaftlichen Fakultät der Eberhard Karls Universität Tübingen.

Tag der mündlichen Qualifikation:	17.02.2021
Stellvertretender Dekan:	Prof. Dr. József Fortágh
1. Berichterstatter:	Prof. Dr. Amir Yazdi
2. Berichterstatter:	Prof. Dr. Stefan Stevanovic

Erklärung / Declaration

Ich erkläre, dass ich die zur Promotion eingereichte Arbeit mit dem Titel:
„The ATF3/IL6-axis as determinator between innate and adaptive immunity”,
selbständig verfasst, nur die angegebenen Quellen und Hilfsmittel benutzt und wörtlich oder inhaltlich übernommene Stellen als solche gekennzeichnet habe. Ich versichere an Eides statt, dass diese Angaben wahr sind und dass ich nichts verschwiegen habe. Mir ist bekannt, dass die falsche Abgabe einer Versicherung an Eides statt mit Freiheitsstrafe bis zu drei Jahren oder mit Geldstrafe bestraft wird.

I hereby declare that I have produced the work entitled
“*The ATF3/IL6-axis as determinator between innate and adaptive immunity”,*
submitted for the award of a doctorate, on my own (without external help), have used only the sources and aids indicated and have marked passages included from other works, whether verbatim or in content, as such. I swear upon oath that these statements are true and that I have not concealed anything. I am aware that making a false declaration under oath is punishable by a term of imprisonment of up to three years or by a fine.

Tübingen, den ....

Datum / Date Unterschrift /Signature

I Acknowledgments

An dieser Stelle möchte ich meinen besonderen Dank nachstehenden Personen entgegenbringen, ohne deren Mithilfe und Unterstützung die Anfertigung dieser Dissertation niemals möglich gewesen wäre.

Mein besonderer Dank gilt Prof. Dr. Amir Yazdi, meinem Doktorvater, für die ausgezeichnet Betreuung, sowie für die enorme Unterstützung bei der Umsetzung der gesamten Arbeit.

Ein großer Dank gilt Prof. Dr. Martin Röcken, für die Betreuung und Ideengebung, die mir einen kritischen Zugang zu dieser Thematik eröffnet haben.

Ich danke Herrn Prof. Dr. Stefan Stevanovic für die hilfsbereite und wissenschaftliche Betreuung als Zweitgutachter.

Ein Dank auch an die gesamte Arbeitsgruppe (Yazdi/Ghoreschi) für die freundschaftliche Arbeitsatmosphäre, viele wertvolle Anregungen und stete Hilfsbereitschaft, die wesentlich zum Gelingen dieser Arbeit beigetragen haben. Insbesondere muss ich hier einen großen Dank an Dr. Marc Burian sowie Ramona Alexandra Eichkorn äußern, die meine Arbeit durch ihre Unterstützung und Gedanken vorangebracht haben.

Zuletzt möchte ich mich besonders bei Peter Müller, meinem Vater, Cornelia Müller, meiner Mutter und Tina Müller, meiner Schwester, sowie meinem Ehemann André Reinknecht bedanken. Ihr habt mich im Rahmen meines Studiums, sowie meinem gesamten Lebenswegs, immer mit Rat, Geduld und lieben Worten begleitet. Ohne euch wäre das alles nicht möglich gewesen, daher widme ich euch diese Arbeit, vielen Dank für die uneingeschränkte, liebevolle und vielseitige Unterstützung.

II List of abbreviations

ACTB/Actb	beta actin
ATF3/Atf3	activating transcription factor 3
***Atf3*$^{-/-}$**	Atf3tm1Dron
***Atf3*$^{-/-}$ x *Il6*$^{-/-}$**	B6.129S2-Il6tm1Kopf/J x Atf3tm1Dron
AP1	activator protein 1
AD	atopic dermatitis
BMDCs	bone marrow derived dendritic cells
BMDM	bone marrow-derived macrophages
$CaCl_2$	calcium chloride
cDNA	complementary DNA
CO_2	carbon dioxide
CREB	cAMP responsive element binding
CsA	cyclosporine A
CXCL/Cxcl	CXC-chemokine ligand
DAMPs	danger-associated molecular patterns
DC	dendritic cells
DMBA	dimethylbutylamin
DMF	dimethylfumarate
DTHR	delayed type hypersensitivity reaction
EDTA	ethylendiamintetraacetat
ELISA	enzyme-linked immunosorbent assay
FBS	fetal bovine serum
GM-CSF	granulocyte macrophage colony stimulating factor
HCl	hydrocholic acid
HPV	human papillomavirus
HPV8	HPV type 8
HPV^{+}	VEGF A$^{fl/fl}$LysMCreHPV8
HPV^{+} x *Atf3* $^{-/-}$	VEGF A$^{fl/fl}$LysMCreHPV8 x Atf3tm1Dron

II List of abbreviations

HPV^{+} x *Il6* $^{-/-}$	VEGF A$^{fl/fl}$LysMCreHPV8 x B6.129S2-Il6tm1Kopf/J (
HO-1	hemoxygenase-1
IL-	interleukin-
***Il6*$^{-/-}$**	B6.129S2-Il6tm1Kopf/J
IFN/Ifn	interferon
MTT	3-(4,5-Dimethylthiazol-2-yl)-2,5-diphenyltetrazoliumbromid
mDCs	mobile dendritic cells
NF- κ B	nuclear factor- κ B
NLRs	Nod-like receptors
Nrf2	nuclear factor (erythroid-derived 2)-like 2
PAMPs	pathogen-associated molecular patterns
PBMCs	peripheral human blood mononuclear cells
PBS	phosphate buffered saline
PKC	protein kinase C
PRRs	pattern recognition receptor
PVDF	polyvinylidene fluoride
qPCR	quantitative polymerase chain reaction
RIG-like helicases	retinoid-inducible helicases
ROS	reactive oxygen species
rpm	revolutions per minute
RT	reverse transcription
SCC	squamous cell carinoma
TLRs	toll-like-receptors
TNF	tumor necrosis factor-α
TPA	12-O-tetradecanoylphrobol 13-acetate
UV	ultraviolet

III Figures

III Figures

IV Tables

IV Tables

V Contents

1 Zusammenfassung

ATF3 ist ein anti-inflammatorischer Regulator; zum Beispiel ist ATF3 nach einer Induktion mittels TLR Ligand dazu in der Lage IL-6 und IL-12/IL-23p40 zu supprimieren. Ebenfalls kann ATF3 direkt an p53 binden, was zu einer Beschleunigung des Zellzyklus führt, welche in einer Erhöhung des Tumorwachstums endet. Das Ziel dieses Projekts war es herauszufinden wie ATF3 eine Entzündung kontrollieren kann und das tumorfördernde und anti-inflammatorische Potential von ATF3 zu untersuchen.

Die humanen *in vitro* Daten dieser Arbeit zeigten einen unterschiedlichen Effekt von den Molekülen CsA und DMF auf myeloide Zellen und Keratinozyten, welche beide ATF3 als Ziel haben. Keratinozyten scheinen sensitiver auf CsA induziertes ATF3 anzusprechen, während das DMF vermittelte, anti-inflammatorische Potential prominenter in myeloiden Zellen ist.

Die murinen Daten dieser Arbeit zeigten *in vivo* eine unerwartete Reduktion der Zellproliferation in der Haut nach TPA Applikation in *Atf3*$^{-/-}$ und *Il6*$^{-/-}$ sowie *Atf3*$^{-/-}$ x *Il6*$^{-/-}$ Mäusen, welche im Vergleich zu *wt* Mäusen eine weniger ausgeprägte epidermale Hyperplasie zeigen. In *Atf3*$^{-/-}$ Mäusen war dies trotz des Anstiegs in der *Il6* Expression der Fall. Am überraschendsten war der hohe Anstieg des Nlrp3 sowie Il-1β Levels der mRNA und des Proteins der entzündeten Haut in *Atf3*$^{-/-}$ Mäusen. Dasselbe Muster zeigte sich in *Il6*$^{-/-}$ sowie *Atf3*$^{-/-}$ x *Il6*$^{-/-}$ Mäusen. Auffällig war der Hohe Anstieg der IL-1 Zytokine in den behandelten Ohren der *Atf3*$^{-/-}$ und *Il6*$^{-/-}$ sowie *Atf3*$^{-/-}$ x *Il6*$^{-/-}$ Mäuse, mit zugleich erniedrigten Level von *Il2* und *Il4* sowie den selben Mengen an *Ifn* und den *Ifn* regulierenden Chemokinen *Cxcl9* und *Cxcl10* im Vergleich zu *wt* Tieren. Diese Daten deuten auf eine Immunreaktion hin zu einer innaten Immunantwort, wenn ATF3 und/oder IL-6 nicht vorhanden sind, während *wt* Tiere eine adaptive Immunantwort aufzeigen. Ebenfalls wurden die Effekte von Anakinra auf eine akute Hautentzündung untersucht, hier zeigte sich, dass Anakina in der Lage ist die Entzündung in *wt* Tieren zu verringern. Dies war interessanterweise in den *Il6*$^{-/-}$ Mäusen nicht der Fall; diese reagierten nicht auf eine Therapie mit Anakinra, was darauf hindeutet, dass IL-6 eine Schlüsselrolle in der Therapie von entzündlichen Hauterkrankungen mit Anakinra spielt.

Murine *in vitro* Analysen lassen darauf schließen, dass dieser hohe Anstieg in *Nlrp3* und *Il1b* mRNA von Keratinozyten ausgelöst wird, da dieser Effekt in Dendritischen Zellen geringer ausfiel. Zusätzlich führte eine Stimulation von Keratinozyten mit UV Bestrahlung zu dem gleichen Resultat für *Nlrp3* und *Il1b*.

Die generierten Daten weisen auf ein faszinierendes Zusammenspiel zwischen IL-1, IL-6 und ATF3 in entzündlicher Haut und der Immunreaktion sowie der Keratinozyten Proliferation hin, welches bisher noch nicht beschrieben wurde. ATF3 scheint eine kritische Rolle in der Regulation zwischen der IL-1 Familie und der IFN Familie, sowie der T Zell Antwort zu spielen, welche nun genauer untersucht wird. Dies ermöglicht es uns, das Verständnis der Mechanismen der Immunantwort unter entzündlichen Bedingungen zu verbessern, was zur Entdeckung und Entwicklung neuer Therapien für entzündliche Hauterkrankungen führen kann.

2 Abstract

ATF3 is known to be a strong anti-inflammatory regulator; for example, ATF3 is able to suppress IL-6 and IL-12/IL-23p40 after induction by TLR ligands. ATF3 can also directly bind to p53, which leads to an acceleration of the cell cycle, and finally tumor promotion. The aim of the project was to determine the control of inflammation via ATF3 and to investigate its tumor promoting and anti-inflammatory potential.

The human *in vitro* data of this work showed different effects of the ATF3-targeting molecules CsA and DMF in myeloid cells and in keratinocytes. Keratinocytes seem to be more sensitive to CsA induced ATF3, whereas the DMF mediated anti-inflammatory potential is more prominent in myeloid cells.

The murine results of this work showed that *in vivo* unexpectedly *Atf3*$^{-/-}$ and *Il6*$^{-/-}$ as well as *Atf3*$^{-/-}$ x *Il6*$^{-/-}$ mice had a reduced cell proliferation in the skin after TPA application, which was associated with less epidermal hyperplasia compared to *wt* controls. For *Atf3*$^{-/-}$ mice this was despite the expected increase in *Il6* expression. Most surprisingly *Atf3*$^{-/-}$ mice displayed higher levels of Nlrp3 and Il-1β mRNA as well as protein in the inflamed skin. The same pattern was found in *Il6*$^{-/-}$ as well as *Atf3*$^{-/-}$ x *Il6*$^{-/-}$ mice. Importantly, ears from *Atf3*$^{-/-}$ and *Il6*$^{-/-}$ as well as *Atf3*$^{-/-}$ x *Il6*$^{-/-}$ mice had higher levels of the IL-1 family cytokines, but at the same time they showed loss of *Il2* and *Il4* and similar levels of *Ifn* and the *Ifn* induced chemokines *Cxcl9* and *Cxcl10* compared to *wt* mice. This results show an immune reaction towards an innate immune response lacking ATF3 and/or IL-6, while wt mice showed an immune reaction towards an adaptive immune response. Additionally, the effects of Anakinra on acute inflammation were investigated showing that, Anakinra is able to lower the inflammation in *wt* mice. Interestingly *Il6*$^{-/-}$ mice did not respond to Anakinra therapy, indicating that IL-6 plays a key role in therapy of inflammatory skin disease with Anakinra.

Murine *in vitro* analysis suggested that this strong increase in *Nlrp3* and *Il1b* mRNA may result from keratinocytes as this effect was minor in dendritic cells. Additionally, stimulation of keratinocytes with UV irradiation showed similar results for *Nlrp3* and *Il1b.*

The generated data point towards a challenging interplay of IL-1, IL-6 and ATF3 in skin inflammation and immune reaction as well as keratinocyte proliferation that had not been described before. This critical role of ATF3 in balancing the regulation between the IL-1 family and the IFN family as well as T cell response is now under further investigation. This enables us to improve the understanding of the mechanisms in immune response under inflammatory conditions, which may result in the discovery and development of new therapies for inflammatory skin disease.

3 Introduction

3.1 Inflammatory skin disease

The most frequent inflammatory skin diseases are psoriasis, atopic dermatitis (AD) and lichen planus. They are characterized by the release of proinflammatory cytokines and the recruitment of inflammatory cells into the skin (1-4). These events result in hyperplasia of the skin which can either be a consequence of hyperproliferation of keratinocytes, lack of differentiation or of apoptosis. Normally proliferation is controlled and does not lead to cancer, only rarely, such as in cases of lichen planus it may result in squamous cell carcinoma (SCC) (1).

Characteristic for skin hyperplasia is the thickening of the non-keratinized layers of the epidermis due to an increased number of epithelial cells. In severe cases the hair follicles can also be affected and are hyperplastic. A large variety of injuries and conditions can trigger hyperplasia, including inflammatory processes, exposure to irritants, to toxic materials or to ultraviolet (UV) light (5). Epidermal thickening most frequently results from skin inflammation, which is a complex defense mechanism including many cell types and mediators of the skin. In healthy skin a balance of regulated interactions between different cellular and microbial components takes place. Imbalance of this components lead to a dysfunction of the epidermal barrier resulting in the pathogenesis of inflammatory skin disease such as AD and psoriasis (6, 7). The inflammatory milieu of these diseases is partly understood, but in contrast the downstream signaling pathway and their cross-talk as well as the function of the involved cytokines are only partially understood (7).

3.1.1 Atopic dermatitis

One of the most frequent skin diseases is AD, which affects 10 to 20% of children and 1 to 3% of adults in industrialized countries (8). AD is associated with pruritic and erythematous plaques on the skin (9). Most of the time it develops during the first years of life, but it can manifest at any age. The first clinical signs are skin dryness and roughness. In the progression of AD, the symptoms can either be continuous for long periods or they can relapse in time intervals. These lesions can affect any part of the body, shown in Figure 1. There is no laboratory or histological findings associated with AD. Therefore the diagnosis only relies on clinical features of the patients. AD patients are susceptible for *S aureus* infections at the lesional skin. Patients suffer from itch, sleep deprivation and social embarrassment because of the visible lesions (10).

The pathogenesis of AD is yet not completely understood but defects in skin barrier function and a dysregulation of the immune system seem to play a key role in the development of the disease. First of all, as a therapeutic treatment of AD inflammation of the skin needs to be controlled and additionally the skin barrier needs to be restored. A successful control of AD needs a complex therapy, which includes an optimal skin care with at the same time treatment of skin infections and an anti-inflammatory treatment with topical corticosteroids or topical calcineurin inhibitors (11).

Figure 1: Atopic dermatitis at different parts of the body. Source: (10, 11)

3.1.2 Psoriasis

Dry, bright red plaques with thick, non-adherent, silver-white scales are characteristic for psoriasis (12). About 0.7 to 3% of children and adults in the EU and US suffer from this disease (13). Psoriasis is subdivided in a number of different phenotypes. In the following we focus on two types of psoriasis: the plaque-type psoriasis and the pustular psoriasis, shown in Figure 2 (14, 15). The classification of the disease is based on clinical appearance which is differentiated according to localization and morphology of the lesions (15).

The most frequent from of the disease is the plaque-type psoriasis, which occurs in about 85-90% of patients (15). Patients suffer from oval or irregularly shaped, red, sharply demarcated, raised plaques covered by silvery scales. The plaques are mainly located on the elbows and knees and on the lower back. As plaque-type psoriasis is a dynamic disease, newly formed lesion can develop slowly into an advanced plaque with keeps on growing and enlarging (15).

Pustular psoriasis is rare compared to the plaque-type form. It is characterized by episodic, widespread skin and systemic inflammation (16). There are different forms of the pustular psoriasis; because of this the disease can be classified into two subgroups: the generalized pustular psoriasis (GPP) and the localized pustular psoriasis. All types of pustular psoriasis have similar presentations; most of the patients develop superficial pustules in a certain area, typically with an erythematous base. In histopathology, parakeratosis, extensive mononuclear and neutrophilic inflammatory infiltrates in the epidermis are observed (17).

Figure 2: Phenotype of pustular psoriasis and plaque-type psoriasis. Source: (15, 17)

3.1.3 Cutaneous squamous cell carcinoma

Cutaneous squamous cell carcinoma is the second most frequent non-melanoma skin cancer. Factors that can increase the risk of SCC include exposure to UV radiation as the greatest risk factor and exposure to human papillomavirus (HPV) types 16, 18 and 31 (18). The SCC can also be divided in different subtypes according to the clinical presentation; it depends on the location and subtype, shown in Figure 3. About 55% of cutaneous SCC occur on the head and the neck because of the high exposure to sunlight (18). But it also often occurs on the legs and the back of patients. In general every area of the body can be affected. SCC develop from epidermal keratinocytes. For the diagnosis of SCC biopsies are taken. Histopathology is done to address the prognosis and to develop the right treatment. The first aim is the complete surgical removal and the histopathological control of the tissue margin. The outcome of a SCC is most of the time good with cure rated that exceed 85% after complete excision (18, 19).

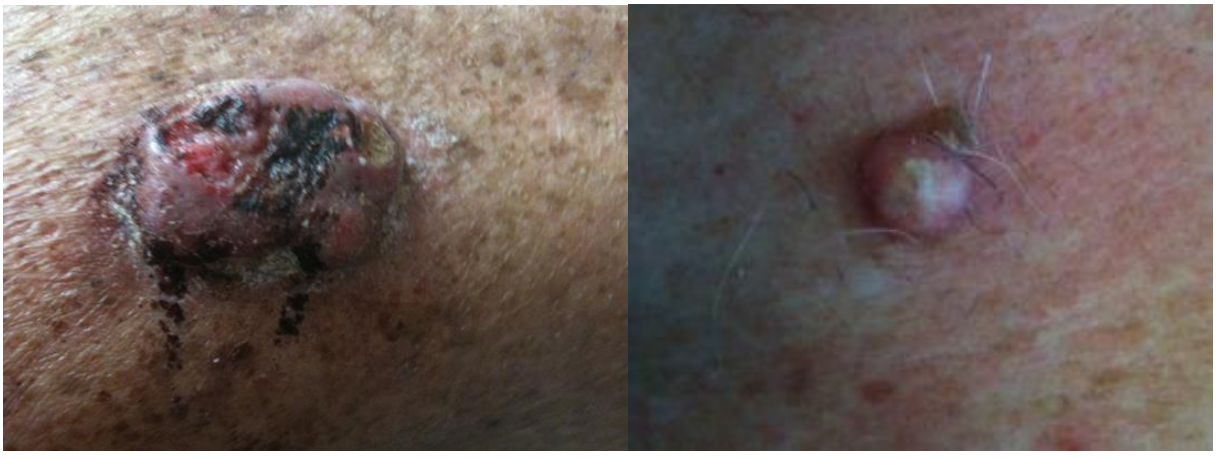

Figure 3: Examples for squamous cell carcinomas. Source: (18)

3.2 The skin as an “active immune organ”

The control of an infection is mainly based on inflammation, while inflammation plays an important role in the control of infection by the recruitment of proteins and cells from the blood into the infected tissues. These components of the blood are now able to address the pathogen directly and increase the flow of lymph carrying microbes and antigen-presenting cells from the infected tissue to nearby lymphoid tissues. When this microbes and cells are present in the lymphoid tissue, the adaptive immune response is activated and leads to the release of lymphocytes (7). If this step is reached effector components of the adaptive immune system, including antibody molecules and effector T cells, are send to the site of inflammation (7). In inflammatory skin disease the migration of leukocytes from the vasculature into damaged tissues is the first step to respond to the agents that are able to induce tissue injury. While acute inflammation is limited to the time of danger exposure, such as the presence of the infectious agent, chronic inflammation is a continuing phenomenon resulting in tissue damage (20). At the beginning of an acute inflammatory response predominantly neutrophils are recruited, but later macrophages dominate (9). In contrast, chronic inflammation is characterized by the presence of macrophages and lymphocytes (8) and is characterized by the promotion of cell proliferation at least in part by continuous delivery of growth promoting cytokines.

The main function of the skin, which is the largest organ of the body, is to build a barrier between the host and the external environment (21). But the barrier is not only a physical or mechanical protection, as it rather forms an active barrier that provides the first line of immunological defense against infection (22). Because of immune competent cells, like mast cells and epidermal langerhans cells, the epidermis itself can function as an “active immune organ” (23) by recruiting and attracting a wide range of inflammatory cells by the secretion of chemokines and cytokines (24). The immune system of the body can be divided into two groups, including the cells of the innate and the cells of the adaptive immune system (25). The function of the innate immune system is to address the skin immune response, in contrast to the adaptive immune system which keeps and amplifies the inflammation. The innate immune system is not based on the reaction to a specific agent, it clears the danger by activation of the complement or recruitment of neutrophils, macrophages, dendritic cells or in the skin the keratinocytes as the first line of defense (26).

3.2.1 Keratinocytes in the immune system

Keratinocytes are epithelial cells which are linked by intercellular bridges so called tight junctions (27). They play important roles in the protection of the body by mechanical and barrier functions of the epidermis and they take part in the inflammatory processes by producing cytokines (28). Epidermal keratinocytes are the major group of the immune competent cells in the skin. Normally their main function is to provide the first line of protection against microbial pathogens as well as physical and chemical danger. But keratinocytes are also pro-inflammatory effector cells, which are able to coordinate the production of anti-microbial peptides, pro-inflammatory cytokines and chemokines after contact with invading pathogens or non-microbial toxins (23). The activation of keratinocytes ensures that there is no way for the pathogen to escape the host immune response. Keratinocytes produce

antimicrobial peptides called defensins and cathelicidins which are part of the cell defense mechanism (29). Under resting conditions keratinocytes do not express high levels of immune mediators (21, 24). In contrast, after the activation by a variety of stimuli, keratinocytes sense danger signals and generate protective immune responses via the release of pro-inflammatory cytokines (21, 24).

3.2.2 Antigen-presenting cells in the immune system

As described above, the innate immune system is the first step for the defense against danger. As a second step, the translocation of an innate into an adaptive response is largely depend on professional antigen-presenting cells, including beside others, dendritic cells and macrophages in the skin (25).

Dermal macrophages are part of the antigen-presenting cells of the skin. They play an important role in tissue repair, because of their function in the phagocytosis of danger signals. At the same time they are poorly migratory and have potent immune-suppressive functions. In healthy skin, they express high levels of IL-10 mRNA (30).

Dendritic cells (DC), as the second group of antigen-presenting cells of the skin, are able to recognize either the danger signals themselves or paracrine signals from keratinocytes (31). After contact with such a danger signal the DC are recruited to the place of inflammation. They are antigen-presenting cells, which are able to induce primary immune responses (32). DC are referred to as “sentinels of the immune systems”, as they sense danger signals to translate them into both innate and adaptive immune responses (33, 34). According to their distribution in the skin they can be subgrouped into Langerhans cells as the main DC of the epidermis and dermal DC. These dermal DC are either located in the entire dermis or at the dermal-epidermal junction. Under inflammatory conditions an additional subset of DC can be recognized the so called inflammatory dendritic epidermal cells. In most immune mediated skin disease dermal DC are increased and are part of the inflammatory response by inducing and regulating the T cell activation (21, 24). The most mobile form of DCs are the so called mDCs, as they are able to drain antigens to the lymph node where they again induce T cell activation. The crosstalk during inflammatory responses between the keratinocytes and DC of the skin leads to the induction of a sufficient immune reaction (9).

3.2.3 Pattern recognition receptors of immune cells

The immune cells of the skin including keratinocytes, macrophages and DCs carry pattern recognition receptors (PRRs) on the cell surface or in the cytoplasm (35). These receptors are able to detect pathogen-associated molecular patterns (PAMPs) or danger associated molecular pattern (DAMPs) (26). This interaction is capable of initiating early immune response (25). PRRs include three main groups: the retinoid-inducible helicases (RIG-like helicases), the Toll-like receptors (TLRs) and the Nod-like receptors (NLRs). Keratinocytes and DC play a key innate role in the detection and defense of pathogens. They express many PRRs including TLRs and NLRs (21, 24), the two most prominent groups of PRRs in the skin. TLRs can be activated mainly by microbial contents such as LPS, flagellin or viral and bacterial DNA or RNA (26). Right now ten human TLRs are already known. They activate

the leucine-rich repeats, a transmembrane domain and an intracellular Toll/IL-1R-domain of the TLRs (36). Most of the TLRs signal via the adaptor molecule MyD88 and then activate the nuclear factor- κ B (NF- κ B) or type I interferons (37). This activation of the immune system via TLRs is of relevance for many skin diseases. DNA or RNA can be detected by TLRs, which are located on the cell surface or within endosomes. While NLRs are located intracellular to detect danger within the cell. NLRs can be divided into three groups: the nucleotide-binding oligomerization domain (NOD), the NLR-leucine-rich repeat and pyrin domain containing (NLRP) and NLR-leucine-rich repeat and pyrin domain containing a CARD (NLRC) (26). NODs are activated by bacterial wall components and end in NF- κ B activation (38).

The largest group of the NLRs is the NLRP family containing a PYD-NACHT-LLR-domain. NLRP1 has in addition two domains, called FIIND and CARD which allow the direct binding to caspase1. The so called activation of the inflammasome, with is part of the immune system, is the oligomerization of NLRPs to recruit caspse-1 into the multiportion complex. The formation of the inflammsome is necessary to activate casase-1, this is done by NLRP1 and NLRP3 but also absent-in-melanoma 2 (AIM2) can form inflammasomes. AIM2 belongs to the family of interferon- inducible proteins and is no NLR (39).

In total the immune system of the skin, with all including components, is of great importance for the protection of the body. In fact also keratinocytes and not only innate immune cells are able to activate the NLR (40, 41). Prior to an initiation of an adaptive immune response, the first line of defense against dangers are the PRRs and cytokines of the skin which lead to an innate immune response.

3.3 Regulating factors in inflammation

As explained above the main function of the skin is to build the first barrier against physical, biological and chemical stress. To perform this function keratinocytes undergo different stages of differentiation including basal cells, which arise from epidermal stem cells, to spinous, granular and transitional cells and result in the corneocytes (12). A correct pass through these different stages is essential for the barrier function of the skin and is regulated by the communication between different cell types. Cytokine are responsible for the control of the differentiation process of the skin, which are produced by keratinocytes and other skin resident cells (12). Transcription factors and cytokines can influence the differentiation and proliferation of the keratinocytes. A deregulation of these factors can result in a dysfunction of the epidermal barrier resulting in many diseases, including AD and psoriasis (7).

3.3.1 Innate cytokine production in the skin

Protein which are secreted by cells are the so called cytokines, they are able to affect the behavior of cells carrying suitable receptors on their surface and play an essential role in both acute and chronic inflammation. Some cytokines released by activated immune cells initiate the inflammation (42). Key inflammatory cytokines signal via receptors that differ structurally from other cytokine receptors, they are called the type I cytokine receptors. These receptors are activated by cytokines including

interleukin- (IL-) 1, IL-6 and tumor necrosis factor-α (TNF) (43). The endothelial cells recognize pro-inflammatory cytokines and change their adhesive properties, this activates leukocytes to stick to them and migrate between the endothelial cells to the site of infection (43). Stimulation of pattern recognition receptors by sterile or microbial agents lead to the production of pro-inflammatory cytokines (43, 44). An overview about the activation of PRRs and the signaling pathways of the TLRs and NLRs is shown in Figure 4.

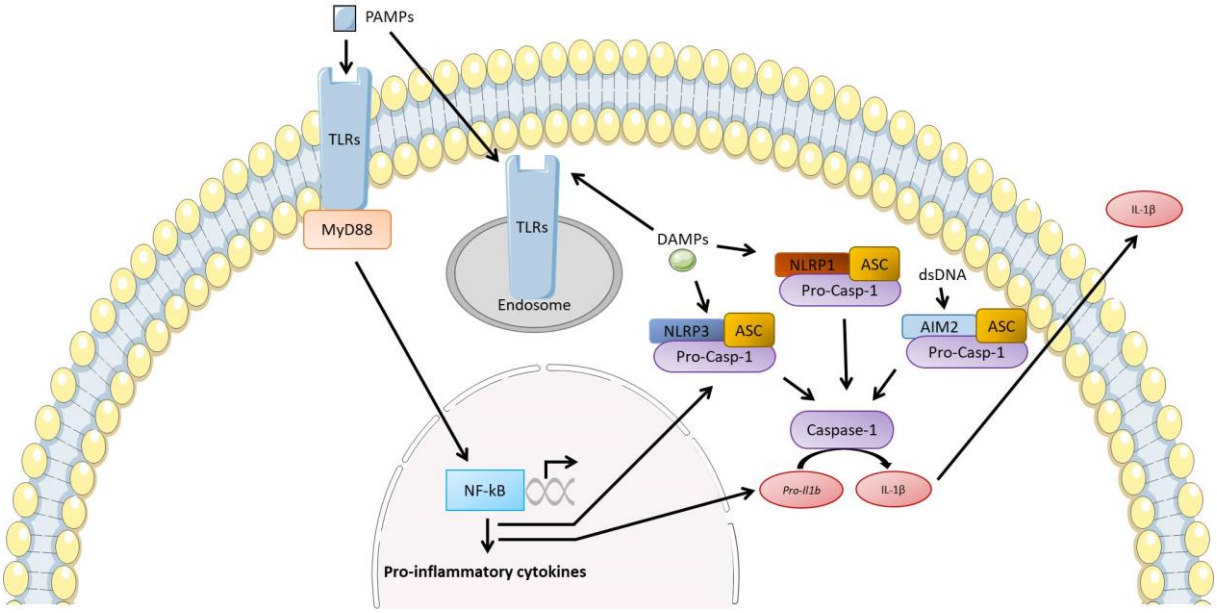

Figure 4: TLR and NLR signaling pathways in the skin.

3.3.1.1 TLR activation

As described above, TLRs are generally considered as sensors for PAMPs. They are expressed in a variety of cell types and in two general cellular locations (45). TLR1, 2 and 4-6 are located on the cell membrane, while TLR3 and 7-9 are located on intracellular compartments such as the endoplasmatic reticulum or endosome (45). They are able to respond to a variety of molecules, such as lipids (TLR1, 2, 4 and 6) and proteins (TLR5) or nucleid acids (TLR3, 7 and 9) (45). All TLRs are expressed in the different cells that are consistent in the skin and upon ligand activation they are able to induce the adaptive immune system. Activated TLRs are able to interact with many intracellular signaling pathways inducing inflammatory cytokines and chemokines, like IL-6 and TNF alpha. These cytokines produced activate the surrounding cells to produce again other chemokines or adhesion molecules. This network between different cells and produced cytokines or chemokines recruits inflammatory cells into the site of inflammation. Both innate and adaptive immune responses are dependent on the production of cytokines and chemokines. They control all aspects of the immune response including direction, amplitude, duration and the remodeling to the tissue. In the skin especially cytokines like TNF alpha, IL-1, IL-6 and IL-12 as well as chemokines such as IL-8 and MIP2 are released after activation of TLRs (45). It was also shown that TLRs are able to modulate tumor development by the release of different cytokines and chemokines. The dermal immune response is triggered by the activation of TLRs of keratinocytes. Keratinocytes express TLRs 1, 2, 3, 4, 5, 9 and 10 (46). TLR

activation, for example, leads to the production of type I interferons resulting in a T helper cell type 1 response (47).

3.3.1.2 NLRs and inflammasome activation

As described above, intracellular NLRs can be activated in a number of immune cells of the skin. They are able to recognize microbial products, irritants and toxins, UV irradiation as DAMPs. Some NLRs can activate inflammasomes and induce pro-inflammatory signaling. Also AIM2 can be activated by cytosolic ds-DNA and especially in the skin AIM2 is functionally (39) and genetically implicated in psoriasis (48).

Activation of these NLRP- or AIM2-associated inflammasomes leads to caspase-1 cleavage and then the secretion of the pro-inflammatory cytokines IL-1β (49). Members of the IL-1 family, including IL-1β, are typically synthesized as precursors without a secretory sequence (43), (50). In immune cells, expression of *pro-Il1b* must be induced before inflammasome activation, for example by TLR stimulation (51), (52). The transcription of *pro-Il1b* is enhanced by the activation of the transcription factor NF-κB. Therefore, the activation of this potent pro-inflammatory cytokine is controlled by two checkpoints: transcription and release (53, 54). For secretion IL-1β must be cleaved to generate the mature cytokine and this is executed by caspase-1 which is activated by inflammasomes (55). Inflammasomes are large multiprotein complexes. Normally constituted by an NLR, the adaptor protein ASC and pro-caspase-1. Upon activation a complex is formed (51). Inflammasomes activate caspase-1 and then the protein complexes are formed, which then proteolytically activates the pro-inflammatory cytokines IL-1β and IL-18 (56). These cytokines are then released via a non-classical secretory pathway (54, 57). In contrast IL-1α is one cytokine which is active in both its precursor and mature forms and remains in the nucleus, the cytoplasm or the cell membrane (43, 58), but can also be released upon inflammasome activation (59). The expression of IL-1α is constitutive in some cells including keratinocytes. In contrast IL-1β expression is induced mainly in response to microbial products, but can also stimulate its own expression. Much more is known about IL-1β. Together with IL-1α it is produced very early in inflammation. Both share the same receptor, called IL-1R. IL-1α receptor activation is the key event in the induction of fever (54). Several diseases are associated with aberrant or excessive signaling by cytokines. In many chronic inflammatory and autoimmune diseases, including type I diabetes, psoriasis and systemic sclerosis, IL-6 and IL-1 are up regulated (43).

3.3.2 The role of Interleukin-1 in inflammation

The IL-1 cytokine family plays an important role in the regulation of the immune system and in inflammatory processes (60). Many disease such as psoriasis, atopic dermatitis, contact dermatitis and cutaneous lupus erythematosus are associated with a dysregulation of the IL-1 system which promotes the manifestation of the disease (61). IL-1α and IL-1β are associated with the differentiation process of the epidermis and the development of skin disease and have pro-inflammatory potential. For example, the cutaneous expression of *IL1A* on mRNA level is reduced in inflammatory skin

disease like psoriasis and AD while no significant changes in the level of *IL1B* were observed (62). But at the same time an increased secretion of IL-1α was observed in the lesional skin of psoriasis patients. An increased expression of IL-1α and IL-1β occurs after acute barrier disruption indicating an protective function of IL-1 in skin disease (63), (64).

3.3.3 Role of Interleukin-6 in inflammation

IL-6 is one of the interleukin type I cytokines. It is a key cytokine with multiple effects on inflammation, immune responses and hematopoiesis. It is able to stimulate the production of acute phase proteins and antibodies as well as the development of effector T-cells (65, 66). Moreover, IL-6 can promote differentiation and proliferation of various non-immune cells (66). Beside its physiological effects IL-6 is also associated with many diseases, including lymphoid malignancies and autoimmune inflammatory disorders (67). In inflammatory skin disease such as psoriasis or lichen planus, IL-6 production by keratinocytes, suggesting an involvement of IL-6 in skin immunity (67). IL-6 functions as first response upon a danger signal, it is one early responsive cytokine in infections (68). Mostly IL-6 is secreted by macrophages and monocytes in inflamed tissues, but it is also secreted by many other cell types. Additionally IL-6 is the most important stimulator o the production from acute phase proteins (69), (20).

In the acute phase of inflammation IL-6 functions as a suppressor of pro-inflammatory cytokines without compromising the level of anti-inflammatory cytokine (43). These anti-inflammatory effects are mediated by the enhanced production of IL-1 receptor antagonist which dampens inflammation by blocking IL-1 receptor signaling (69). In conclusion IL-6 has two different effects; at some levels it acts as a defense mechanism but in chronic inflammation it is rather pro-inflammatory.

There is a correlation between the level of psoriasis and IL-6 in the serum of the patients (70). After barrier disruption of the skin an increased expression and localization of IL-6 and its receptors is found. In a transgenic mouse model, IL-6 is also able to increase the proliferation and epidermal thickening on keratinocytes (71), (12). These findings suggest a role of IL-6 in wound healing by promoting keratinocyte proliferation. The increased level of IL-6 in patients with psoriasis could be due to the disruption of the skin barrier which promotes the synthesis of IL-6 by immune cells.

3.3.4 Role of the activating transcription factor ATF3 in inflammation

The outcome of an inflammatory skin disease is mediated by the intensity of the hyper proliferation of the skin, one factor which might control and regulate this mechanism is the activating transcription factor 3 (ATF3). It is a member of the cAMP responsive element binding (CREB) family of transcription factors (72, 73) and can dimerize with other ATF/CREB proteins including ATF3, c-Jun and JunB (73).

Expression of ATF3 is induced by stress signals such as cAMP, UV radiation, calcium influx and cytokines (74). The gene promoter of ATF3 binds to several transcription factors including ATF/CRE, activator protein 1 (AP1) and NF-κB. ATF3 is able to form dimers under stress stimuli and then activates or represses gene expression. ATF3 is involved in the pathogenesis of many diseases as it modulates the immune response, atherogenesis, cell cycle, apoptosis and glucose homeostasis (74, 75).

Besides this function ATF3, is an important transcriptional modulator with its ability to limit the inflammatory response by the control of cytokine and chemokine expression. Furthermore, it regulates the inflammatory response in immune cells which are involved in inflammation. Thus ATF3 bind to the promoter region of IL-6 (76). For governing basal interferon (IFN)-β in macrophages, the expression of ATF3 is necessary (77). In resting macrophages, NK cells and CD4+ T cells, ATF3 expression is maintained at low levels but upon activation with various factors, ATF3 expression is induced. Due to the ability of ATF3 to directly interfere with NF-κB and AP-1 driven promotors it can decrease the expression of inflammatory cytokines such as IL-6 (78). AP-1 transcription factors regulate inflammation, therefore a dysregulation shows effects on the initiation of skin reactions (22).

Cyclosporine A (CsA) is one of the most potent inducers of ATF3 (79). CsA is an immunomodulator used to prevent from organ transplant rejection. Besides its key clinical application CsA is used for the treatment of rheumatoid arthritis, atopic dermatitis, psoriasis, Crohn's disease and nephrotic syndrome (80-83). By the formation of a complex with cyclophiln, CsA is able to dampen lymphocyte activation. The complex blocks the phosphatase activity of cylcineurin that in turn decreases the production of inflammatory cytokines produced by T lymphocytes (84). Its medical efficacy is limited due to the strongly increased risk of non-melanoma skin cancer, especially after chronic UV exposure (85) via the suppression of p53-dependent senescence (79). An inflammatory microenvironment and oncogenic mutations can support and induce carcinogenesis. So on the one hand the induction of ATF3 can promote cancer by the suppression of p53 but on the other hand ATF3 induction significantly decreases the expression of pro-inflammatory cytokines, especially of IL-6 (86) or IL-8 (87) as well as TNFα and IL-1β (88).

This interplay between anti-inflammatory and pro-oncogenic aspects of ATF3 is important for the treatment of psoriasis or multiple sclerosis with Dimethylfumarate (DMF). DMF is able to induce ATF3 transcription (89), but as well it can induce type II dendritic cells via increased hemoxygenase-1 (HO-1) and activating the nuclear factor (erythroid-derived 2)-like 2 (Nrf2) pathway (90). Induced ATF3 is able to suppress the transcription of IL-6 which has an anti-inflammatory effect in psoriasis. Although ATF3 is induced and alters p53 activation, even long term DMF-treated psoriasis patients showed no increased risk of non-melanoma skin cancer (91).

In general, both DMF and CsA induce the pro-tumorigenic ATF3, but only CsA treatment is associated with increased risk of non-melanoma skin cancer. Therefore, ATF3 seems to play a bimodal role as a tumor suppressor or as tumor promoter (92). Uncontrolled hyperproliferation of the skin is the result of an induction of ATF3 which finally results in skin cancer only upon CsA, but not after DMF treatment. In SCC development in organ transplant recipients, ATF3 is severely induced, as its expression is potentiated by combination of CsA and UVA (93).

3.3.5 Link between ATF3, IL-6 and IL-1 in skin inflammation

IL-6 is one important factor of the innate immune system. It is induced by IL-1 and its expression is regulated by the transcription factor ATF3. ATF3 cannot only suppress inflammation by repression of IL-6, but it can also induce the proliferation of the keratinocytes by direct suppression of p53. For the

treatment of psoriasis fumaric acids are used. They can induce ATF3 and therefore dampen IL-6. IL-6 then decreases IL-12/23 (94) as an important messenger, which regulates the adaptive T-cell mediated immune response in psoriasis. ATF3 is able to suppress the transcription of IL-6. By knocking down endogenous levels of ATF3 higher levels of IL-6 can be transcribed. So ATF3 seems to be involved in suppressing cytokine expression during infection (95).

The both most frequent inflammatory skin disease are psoriasis and atopic dermatitis. These diseases are mediated by the release of proinflammatory cytokines and the invasion of inflammatory cells like mast cells, macrophages or DC (96). Furthermore, chronic inflammation leads to skin hyperplasia which is most of the time controlled and does not result in cancer progression. Although ATF3 mediates proliferation by the direct suppression of p53 in patients treated with DMF, a reduction of the inflammatory hyperplasia can be seen, what may prevent tumor growth. This can be explained by the suppression of IL-6 via ATF3. In contrast Cyclosporin A, which is a calcineurin-inhibitor, and also used for the treatment of atopic dermatitis and psoriasis, leads to an increase risk of epithelial skin cancer. CsA is also able to induce ATF3 but here the stronger influence of ATF3 on the cell cycle and p53 seems to play the important role.

3.4 Mouse models of inflammatory and cell cycle mediated inflammation

3.4.1 TPA-mouse model of acute innate skin inflammation

To induce an skin inflammation and epidermal hyperplasia that has the same hallmarks like psoriasis, 12-O-tetradecanoylphrobol 13-acetate (TPA) a protein kinase C activator, is applied to the skin (97, 98). The application of one dose of TPA to mouse ears, is known to induce an acute inflammatory reaction which has some hallmarks like psoriasis including erythema, edema and polymorphonuclear leukocyte (PMN) infiltration (99). In contrast, the multiple topical applications of TPA to mouse ears is able to produce a prolonged inflammatory reaction which is characterized by increases in epidermal thickening, inflammatory cell infiltration and ear swelling (100). After inducing Ras-mutation by the topical application of Dimethylbutylamin (DMBA) TPA delivers the pro-inflammatory environment needed for the induction of skin papillomas, which in some mouse strains result in squamous cell carcinoma. This model depends on innate inflammatory cytokines, such as TNF, IL-1α and IL-1β (101). Skin proliferation and hyperplasia are promoted by chronic inflammation that results from repetitive TPA application alone.

Without the induction of Ras-mutations by DMBA, TPA alone mediates the recruitment of an inflammatory infiltrate and skin inflammation. This results in skin hyperplasia that shares many similarities with inflammatory skin diseases, such as psoriasis, atopic dermatitis or lichen planus (102). TPA activates protein kinase C (PKC) and induces a variety of tissue responses which lead to a strong inflammatory reaction (101). PKC activation in keratinocytes leads to many events critical for differentiation, such as cell-cycle exit and apoptosis (103).

3.4.2 HPV-mouse model of a cell cycle mediated inflammation

Human papilloma viruses (HPV) are part of a large family which consists of small DNA viruses. They are able to induce hyperproliferation in cutaneous and mucosal epithelia (104). They have the ability to extend from benign to malignant lesions (105). It was shown that cutaneous HPV type 8 (HPV8) is carcinogenic in patients with epidermodysplasia verruciformis (106). These patients suffer from flat warts during their childhood and in the later stage of life most of them develop SCC in sun exposed skin (107). Transgenic mice with the complete early region of HPV8, were able to spontaneously develop papillomas, dysplasia and SCC of the skin (108). Additionally, the synergistic effects of UV light were investigated with treatment of the mice with UVA/UVB light, showing that irradiation with UVA and UVB light induced papillomas at an earlier time point in mice (105). In cooperation with Prof. Herbert Pfister, Virology, University of Cologne, HPV8-K14 mice were bred. These mice overexpress the viral HPV8 protein in epidermal keratinocytes and should develop papilloma spontaneously.

4 Aim of the project

Proliferation in chronic inflammatory skin disease such as psoriasis or lichen planus is most of the time controlled. However, chronic inflammation may serve as a precursor for tumor growth, exemplified by squamous cell carcinomas developing in chronic lichen planus. The aim of the project is therefore to determine the control of inflammation which eventually prevents tumor growth.

One key factor which might control and regulate proliferation is ATF3. But ATF3 seems to play two different roles in inflammation (Figure 5). On the one hand fumaric acid is used as a treatment of inflammatory skin disease such as psoriasis. It is known that DMF leads to reactive oxygen species (ROS) which than can induce ATF3. ATF3 is able to suppress the transcription of IL-6. This reduces inflammation and skin hyperplasia without any increase in tumor growth.

On the other side ATF3 suppresses p53 and thus promotes the proliferation of keratinocytes. CsA is administered to organ recipients to prevent a rejection reaction. Here, CsA induces ATF3 which than promotes the proliferation of keratinocytes by the direct suppression of p53 which leads to an acceleration of the cell cycle. Upon additional chronic UV exposure, the risk of developing epithelial skin cancer is highly increased. Therefore ATF3 seems to have an additional tumor promoting effect in combination with specific other stimuli, like UV exposure.

Therefore, the aim of the project is to decode mechanisms in inflammation which distinguish the anti-inflammatory from the tumor promoting effect of ATF3.

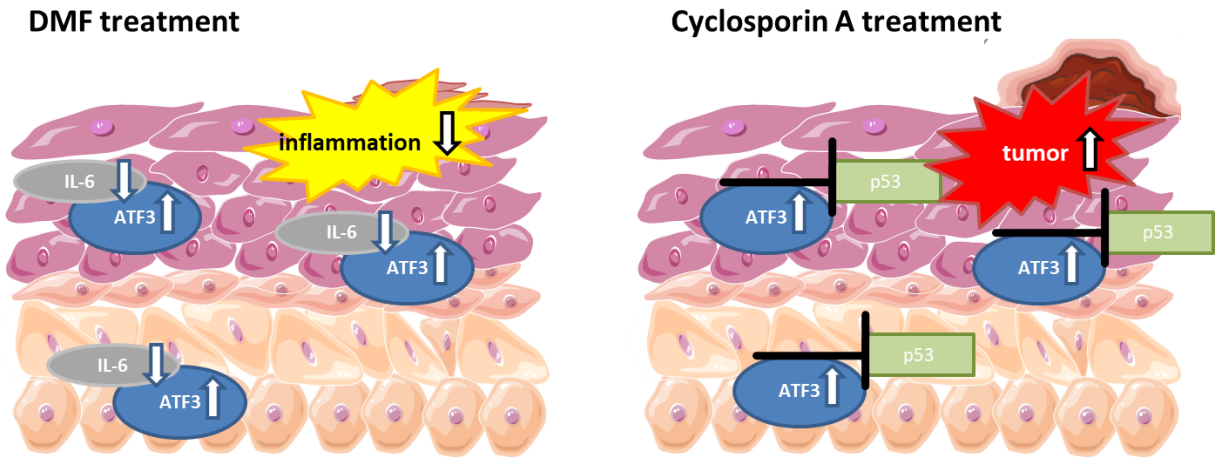

Figure 5: Role of ATF3 in inflammation. ATF3 might control and regulate proliferation, but it seems to play two different roles in inflammation. Under DMF treatment ATF3 is induced to suppress the transcription of IL-6. This leads to an anti-inflammatory effect and reduced inflammation. CsA treatment induces ATF3 which then promotes proliferation by direct suppression of p53.

Materials and Methods

4.1 Materials

This chapter lists all materials and equipment required for the reproducibility of the dissertation.

Material	**Manufacturer**	**Oder number**
96-Well PCR plate	Biozym	# 710897
ACK Lysispuffer	Lonza	# 1054BE
Agarose	Lonza	# 50004
Anakinra	Sobi	# 3197418
Anti Actin mAB	Merck	# MAB1501R
ATP	Invivogen	# tlrl-atp
BD PlastipakSpritze mit Luer-Ansatz, ohne Kanüle, einzeln steril verpackt, 1ml	BD	# 300013
Biocoll	Biochrom	# L6155
Cell cultre flask (75cm^2)	Cellstar	# 658175
Cell strainer	Greiner Bio-One	# 542070
Centrifuge	Heraeus	Multifuge 3LR
CnT-07	CELLnTEC	CnT-07
cOmplete™, Mini, EDTA-free Protease Inhibitor Cocktail	Roche	# 4693159001
Corneregel®	Bausch+Lomb	
Corning® BioCoat™ Collagen I 75cm²	Corning	# 354485
CPG (ODN 2395)	Invivogen	# tlrl-2395

Cyclosporin A	Enzo	# ALX-380-002
DirectPCR Lysis Reagent (Ear) 50 ml	Viagen	# 402-E
Dispase II	Roche	# 04942078001
DMF	Roth	# 0702.1
DuoSet ELISA Ancillary Reagent Kit 2	R&D Systems	# DY008
Ebselen	Enzo	# ALX-270-097
Ethanol absolut	VWR	# 20.821330
Fetal Bovin Serum	Sigma	# 77524
GE Healthcare Whatman™ 17 Chr Chromatography Paper	Fischer scientific	3017915
Gentamycin/Amphotericin	CELLnTEC	# CnT-GAB10
Human IL-1α/IL1F1 DuoSet ELISA	R&D Systems	# DY200
Human IL-1β/IL1F2 DuoSet ELISA	R&D Systems	# DY201
Human IL-6 DuoSet ELISA	R&D Systems	# DY206
Il1b Rabbit mAB	abcam	# ab9722
Immobilon-FL PVDF Membran	Merck	# IPFL00010
Incubator	Eppendorf	Galaxy 170S
Insulinkanüle 26G	BD	# 303800
Isofluran	Apotheke	0155-080-202
LightCycler 480	Roche	

LightCycler® 480 Probes Master	Roche	# 04887301001
Lipofectamin	Invitrogen	# 13778_15
LPS	Invivogen	# tlrl-peklps
Maxima First Strand cDNA Synthesis Kit	Thermo Scientific	# K1671
Mouse IL-1α/IL1F1 DuoSet ELISA	R&D Systems	# DY400
Mouse IL-1β/IL1F2 DuoSet ELISA	R&D Systems	# DY401
Mouse IL-6 DuoSet ELISA	R&D Systems	# DY406
MTT	Thermo Scientific	# M6494
Multiscan Ex	Thermo Scientific	# 51118170
Nlrp3 Rabbit mAB	Cellsignal	# D4D8T
Odyssey® Blocking Buffer in PBS	Li-cor	927-40000
Ohrmessgerät	Kroeplin GmbH	# C1X018
Opti MEM	Gibco	# 31985047
PageRuler™ Prestained Protein Ladder	ThermoFischer	# 26616
PBS	Sigma	# D8537
Penicillin/Streptomycin	Biochrom/Merck	# A 2212
peqGOLD Taq- und Hot Taq-DNA-Polymerase	Peqlab/VWR	# 01-1020
peqGOLD Total RNA Kit	Peqlab/VWR	# 732-2868
PMA	Invivogen	# tlrl-pma

Poly (I:C)	Invivogen	# trl-pic
Primer and probes	TibMol Biol	
Proteinase K	Merck	# 3115836001
R837	Invivogen	# tlrl-imq
Recombinent murine GM-CSF	Peprotech	# 315-03
RNAlater™ Stabilization Solution	Thermo Scientific	# AM7021
RPMI Media 1640	Biochrom	# 12633012
Sealing foils	Genaxxon	# 2248.0100
Thermo Scientific™ Pierce™ BCA™ Protein-Assay	Fischer scientific	23228
Trypsin/EDTA-Lösung (0,05 %/0,02 %)	Biochrome/ Merck	# L2143
Tubes	Eppendorf	
Tween 20	Merck	8221840500
UVA / UVB Psoriasis Comb	Schulze & Böhm	
Well plates	Costar	# 3512
Work bench	MSC Adventures	S1025430

4.2 Methods

This chapter lists all methods required for the reproducibility of the dissertation. All methods of cell culture were performed in biological safety level 1 laboratory under the sterile bench. The cultivation of human cells was carried out in an incubator at 37°C, 95% humidity and 5% carbon dioxide (CO_2) concentration of the air. Murine cells were cultured in an incubator at 37°C, 95% humidity and 7.5% CO_2 of the air. Solutions and materials were sterile or autoclaved.

4.2.1 Isolation and cultivation of human cells

The isolation of primary human cells was approved by the medical ethical committee of the Eberhard Karls University (protocol 109/2019BO2) and performed in accordance with the Declaration of Helsinki principles. Primary human keratinocytes were isolated from healthy human skin samples provided. Skin explants were collected in HBSS. The fatty tissue of the skin was removed; epidermis and dermis were cut into slim pieces. To separate the epidermis from the dermis the pieces were incubated over night at 4°C with 10mg/ml Dispase II. The epidermal strips were removed, chopped, and incubated in 0.05% Trypsin/Ethylendiamintetraacetat (EDTA) for 10 to 30 minutes at 37°C. The reaction was stopped with RPMI including 10% FBS, after pipetting up and down several times the cell suspension was filtered through a 100-µm mesh. The cells were then centrifuged for 5 minutes with 1500 revolutions per minute (rpm) and cultured in CnT-07 medium with supplements and gentamycin/amphotericin until the cells reached 100% confluency. Then the cells were washed with phosphate buffered saline (PBS) and detached with 0.05% Trypsin/EDTA. Trypsin is blocked with RPMI containing 10% FBS and the cell suspension was centrifuged for 5 minutes at 1500 rpm. Cells were again seeded out and cultured with CnT-07 medium with supplements and penicillin/streptavidin. Human keratinocytes were used for the experiments at passage 2 after differentiation with calcium chloride ($CaCl_2$) (1.7mM) for 24 hours.

Peripheral human blood mononuclear cells (PBMCs) were isolated from full blood by Ficoll gradient centrifugation. The blood was collected from healthy donors and diluted 1:1 with PBS. 20ml of the diluted blood was layered gently over 12ml Ficoll. The cell suspension was centrifuged for 25 minutes with 2000 rpm (400g) without break. The interphase was collected and diluted with up to 50ml PBS. Cells were again centrifuged for 5 minutes at 1500 rpm. For adherence, PBMCs were cultured for 1 h in RPMI without FBS and the adherent cell fraction was further cultivated for 24 hours in RPMI with 10% FBS then human PBMCs were used for the experiments.

4.2.2 Isolation and cultivation of murine cells

The generation of murine cells was carried out according to the German law and the recommendation of the guide for care and use of laboratory animals of the National Institutes of Health for the Welfare of Animals. Killing of the animals and generation of cells were approved by the respective government

authority of the state Baden-Württemberg (Regierungspräsidium) §4 Anzeige vom 13.02.2017 “ATF3 und Interleukin 6 bei entzündlicher Hauthyperlasie, SFB Transregio 156 Teilprojekt B06”.

Primary adult murine tail epidermal keratinocytes were isolated either from wt, *Il6*$^{-/-}$ or *Atf3*$^{-/-}$ adult mice. The skin of the tail was removed and cut into slim pieces. The pieces were digested overnight in 10 mg/ml Dispase II. After removal of the epidermal sheets and trypsin digestion (0.05% Trypsin/EDTA), the digestion was stopped with RPMI with 10% FBS and the epidermal suspension was filtered through a 100-µm mesh. The cells were centrifuged for 5 minutes with 1500 rpm and cultured in CnT-07 medium with supplements and gentamycin/amphotericin on collagen-coated dishes. After the murine keratinocytes were 100% confluent, cells were washed with PBS and detached with 0.05% Trypsin/EDTA. The reaction was stopped with RPMI with 10% FBS and the suspension was centrifuged for 5 minutes at 1500 rpm. Murine keratinocytes were seeded out into well plates and used for the experiment after differentiation with $CaCl_2$ (1.7mM) for 24 hours.

Bone marrow-derived dendritic cells (BMDCs) were differentiated from tibial and femoral bone marrow progenitors of either wt, *Il6*$^{-/-}$ or *Atf3*$^{-/-}$ mice. Mice were killed with CO_2 and disinfected with 80% ethanol. Tibial and femoral bones were separated and rinsed with 5ml PBS for each bone. The cell suspension of all bones was centrifuged for 5 minutes at 1500 rpm. Erythrocytes were lysed with ACK lysis puffer for 2 minutes and the reaction was stopped with PBS. The cell suspension was again centrifuged and the pellet was resuspended in RPMI medium with 10% FBS, 10% granulocyte macrophage colony-stimulating factor (GM-CSF) and penicillin/streptomycin and filtered through a 70-µm mesh. The cell count was determined and $2*10^6$ cells were seeded into each 10cm dish. Three days after isolation 10 ml medium was added to the cell culture dish and at day 6 after isolation medium was changed. BMDCs were used for the experiment at day 7.

4.2.3 Stimulation of keratinocytes

To investigate the induction of cytokines and related genes human or murine keratinocytes were treated with different agonists. In Table 1 each stimulation condition is listed.

Table 1: Agonists for the stimulation of keratinocytes

agonist	concentration	incubation	cell type
DMF	70µM/35µM	2 to 6 hours	human/murine keratinocytes
CsA	10µM/5µM	2 to 6 hours	human/murine keratinocytes

Ebselen	20µM/10µM	2 to 6 hours	human/murine keratinocytes
PMA/TPA	5µg/ml/100nM	16 hours	human/murine keratinocytes
R837	20µg/ml	2 to 4 hours	human/murine keratinocytes
Poly (I:C)	10µg/ml	4 to 18 hours	Human/murine keratinocytes
UVA	5J/cm^2	4 to 16 hours	human/murine keratinocytes
UVB	50mJ/cm^2	4 to 16 hours	human/murine keratinocytes

4.2.4 Stimulation of myeloid cells

To investigate the induction of cytokines and related genes PBMCs and BMDCs were treated with different agonists. In Table 2 the respective conditions are listed.

Table 2: Agonists for the stimulation of myeloid cells

agonist	concentration	incubation	activation
LPS	100ng/ml	3 hours	PBMCs/BMDCs
DMF	70µM	2 hours	PBMCs/BMDCs
ATP	5mM	0.5 hours	PBMCs/BMDCs
R837	20µg/ml	3 hours	BMDCs
CPG	1µM	2 hours	BMDCs

4.2.5 3-(4,5-Dimethylthiazol-2-yl)-2,5-diphenyltetrazoliumbromid Assay

For determination of the cell viability a 3-(4,5-Dimethylthiazol-2-yl)-2,5-diphenyltetrazoliumbromid (MTT) assay was performed. Therefore, keratinocytes were seeded out in 96 well plates in a volume of 100µl per well. Keratinocytes were differentiated over night with $CaCl_2$ (1.7mM) after they were 100% confluent and then stimulated with UVA or UVB light for several time points. After the stimulation

10µl MTT were added to the medium and resuspended gently. The 96 well plate was stored at 37°C up to 4 hours. The reaction was stopped with 100µl isopropanol with 0,04 N hydrochloric acid (HCl) after the solution turned black. The solution was pipetted several times up and down and the absorption was detected at 595nm wavelength. Cell viability was calculated out of absorption values.

4.2.6 Transfection of human keratinocytes with siRNA

For the transfection of human keratinocytes with siRNA the ON-TARGET plus siRNA (Dharmacon) sequences were used as shown in Table 3.

Table 3: ON-Target plus Human ATF3 si RNA- SMARTpool

ON-TARGETplus SMARTpool siRNA J-008663-05, ATF3 **Target Sequence: GAGCUAAGCAGUCGUGGUA**
ON-TARGETplus SMARTpool siRNA J-008663-06, ATF3 **Target Sequence: GCAAAGUGCCGAAACAAGA**
ON-TARGETplus SMARTpool siRNA J-008663-07, ATF3 **Target Sequence: AGAAGCAGCAUUUGAUAUA**
ON-TARGETplus SMARTpool siRNA J-008663-08, ATF3 **Target Sequence: CGAGAAAGAAAUAAGAUUG**

Human keratinocytes were used for the experiments after they were seeded out into 12-well plates. Cells rest till they were about 60% confluent. Keratinocytes were washed with PBS and 875µl Opti-MEM is applied to each well.

For the transfection three dilutions were generated:

- Lipofectamin dilution: 100µl Opti-MEM per well + 6µl Lipofectamin RNAiMax per well
- siRNA dilution: 100µl Opti-MEM per well + 2µl siRNA (control/ATF3 siRNA 10µM) per well
- 1:1 mixture of siRNA dilution and Lipofectamin dilution:
    - Control si RNA: 62.5 µl siRNA dilution + 62.5µl Lipofectamin dilution per well
    - ATF3 si RNA: 62.5 µl siRNA dilution + 62.5µl Lipofectatmin dilution per well

The 1:1 mixture was incubated for 5 minutes at room temperature and 125µl per well was added to the cells. Human keratinocytes were transfected for 24 hours. Cells were washed with PBS and CnT-07 medium was added to the cells. Then a specific stimulation of the cells was performed.

4.2.7 Blocking of the IL-1 receptor with Anakrina

Anakinra is a recombinant IL-1 Receptor antagonist. To use it in murine BMDCs, cells were isolated as described and seeded out into 12-well plates. Anakinra was used at a concentration from 100ng/ml to 500ng/ml. Cells were preincubated for 1 hour with Anakinra and then stimulated with different agonists to investigate the effect of IL-1 receptor blocking.

As a second experiment cells were preincubated for 1 hour with 250ng/ml Anakinra and treated with different concentrations of LPS for 2 hours and ATP for 0.5 hour.

4.2.8 RNA isolation and gene expression analysis

RNA isolation is the extraction and purification of RNA from biological samples. In the reverse transcription (RT) reaction RNA is first transcribed into cDNA and subsequently qPCR is performed. The RNA is used as a template, which is then amplified. The first step of the RT is to generate a DNA/RNA hybrid; here the reverse transcriptase has an RNase H function which is able to degrade the RNA protein of the hybrid. The DNA-dependent polymerase activity of the reverse transcriptase completes the single stranded DNA into cDNA (109).

Quantitative Polymerase chain reaction (qPCR) is used to quantify, detect and characterize nucleic acids for many applications in science. To amplify a single DNA molecule into numerous copies in a short time, the biochemical process PCR is used.

The Amplification can be divided into different steps:

(1) denaturation, here double-stranded DNA is heaten up to separate it into two single strands.

(2) annealing, here short DNA molecules, the so called primers, bind to the regions of interest of DNA.

(3) extension, here the 3´end of the specific primer is extended by the DNA polymerase alsong the template stand.

The advantage of probe-based qPCR is that many targets can be detected at the same time in each sample, therefore an optimization and the design of a target specific probe used in addition to primers is required. The most common type is the hydrolysis probe, which contains fluorophore and quencher. While the probe is intact, fluorescence resonance energy transfer prevents the emission of the fluorophore via the quencher. It binds to the probe and is hydrolyzed, during the primer extension and amplification of a specific sequence. This leads to the cleavage of the probe, this mechanism separates the fluorophore form the quencher and results in an amplification-dependent increase in fluorescence. In summary the fluorescence signal from a probe-based qPCR reaction is proportional to the amount of the probe target sequence present in the sample (110).

After the experiments cells were lysed with 300 µl RNA lysis puffer, RNA was isolated and RT was performed. Total RNA (Peq Gold total RNA Kit Sline, VWR, Erlangen, Germany) and reverse transcription (Maxima First Strand cDNA Synthesis Kit for RT-qPCR, Thermo Fischer Scientific, Waltham, Massachusetts) were carried out according to the manufacturer's instructions. To calculate

RNA concentration after the RNA isolation the absorption was measured via NanoDrop 1000 at 260 nm. The concentration was calculated as following:

$$RNA\ concentration\ \left(\frac{\mu g}{ml}\right) = absorption_{260} * 40$$

The reaction mix for cDNA synthesis was incubated for 10 minutes at 25 °C and then for 30 minutes at 50° C. Afterwards the enzyme was inactivated at 85° C for 5 minutes. CDNA was stored at -20° C.

Quantitative Polymerase chain reaction (qPCR) was executed to determine gene expression using the LightCycler 480 instrument.

For each reaction of probe based qPCR the following substances were used:

- 0.5 µl primer forward
- 0.5 µl primer reverse
- 0.5 µl probe
- 2.5 µl H_20
- 5 µl probes master.

To each well 9 µl master mix and 1 µl complementary DNA (cDNA) template were added.

The expression of the specified genes was calculated relative to the expression of the housekeeping gene ß-actin. The PCR was performed for 50 cycles. As housekeeping gene ACTB was employed (referred to as “control” below). For every sample duplicates were made. Values with a standard derivation higher than 0.5 were excluded. The data was analyzed using the comparative C_t method:

$$R = 2^{-[(\Delta Ct_{treated} - \Delta Ct_{control}) - (\Delta Ct_{untreated} - Ct_{control})]}$$

Human primer and probe sequences are listed in Table 4, murine primer and probe sequences are listed in Table 5.

Table 4: Human oligonucleotide primers and LightCycler hybridization probes

Target gene	Gene ID NCBI	Primer	Primer sequence	Purpose
ATF3	467	ATF3 A	AAATGCTGCTTCTCGTTCTTGA	qPCR
		ATF3 S	GGAGTGCCTGCAGAAAGAGTC	qPCR
		ATF3 P	6FAM-TCCTCAATCTGAGCCTTCAGTTCAGCA--BBQ	Hybridization Probe

ACTB	60	ß-Actin F	AGCCTCGCCTTTGCCGA	qPCR
		ß-Actin R	CTGGTGCCTGGGGCG	qPCR
		ß-Actin TM	6FAM-CCGCCGCCCGTCCACACCCGCC--BBQ	Hybridization Probe
IL1A	3552	IL1A F	GAAGGCTGCATGGATCAATCTGT	qPCR
		IL1A R	GTGAGGTACTGATCATTGGCTCG	qPCR
		IL1A TM	6FAM-CGGGAAGGTTCTGAAGAAGAGACGGT--BBQ	Hybridization Probe
IL1B	3553	IL1B S	CAGGGACAGGATATGGAGCAA	qPCR
		IL1B R	ATGTACCAGTTGGGGAACTG	qPCR
		IL1B TM	6FAM-AGAATCTGTACCTGTCCTGCGTGTTGAA--BBQ	Hybridization Probe
IL6	3569	IL6 U	CCAGAGCTGTGCAGATGAGTACA	qPCR
		IL6 B	CCTGCAGCTTCGTCAGCA	qPCR
		IL6 TM	6FAM-CATTTGTGGTTGGGTCAGGGGTGGT--BBQ	Hybridization Probe
HMOX1	3162	HMOX1 F	ACTGCGTTCCTGCTCAACAT	qPCR
		HMOX1 R	GCATAAAGCCCTACAGCAACTG	qPCR
		HMOX1 TM	6FAM-CAGGAGCTGCTGACCCATGACACCAA--BBQ	Hybridization Probe
NLRP1	22861	NLRP1 F	CACTTTATATGGGCTGTCGTTACA	qPCR
		NLRP1 R	CTCATCTTTCTTGTCTTTCACTTGC	qPCR
		NLRP1 P	6FAM-CTCCAGGGCTTCGATAGCAGAGCT--BBQ	Hybridization Probe
NLRP3	114548	NLRP3 F	CACTTCTGACCTCCAGCCA	qPCR

		NLRP3 R	AGGCTCAAAGACGACGGT	qPCR
		NLRP3 P	6FAM-CTGAAACAGCAGAGCTGCCTCCTG--BBQ	Hybridization Probe
CXCL8	3576	IL8 A	ACATGAAGTGTTGAAGTAGATTTGCT	qPCR
		IL8 S	AGAAGTTTTTGAAGAGGGCTGAG	qPCR
		IL8 P	6FAM-AGTTTCACTGGCATCTTCACTGATTCTTGG--BBQ	Hybridization Probe

Table 5: Murine oligonucleotide primers and LightCycler hybridization probes

Target gene	**Gene ID NCBI**	**Primer**	**Primer sequence**	**Purpose**
Atf3	11910	mu Atf3 S	GCGAAGACTGGAGCAAAATGA	qPCR
		mu Atf3 A	TGACAAAGGGTGTCAGGTTAGC	qPCR
		mu Atf3 P	6FAM-CTCAAATACCAGTGACCCAGGAGGTGA--BBQ	Hybridization Probe
Actb	11461	rodAct for	ACCCACACTGTGCCCATCTA	qPCR
		rodAct rev	GCCACAGGATTCCATACCCA	qPCR
		Actin Tm	6FAM-CATCCTGCGTCTGGACCTGGC--BBQ	Hybridization Probe
Il1a	16175	Il1a A	CGCTCACGAACAGTTGTGAATC	qPCR
		Il1a S	AACACTATCTCAGCACCACTTGGTT	qPCR
		Il1a TM	6FAM-TGACCTGCAACAGGAAGTAAAATTTGACAT--BBQ	Hybridization Probe

Il1b	16176	Il1b S	GACGGACCCCAAAAGATGAA	qPCR
		Il1b A	GAAGGTCCACGGGAAAGACAC	qPCR
		Il1b TM	6FAM-CAGGCAGTATCACTCATTGTGGCTGT--BBQ	Hybridization Probe
Il6	16193	IL6_F	CGGAGGCTTAATTACACATGTTCTC	qPCR
		IL6_R	GGTAGCTATGGTACTCCAGAAGACCA	qPCR
		IL6_FAM	6FAM-ACGATGATGCACTTGCAGAAAACAATCTGA--BBQ	Hybridization Probe
Hmox1	15368	Hmox1 S	TGCTCGAATGAACACTCTGGAGA	qPCR
		Hmox1 R	GTTTCCCTCGGGGTGTCT	qPCR
		Hmox1 TM	6FAM-ACGAAGTGACGCCATCTGTGAGGGA--BBQ	Hybridization Probe
Nlrp1a	195046	mNLRP1a_x7/8_F	GCAGAGACAGCAGTCAGGAG	qPCR
		mNLRP1a_x8/9_R	CCATGGGTAACTGAACTCGGTA	qPCR
		mNLRP1a_Probe	6FAM-CACATGGAACCTCTGGGGACTGA--BBQ	Hybridization Probe
Nlrp3	216799	Nlrp3 S	TCTCTGACCAGACTGTACATTGGA	qPCR
		Nlrp3 A	GAATTCACCAACCCCAGCTT	qPCR
		Nlrp3 P	6FAM-CTTGGACTCCTGAGTCTCCCAAGGCATT--BBQ	Hybridization Probe
Cxcl1	14825	muCxcl1 F	CCAAACCGAAGTCATAGCCAC	qPCR
		muCxcl1 A	TCCGTTACTTGGGGACACCT	qPCR
		muCxcl1 TM	6FAM-AATGGTCGCGAGGCTTGCCT--BBQ	Hybridization Probe
Cxcl9	17329	mCxcl9 F	TGCAACAAAACTGAAATCATTGCT	qPCR
		mCxcl9 R	CTTCCTTGAACGACGACGACTT	qPCR

		mCxcl9 P	6FAM-CACTGAAGAACGGAGATCAAACCTGCCT--BBQ	Hybridization Probe
Cxcl10	15945	mCxcl10 F	AGCGTTTAGCCAAAAAAGGTCTA	qPCR
		mCxcl10 R	CAATTAGGACTAGCCATCCACTG	qPCR
		mCxcl10 P	6FAM-AGCCACGCACACACCCCGGT--BBQ	Hybridization Probe
Il2	16183	mIL-2 S	CCCCAGGATGCTCACCTT	qPCR
		mIL-2 A	CCAAGTTCATCTTCTAGGCACTG	qPCR
		mIL-2 TM	6FAM-CCCAAGCAGGCCACAGAATTGAAAG--BBQ	Hybridization Probe
Il4	16189	mIl4 S	CCAAACGTCCTCACAGCAAC	qPCR
		mIl4 R	GCATCGAAAAGCCCGAAAG	qPCR
		mIl4 TM	6FAM-AGAACACCACAGAGAGTGAGCTCGTCTGTA-BBQ	Hybridization Probe
Ifng	15978	mIfng S	CGAAAAAGGATGCATTCATGAGTA	qPCR
		mIfng A	GCTGGTGGACCACTCGGA	qPCR
		mIfng TM	6FAM-TGCCAAGTTTGAGGTCAACAACCCA-BBQ	Hybridization Probe

4.2.9 Cytokine analysis by ELISA

The enzyme-linked immunosorbent assay (ELISA) is used as an immunological assay for detection of proteins, antibodies, antigens or cytokines in cell supernatants or serum. The ELISA allows measuring multiple samples in a single experiment.

For this project solid phase sandwich ELISA from R&D were used. In this method two sets of antibodies are used to detect for instance cytokines out of cell free supernatant. In the first step the ELISA plate was coated with a capture antibody overnight at room temperature in a defined concentration according to the manufacturer ´s instructions. The capture antibody is raised against the antigen of interest. After the incubation time unbound antibodies are washed from the plate. The plate was than blocked for one hour with 1% BSA in PBS to prevent unspecific binding of the detection

antibody. After washing away the blocking solution, the supernatants from the experiments were centrifuged and cell free supernatants were added to the plate to bind to the capture antibody coated on the plate. Samples were analyzed in duplicates. To quantify the measurements a reaction standard with known amounts of the cytokine were used. Seven concentrations using 2-fold serial dilutions in 1% BSA in PBS were applied to the plate in triplicates according to the manufacturer´ s instructions. After incubation for two hours any excess sample was washed away. In the next step detection antibody was added to the plate for two hours in a defined concentration. This antibody is labelled with Biotin and binds to any target antigen already bound to the plate. After washing away unspecific antibodies the Streptavidin HRP consisting out of streptavidin conjugated to horseradish peroxidase was added to the plate for 20 minutes. After a washing step the substrate consisting of 1:1 mixture of Color Reagent A (H_2O_2) and Color Reagent B (Tetramethylbenzidine) was added to the plate to form a colored product which can be measured using a plate reader. The reaction is stopped with a stop solution consisting of 2 N H_2SO_4. Determination of antigen concentration in a sample requires production of a standard curve using known concentrations. Via this curve, the concentration of specific protein in a sample can then be calculated using the optical density measured with a microplate reader at 450 nm.

Human and murine IL-1α, IL-1β/ and IL-6 secretion was measured in cell-free supernatants using R&D ELISA kits (Human/Mouse IL-1β/IL1F2 DuoSet ELISA, Human/Mouse IL-1α/IL1F1 DuoSet ELISA, Human/Mouse IL-6 DuoSet ELISA) according to the manufacturer’s instructions.

4.2.10 Statistical methods

If not otherwise stated, experiments were performed with three independent biological replicates. Statistical analysis was performed with Graph Pad 8 (GraphPad Software, San Diego, CA, USA) using the one-way ANOVA test followed by Dunnett’s multiple comparisons test.

4.2.11 Western Blot

Via gel electrophoresis it is possible to visualize specific antibodies to identify proteins that have been separated based on their size. This mechanism is called western blot and uses a membrane made of PVDF (polyvinylidene fluoride). The gel, containing the proteins, is placed next to the membrane. Application of an electrical current induces the proteins to migrate from the gel to the membrane. Using specific antibodies for the target of interest, the proteins on the membrane can be visualized using secondary antibodies and detection reagents.

A list of the used buffers and solution for the western blot can be seen below.

Lysis buffer

1 mM	EDTA (0.5 M stock solution)	100 µl
0,005 %	Tween-20	2.4 µl
0.5 %	Triton X-100	250 µl

5 mM	NaF (0.5 M stock solution)	500 µl
6 M	Urea	18 g
	dH2O	ad 50 ml

➔ 10 ml + 1 tablet Complete Protease Inhibitor (Roche)

2x SDS-sample buffer

10 %	Glycerin	1 ml
100 mM	DTT	0.7 g
2 %	SDS	0.2 g
0,01 %	Bromphenolblau	0.001 g
125 mM	Tris-HCl pH 6.8	
	(0.5 M stock solution)	2.5 ml
	dH2O	ad 10 ml

10x SDS-Page running buffer

250 mM	Tris	30 g
2 M	Glycin	144 g
	pH 8.3 – 8.5	
1 %	SDS	10 g
	dH2O	ad 1000 ml

1x SDS-Page running buffer

100ml 10x SDS-Page running buffer + 900ml dH2O

Western Blot Semi-Dry buffer

25 mM	Tris	3.3 g
0.2 M	Glycin	15.01 g
20 %	Methanol	200 ml
	pH 8.5	

	dH2O	ad 1000 ml

seperation gel buffer

1.5 M	Tris	18.17 g
0.4 %	SDS (10 % stock solution)	4 ml
	pH 8.8	
	dH2O	ad 100 ml

collection gel buffer

0.5 M	Tris	6.06 g
0.4 %	SDS (10 % stock solution)	4 ml
	pH 6.8	
	dH2O	ad 100 ml

PBST

0.1 %	Tween-20	500 µl
	PBS	500 ml

For the preparation of lysates the tissue of the ears was dissected with clean tools, on ice as quickly as possible to prevent degradation by proteases. Half of the ear was placed in 300µl lysis buffer for western blot. The tissue was shredded with metal balls out of the -20°C fridge for 40 seconds 3 times. The suspension was centrifuged with 12000 rpm for 4 minutes and the supernatant was used for protein determination.

To quantify the protein a 96 well plate was used. 50µl of the standards and blank (PBS) were applied in duplicates. The samples were diluted 1:10 also up to 50µl. The work solutions A and B were mixed 15:1. And 100µl of the mixture was applied to each well. The well plate was incubated for 30 minutes at 37°C. Determination of protein concentration in a sample requires production of a standard curve using known concentrations. Via this curve, the concentration in a sample be calculated using the optical density measured with a microplate reader at 492 nm. 20µg of protein were loaded for western blot.

For the SDS-gel electrophoresis a gel which contains separation and collection gel according to Table 6 and Table 7 were generated. For the detection of Nlrp3 (100kDa) a 10% gel was used, while for the detection of *pro-Il1b* and IL-1β (17.31kDa, 34.6kDa) a 15% gel was used.

Table 6: Composition of separation gel

	8%	10%	12%	15%
separation gel buffer	2.55ml	2.55ml	2.55ml	2.55ml
acrylamid	2.67ml	3.33ml	4.00ml	5.00ml
dH_20	4.78ml	4.12ml	3.45ml	2.45ml
TEMED	6.25µl	6.25µl	6.25µl	6.25µl
APS 10%	50µl	50µl	50µl	50µl

Table 7: Composition of collection gel

	5%
collection gel buffer	1ml
acrylamid	0.67ml
dH_20	2.33ml
TEMED	5µl
APS 10%	40µl

For the SDS gel electrophoresis running buffer was kept at 4°C till use. The samples (20µg) were diluted 1:1 with 2xSDS sample buffer and heated for 5 minutes at 95°C. 1x running buffer was used for the SDS electrophoresis. Equal amounts of protein were loaded into the wells of the SDS-PAGE gel, along with a molecular weight marker. The gel was run for half an hour at 80V and for 1–2 h at 120 V.

For the transfer of the protein from the gel to a membrane, the PVDF membrane was activated with methanol for 1 minute and rinsed with transfer buffer. The transfer buffer was also kept at 4°C till use. The sponge and filter paper had to be wet and kept in transfer buffer. The order for blotting can be seen below. Transfer for 2 hours at 200mA.

Figure 6: Shema of western blot transfer to the membrane.

After the transfer the membrane was blocked with blocking buffer for 1 hour at room temperature. Then the membrane was incubated over night at 4°C with the specific primary antibody in 10ml blocking buffer and PBST (1:1) for each membrane:

- 1:5000 mouse mAb α-Actin (housekeeping gene)
- 1:1000 rabbit mAb α-Nlrp3
- 1:1000 rabbit mAb α-IL-1β

The next day the membrane was washed three times with TBST for 10 minutes while shaking. Then the membrane was incubated for 1 hour at room temperature with the needed secondary antibody in 10ml blocking buffer and PBST (1:1) for each membrane:

- 1:14000 α-mouse IgG red (for Actin)
- 1:14000 α-rabbit IgG green (for NLRP3 and IL-1β)

The membrane was washed again three times with PBST and signals were detected with Li-Cor at a wavelength of 700nm (red) and 800nm (green).

4.2.12 Generation of mice strains for TPA mouse model

For the mice experiments different mice strains were used. The Atf3tm1Dron (*Atf3*$^{-/-}$) mice were already established in Tübingen (89) and the B6.129S2-Il6tm1Kopf/J (*Il6*$^{-/-}$) mice were ordered form Jackson.

To generate double knockout mice for both *Atf3*$^{-/-}$ and *Il6*$^{-/-}$, *Atf3*$^{-/-}$ and *Il6*$^{-/-}$ mice were crossed. The descendants of the F1 generation are heterozygous *Atf3*$^{+/-}$ x *Il6* $^{+/-}$ mice. Crossing descendants of the F1 generation leads to the F2 generation results in 3 putative genotypes. Here *Atf3*$^{+/+}$ x *Il6* $^{+/+}$, *Atf3*$^{+/-}$ x *Il6* $^{+/-}$ and *Atf3*$^{-/-}$ x *Il6*$^{-/-}$ are possible. Having the double knockout mice B6.129S2-Il6tm1Kopf/J x Atf3tm1Dron (*Atf3*$^{-/-}$ x *Il6*$^{-/-}$) in the F2 generation enables the crossing of two double knockout mice. The descendants are always double knockout mice. The crossing scheme is listed in Figure 7.

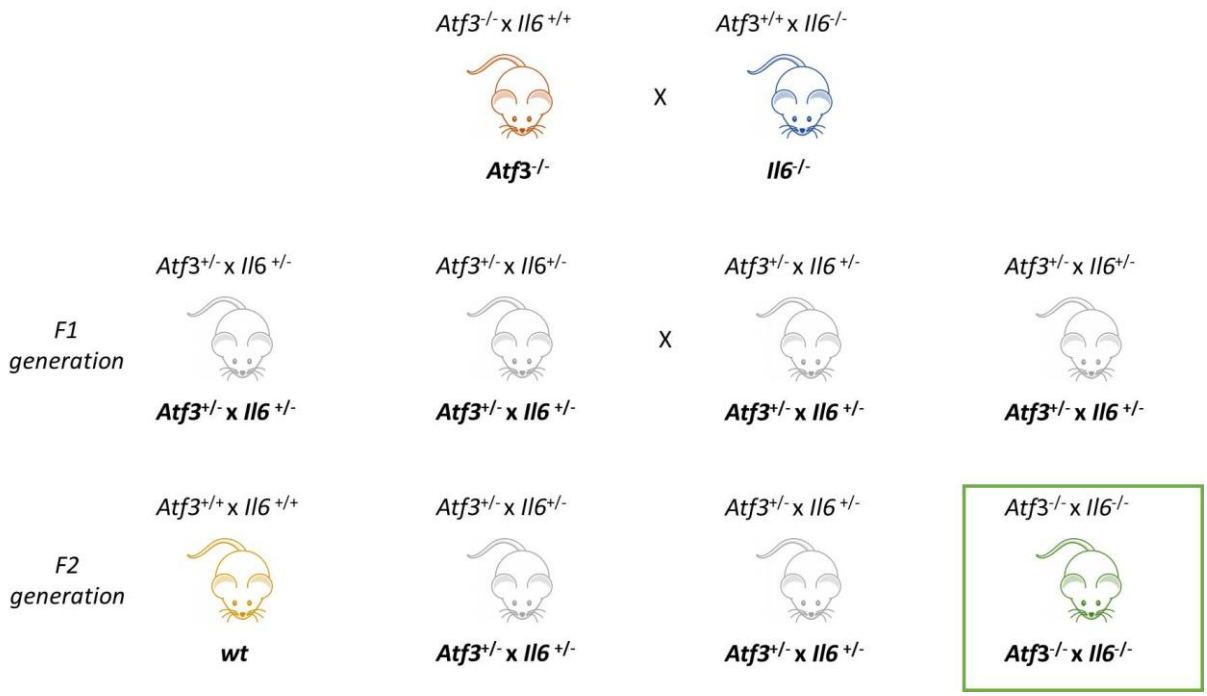

Figure 7: Crossing schema of double knockout mice. Crossing *Atf3*$^{-/-}$ mice with *Il6*$^{-/-}$ mice leads to a F1 generation including *Atf3*$^{+/-}$ x *Il6*$^{+/-}$ mice. Crossing this generation again leads to an F2 generation including the double knockout mice *Atf3*$^{-/-}$ x *Il6*$^{-/-}$.

4.2.13 Genotyping of mice strains for TPA mouse model

For the crossing of the double knockout mice in the F2 generation genotyping of the mice was performed to screen whether they have the desired genotype. In this project *Atf3*$^{-/-}$ x *Il6*$^{-/-}$ were generated in a pure double knock-out bred, resulting in exclusively double-homocygous. No regular genotyping was indicated only for control in spaced intervals it was preferred.

For genotyping, biopsies were taken from the ears of the mice. Each biopsy was lysed with 99 µl lysis puffer and 1 µl proteinase K to disrupt the tissue. The samples were digested in a rotating heatblock at 56°C overnight. On the next day, the digested was heated up to 95°C for 10 minutes to stop proteinase activity and mixed till the whole tissue was lysed.

Primers for the genotyping of *Atf3* and *Il6* are listed in Table 8 and used at a concentration of 10µM.

Table 8: Genotyping primer for *Atf3* and *Il6*

Target gene	Primer	Primer sequence	Primer type	Stock concentration	Working concentration
Atf3	for	AGAGCTTCAGCAATGGTTTGC	Common	100µM	10µM
	rev	TGAAGAAGGTAAACACACCGT	Wild type	100µM	10µM

			Reverse		
	neo	ATCAGCAGCCTCTGTTCCAC	Mutant Revers	100µM	10µM
Il6	oIMR2012	TTCCATCCAGTTGCCTTCTTGG	Common	100µM	10µM
	oIMR2013	TTCTCATTTCCACGATTTCCCAG	Wild type Reverse	100µM	10µM
	oIMR2014	CCGGAGAACCTGCGTGCAATCC	Mutant Revers	100µM	10µM

For the genotyping with Peqlab Tag Polymerase following substances were used for each biopsy:

- 2 µl 10x Buffer
- 1 µl dNTPs
- 1 µl $MgCl_2$
- 1 µl Taq DNA polymerases
- 1 µl primer (10µM)
- 10 µl H_20

For each sample 18 µl of the master mix and 2 µl of the template were used.

Performed program in the light cycler:

denaturation:	95°C	3 minutes
30 cycles:	94°C	30 seconds
	63°C	30 seconds
	72°C	30 seconds
	72°C	3 minutes
hold:	4°C	

Agarose gels were used for the separation of the fractions. For *Atf3* a 3% gel is needed while for *Il6* a 1% gel is used. The gel electrophoresis was performed with TEA buffer 0.5x. The PCR product was mixed with 5 µl loading buffer and 10 µl of this mixture was loaded into the gel. To check the size of the product a size standard marker was loaded into the gel, here the loading puffer was already

included. The gel was run at 140V for 40 minutes. UV-transilluminators are used to visualize DNA separated by electrophoresis. The loading buffer includes a fluorescent dye which binds to nucleic acid. The result was captured by a photo of the gel, example shown in Figure 8.

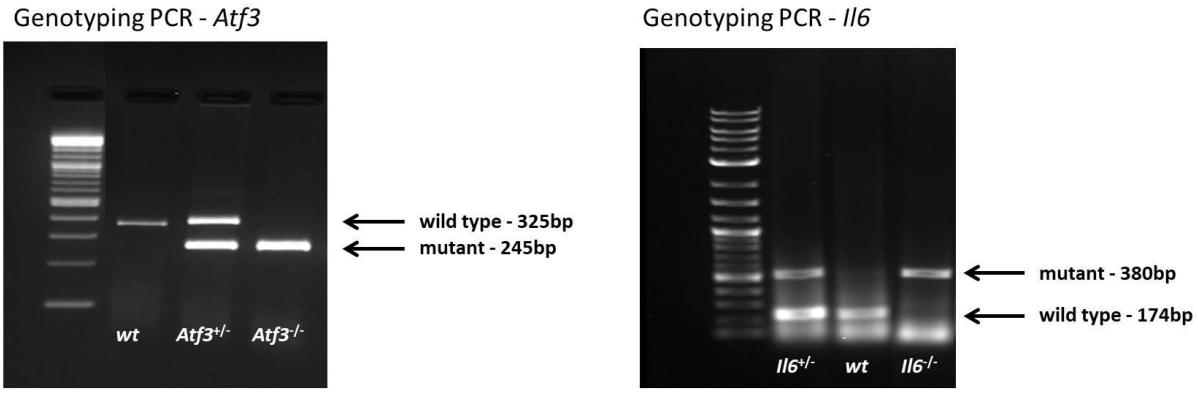

Figure 8: Representative results for genotyping PCR for *Atf3*$^{-/-}$, *Il6*$^{-/-}$ and *Atf3*$^{-/-}$ x *Il6*$^{-/-}$ mice

4.2.14 TPA induced inflammation in vivo

All animal experiments were carried out according to the German law and the recommendation of the guide for care and use of laboratory animals of the National Institutes of Health for the Welfare of Animals. Animal experiments were approved by the respective government authority of the state Baden-Württemberg (Regierungspräsidium) HT06/18G “ATF3 and Interleukin-6 bei aktuer Hautentzündung, Transregio CRC 156, Teilprojekt B06”.

In this experiment TPA activates proteinkinase C, which leads to an inflammatory induced skin inflammation in mice. Thereby we mimic an inflammatory hyperplasia of the skin.

For the experiments *wt*, *Atf3*$^{-/-}$, *Il6*$^{-/-}$ and Atf3$^{-/-}$ x *Il6*$^{-/-}$ mice at an age of 8 weeks were used. Mice were anesthetized with 5% Isoflurane, the narcosis was kept up with 1.5% Isoflurane. To avoid any damage to the eyes, the eyes were covered by a moisturizing cream. The ear swelling of the mice was measured. 25 µg/ml TPA, diluted in ethanol, was applied to the right ear and ethanol was utilized as a negative control on the left ear. After that weight was measured and the mice housed in their cage. Mice were treated accordingly with 25µg/ml TPA or ethanol daily from day 1 to day 5. Each the skin was evaluated, the weight and the ear swelling were controlled. The endpoint was at day 7 then the samples for RNA analysis and histology were taken. Samples for histology were stored overnight in 4.5% formaldehyde and immunohistochemical stainings for HE, Ki67, p53 and IL-1β were performed. For RNA analysis the biopsies were stored in RNAlater over night for 4°C, the next day the biopsies were shredded and RNA were isolated, cytokines were investigated by qPCR as previously described. Samples for western blot were lysed with western blot lysis buffer, shredded three times, centrifuged and supernatants were used for western blot. Experimental setup is shown in Figure 9.

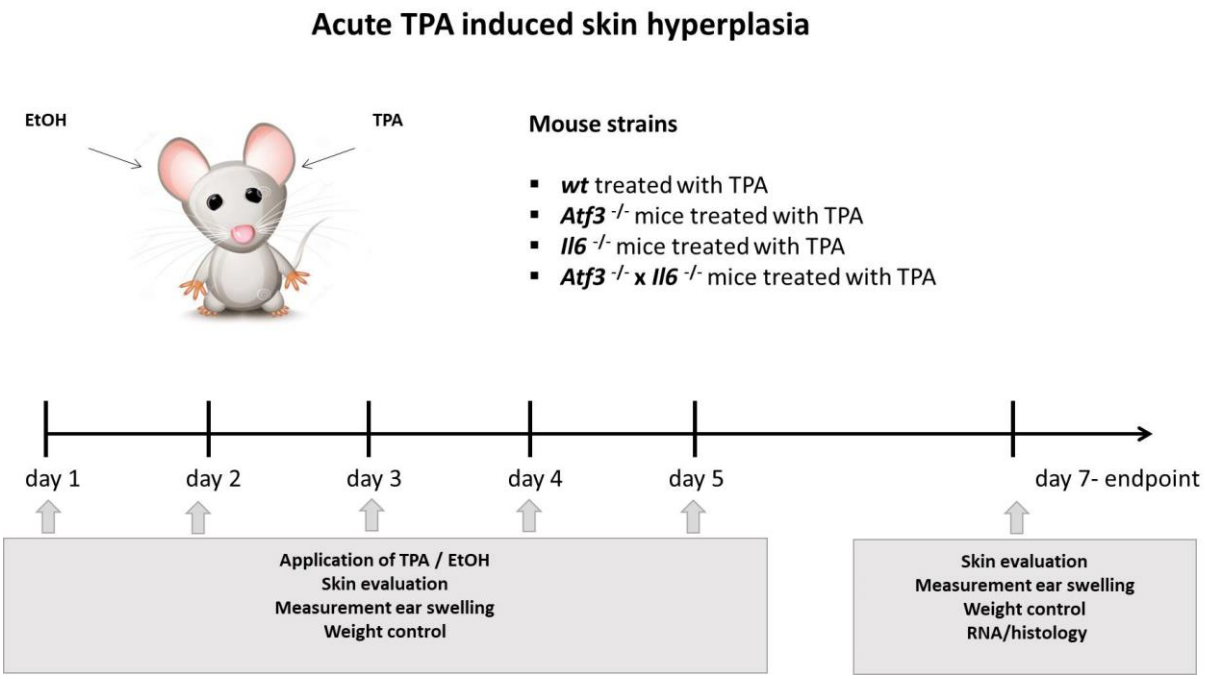

Figure 9: Experimental setup for 7 days TPA application.

To have a look at the effects of Anakinra *in vivo* certain mice were additionally treated with Anakinra during the treatment with TPA in *wt* and *Il6*$^{-/-}$ mice.

Anakinra (5mg/kg weight, diluted in isotonic saline solution of 100µl) was injected interperitoneally on day 1, day 3 and day 5 under isofloran narcose. Additionally ear swelling and weight was controlled on these days. The endpoint of the experiment was on day 7. The specimens were analyzed as described in section 3.2.13; the experimental setup is shown in Figure 10.

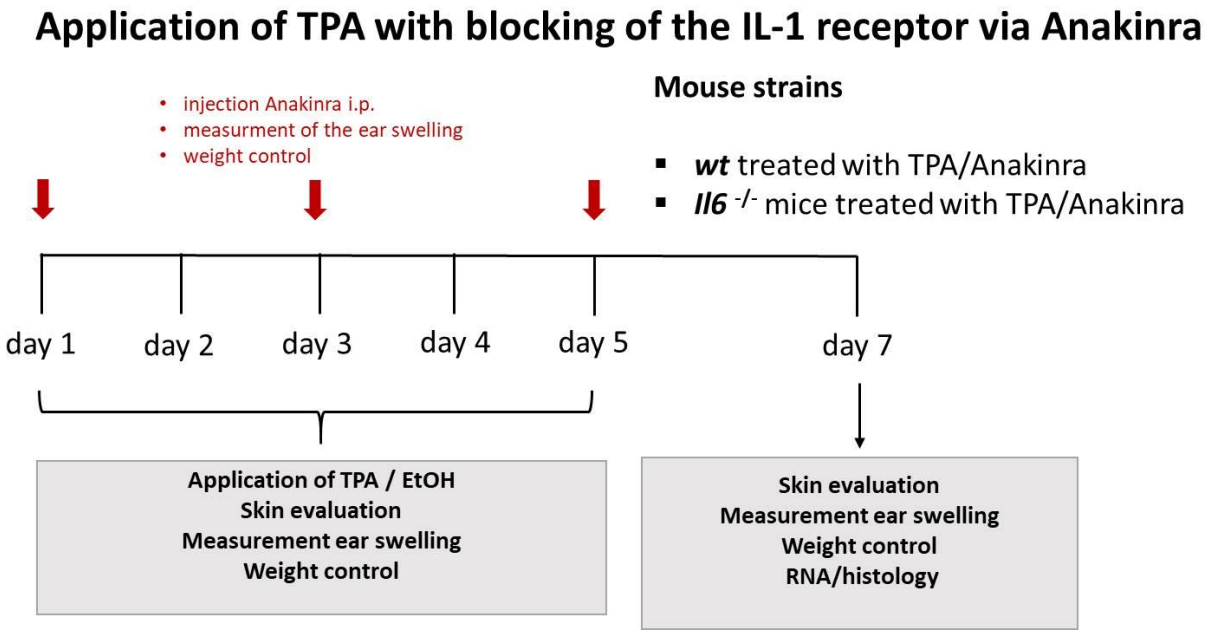

Figure 10: Experimental setup for additional Anakinra treatment to TPA application.

4.2.15 Generation of mice strains for HPV mouse model

VEGF $A^{fl/fl}$LysMCreHPV8 (HPV^{+}) mice overexpress the E6 protein of the human papilloma virus 8 in keratinocytes. These mice were generated in the Institute of Virologie, University of Cologne (AG Pfister) and a breed was established in Tübingen.

To generate the required VEGF $A^{fl/fl}$LysMCreHPV8 x Atf3tm1Dron (HPV^{+} x *Atf3* $^{-/-}$) and VEGF $A^{fl/fl}$LysMCreHPV8 x B6.129S2-Il6tm1Kopf/J (HPV^{+} x *Il6* $^{-/-}$) both knockout mice were crossed with the HPV transgenic mice. The HPV gene is homozygous therefore the overexpression is passed onto each descendant. The descendants of the F1 generation are heterozygous *Atf3*$^{+/-}$ or *Il6* $^{+/-}$ mice positive in HPV. Crossing descendants of the F1 generation leads to the F2 generation resulting in 3 putative genotypes. Here *Atf3*$^{+/+}$ or *Il6* $^{+/+}$, *Atf3*$^{+/-}$ or *Il6* $^{+/-}$ and *Atf3*$^{-/-}$ or *Il6*$^{-/-}$ are possible. The *Atf3*$^{-/-}$ or *Il6*$^{-/-}$ mice are the right genotype for the further investigations, lacking *Atf3* or *Il6,* at the same time they are positive for HPV.

4.2.16 Genotyping of mice strains for HPV mouse model

The genotyping was performed as explained in 4.2.12.

The result for the genotyping of HPV was captured by a photo of the gel, example shown in Figure 11.

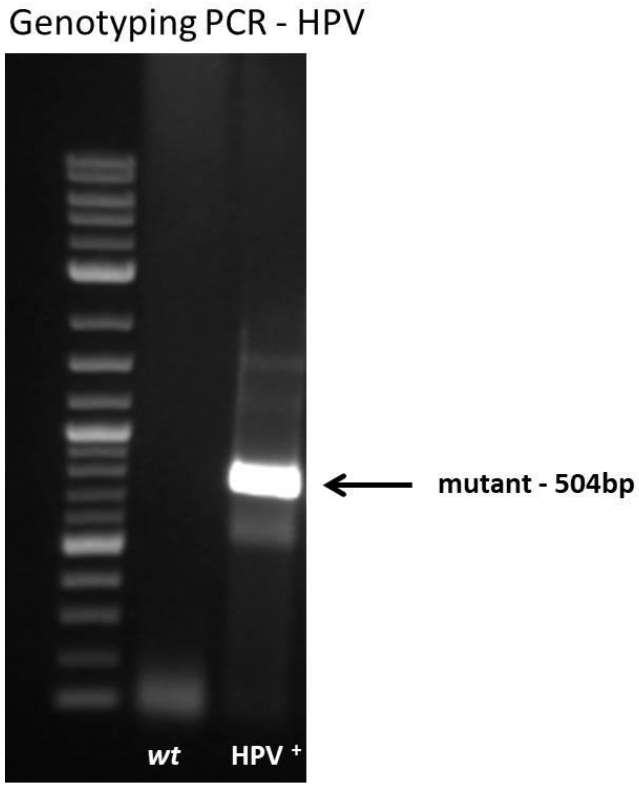

Figure 11: Representative results for genotyping PCR for HPV^{+} mice.

Primer for the genotyping of *Atf3*, *Il6* and HPV are listed in Table 9 and used at a concentration of 10µM.

Table 9: Genotyping primer for HPV, *Atf3* and *Il6*

Target gene	Primer	Primer sequence	Primer type	Stock concentration	Working concentration
Atf3	for	AGAGCTTCAGCAATGGTTTGC	Common	100µM	10µM
	rev	TGAAGAAGGTAAACACACCGT	Wild type Reverse	100µM	10µM
	neo	ATCAGCAGCCTCTGTTCCAC	Mutant Revers	100µM	10µM
Il6	oIMR2012	TTCCATCCAGTTGCCTTCTTGG	Common	100µM	10µM
	oIMR2013	TTCTCATTTCCACGATTTCCCAG	Wild type Reverse	100µM	10µM
	oIMR2014	CCGGAGAACCTGCGTGCAATCC	Mutant Revers	100µM	10µM
HPV	HPV8E6 fw	GGATCCTTTCCTAAGCAAATGGACGGG	Common	100µM	10µM
	HPV8E9 bw	GGATCCGCATGCCACAAAATCTTGCA CAGTGACCTC	Wild type Reverse	100µM	10µM

4.2.17 Cell cycle mediated inflammation in vivo

All animal experiments were carried out according to the German law and the recommendation of the guide for care and use of laboratory animals of the National Institutes of Health for the Welfare of Animals. Animal experiments were approved by the respective government authority of the state Baden-Württemberg (Regierungspräsidium) HT6/15 “ATF3 und Interleukin-6 bei entzündlicher Hauthyperplasie, Transregio CRC, Teilprojekt B06”.

Mice which overexpress the HPV8 protein in epidermal keratinocytes should develop spontaneous papillomas. Therefore mice were inspected once a week to check for the development of papillomas

Because of the fact that the mice did not develop spontaneous papillomas as expected they were additionally treated with UVA and UVB to induce the development of papillomas. According to published data, mice were irradiated once with 10J/cm^2 UVA and 1J/cm^2 UVB light (111) at the age of 6 weeks. Mice were narcotized with Isofluran and the back skin of the mice was shaved 2 cm above

the tail. Before irradiation mice were covered with aluminium foil with a hole of 4cm^2. After that mice were irradiated with a UVA (320-400nm) and UVB-light (280- 360nm). The mice were then investigated macroscopically for 18 weeks to check for the development of papillomas. The experimental setup is shwon in Figure 12.

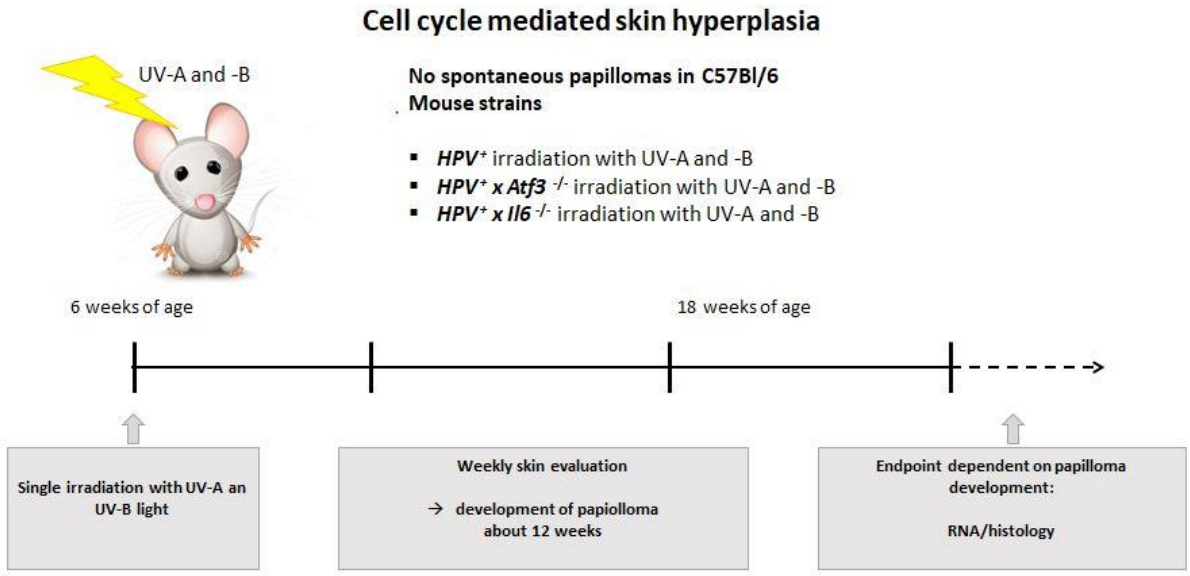

Figure 12: Experimental setup for UV induced skin hyperplasia

5 Results

5.1 Differential induction of *ATF3* and *HMOX1* in PBMCs and keratinocytes via DMF or CsA

5.1.1 Induction of *ATF3* via DMF, Ebselen or Cyclosporin A in human PBMCs and keratinocytes

To dissect the bi-modal role of ATF3 we pharmalogically induced it in human PBMCs and keratinocytes. Cells were treated with DMF, Ebselen or CsA in two different concentrations for 2 to 6 hours (Figure 13). CsA is a known inducer of ATF3, while it is also a calcineurin inhibitor. Ebselen is a gluthatione peroxidase mimetic and ROS scavenger, whose anti-inflammatory potential is currently clinically evaluated (92). DMF is licensed for the treatment of psoriasis and multiple sclerosis.

First the regulation of *ATF3* in human PBMCs was analyzed (Figure 13a). *ATF3* was most prominently induced on mRNA level in a time and dose dependent manner by Ebselen in human PBMCs. CsA and DMF showed fewer effects on *ATF3* in this cell type. The amounts of mRNA induced varied strongly between the different donors and were also very small, but the showed no time dose dependency.

The inflammatory microenvironment in SCC development can promote or attenuate tumor growth. In carcinoma, keratinocytes are the cells that proliferate, while the tumor associated macrophages or lymphocytes control tumor promotion positively or negatively (112).

Therefore, *ATF3* expression was also investigated in human keratinocytes (Figure 13b). *ATF3* induction in keratinocytes differed strongly from *ATF3* regulation in PBMCs. CsA was the most prominent inducer of *ATF3* expression. The induction was dose dependent and peaked at 4 hours of incubation. Ebselen and DMF showed lower effects, with DMF being the weakest direct inducer of the three compounds tested.

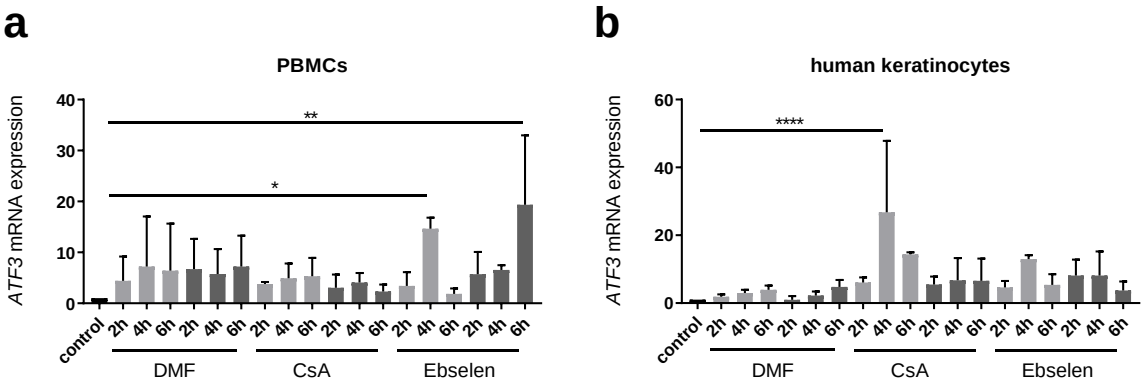

Figure 13: Induction of *ATF3* via DMF, Ebselen or Cyclosporin A in human PBMCs and keratinocytes. Treatment with DMF (70µM light grey and 35µM dark grey), CsA (10µM light grey and 5µM dark grey) and

Ebselen (40µM light grey and 20µM dark grey) for 2 to 6 hours **a** in human PBMCs and **b** in human keratinocytes. Quantitative mRNA expression for *ATF3* relative to *ACTB* is shown at the indicated time points. Significance is implicated by stars *: p<0.05; **: p<0.01; ***: p<0.001.

5.1.2 Similar induction of *HMOX1* and *ATF3* in PBMCs but different induction in keratinocytes

Because of the fact that HO-1 and ATF3 are both induced by cellular stress, the next step was to analyze the correlation between ATF3 induction and HO-1 increase in myeloid cells and in keratinocytes. Cells were treated with DMF, CsA and Ebselen for 2 to 6 hours (Figure 14).

To investigate the effects of ATF3 and HO-1 and their anti-inflammatory potential we investigated the correlation between ATF3 induction and HO-1 increase in keratinocytes as well as myeloid cells. As seen before for *ATF3*, DMF was also able to induce *HMOX1* in myeloid cells and in keratinocytes. The ROS scavenger Ebselen also elevated the transcription of *HMOX1* and *ATF3* in human PBMCs. CsA the most prominent inducer of *ATF3* in keratinocytes did not alter intracellular ROS (Figure 14a). CsA failed to induce *HMOX1* expression in keratinocytes. Here only DMF was able to induce *HMOX1* on mRNA level (Figure 14b).

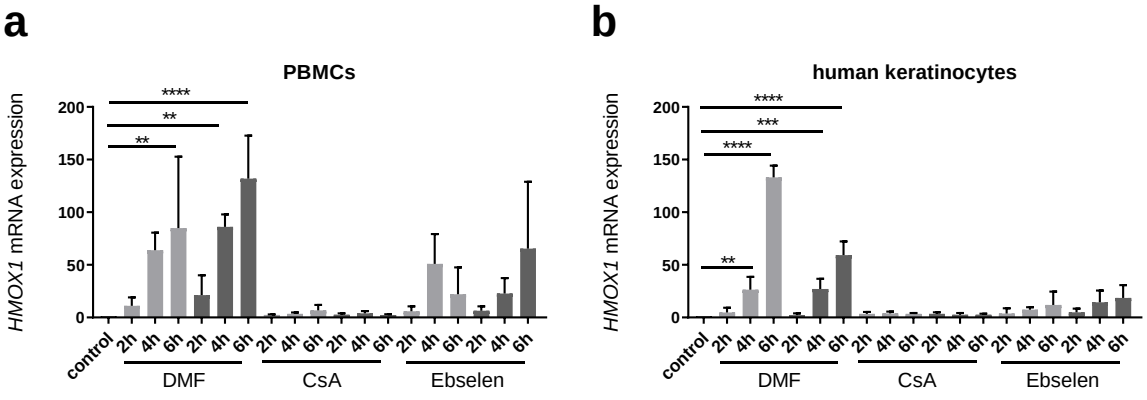

Figure 14: Similar induction of *HMOX1* and *ATF3* in PBMCs but different induction in keratinocytes. Treatment with DMF (70µM light grey and 35µM dark grey), CsA (10µM light grey and 5µM dark grey) and Ebselen (40µM light grey and 20µM dark grey) for 2 to 6 hours **a** in human PBMCs and **b** in human keratinocytes. mRNA expression for *HMOX1* relative to *ACTB* is shown at the indicated time points. Significance is implicated by stars *: p<0.05; **: p<0.01; ***: p<0.001.

5.1.3 *ATF3* induction by TLR-agonists in PBMCs and by protein kinase C activation in keratinocytes

As ATF3 was first characterized as a suppressor of TLR4-induced transcription of IL6 and related cytokines, PBMCs and keratinocytes were stimulated with LPS to activate the TLR or with PMA to activate the protein kinase C (Figure 15).

TLR4 activation by LPS resulted in an increased transcription of *IL1B* (Figure 15a) and *IL6* (Figure 15b), while treatment with the known inducers of ATF3 showed no effect on cytokine expression. The small *ATF3* expression induced by a TLR4 depended signaling peaked after 2 hours (Figure 15c). TLR-mediated *ATF3* transcription did not correlate with *HMOX1* mRNA expression, but rather impaired *HMOX1* expression in PBMCs (Figure 15d). In human primary keratinocytes *ATF3* expression peaked after 2 hours by PMA-treatment (Figure 15e), this effect was independent of *HMOX1* (Figure 15f).

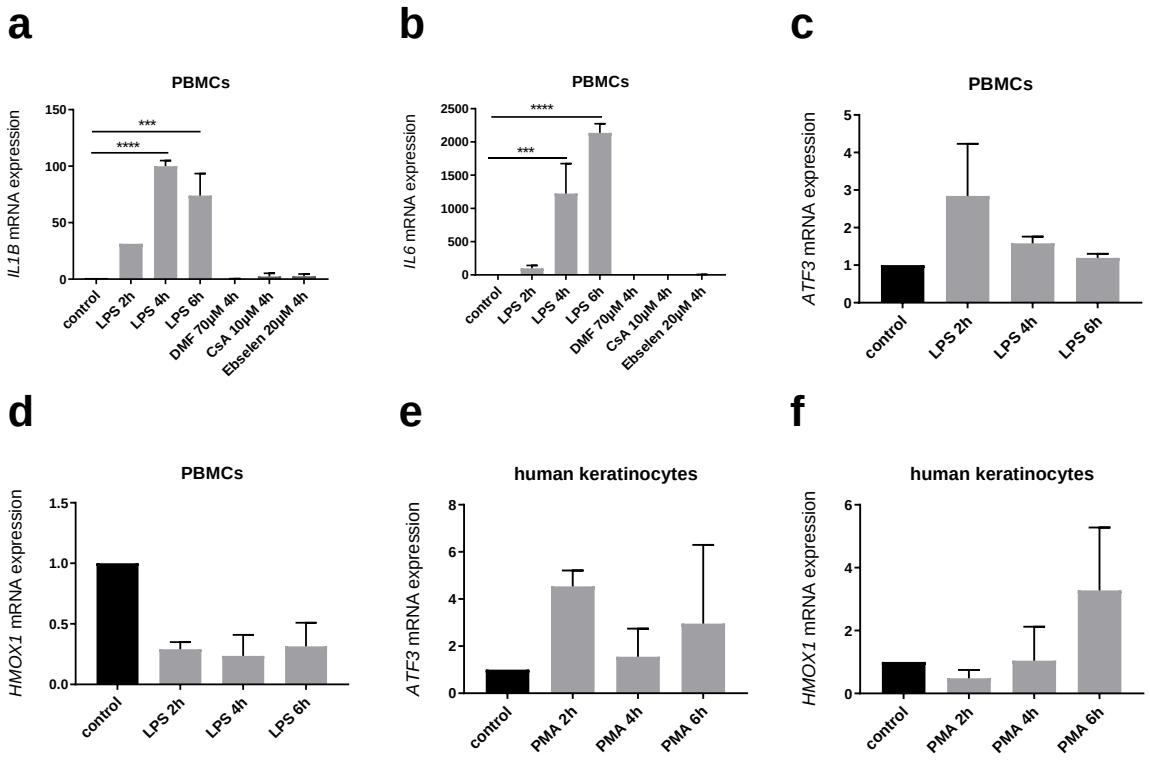

Figure 15: Induction of stress enhances *ATF3*, but not *HMOX1* transcription. a-d PBMCs were treated with LPS (100ng/ml), DMF (70µM), CsA (10µM) and Ebselen (20µM) for the indicated time points and **e-f** keratinocytes treated with PMA (100nM) for 2 to 6 hours. Quantitative mRNA analysis was performed for **a** *IL1B*, **b** *IL6*, **c/e** *ATF3* and **d/f** *HMOX1*. Significance is implicated by stars *: p<0.05; **: p<0.01; ***: p<0.001.

5.1.4 Inhibition of LPS-mediated transcription of *IL6*, *IL1A* and *IL1B* by DMF in PBMCs

Pro-IL1A, *pro-IL1B* and *IL6* must be transcriptionally induced in PBMCs by cytokines or TLR agonist. ATF3 is known to suppress TLR4 induced IL-6 synthesis, therefore the effect of ATF3-induction on TLR-induced transcription of pro-inflammatory mediators was investigated (Figure 16). Without additional TLR-activation, *ATF3* induction by DMF alone neither amplified nor diminished *pro-IL1* or *IL6* transcription, while LPS treatment induced these cytokines (Figure 15a, Figure 15b) in PBMCs.

For TLR4 activation cells were treated with LPS for 2 to 6 hours which led to a direct secretion of IL-6 after its mRNA induction (Figure 16a) while only very low amounts of IL-1β were secreted like expected (Figure 16b). If cells were pretreated prior to LPS-treatment with DMF, *ATF3* was super-induced (Figure 16c) while *HMOX1* (Figure 16d) remained unaltered.

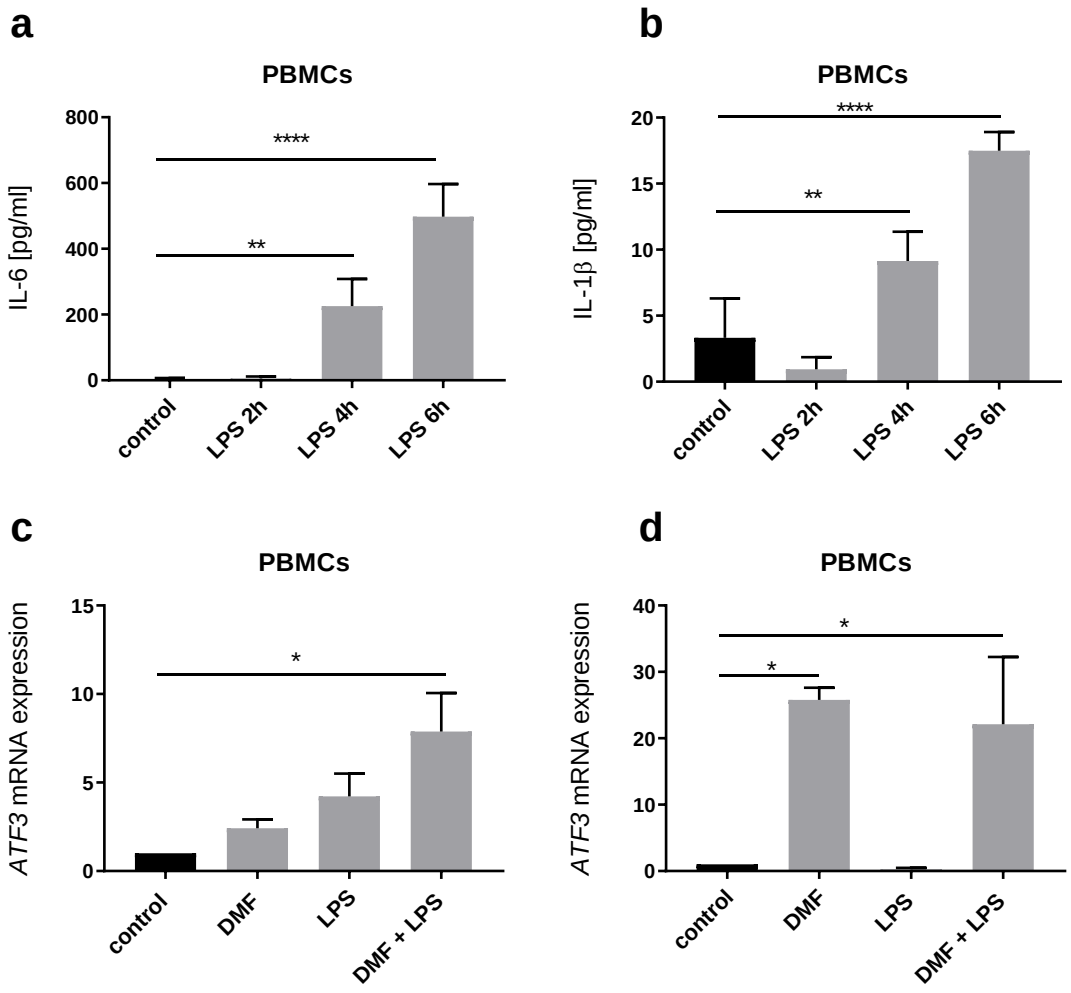

Figure 16: IL-6, but not IL-1β is secreted after TLR activation. a IL-6 and **b** IL-1β secretion of PBMCs after stimulation with LPS for 2 to 6 hours by ELISA**.** Relative transcripts of **c** *ATF3* and **d** *HMOX1* mRNA were measured by qRT-PCR. RNA was isolated from PBMCs treated with 70µM DMF (4h), 100ng/ml LPS (2h) and a combination of both. Significance is implicated by stars *: p<0.05; **: p<0.01; ***: p<0.001.

In consequence, DMF was capable of drastically reducing LPS-induced transcription of *IL6* (Figure 17a), *IL1A* (Figure 17b) or *IL1B* (Figure 17c). To investigate the impact of NLRP3 activation, PBMCs were additionally treated with the NLRP3 agonist ATP. Due to less *pro-IL1*B transcribed, DMF also dramatically reduced IL-1β secretion in PBMCs (Figure 17d).

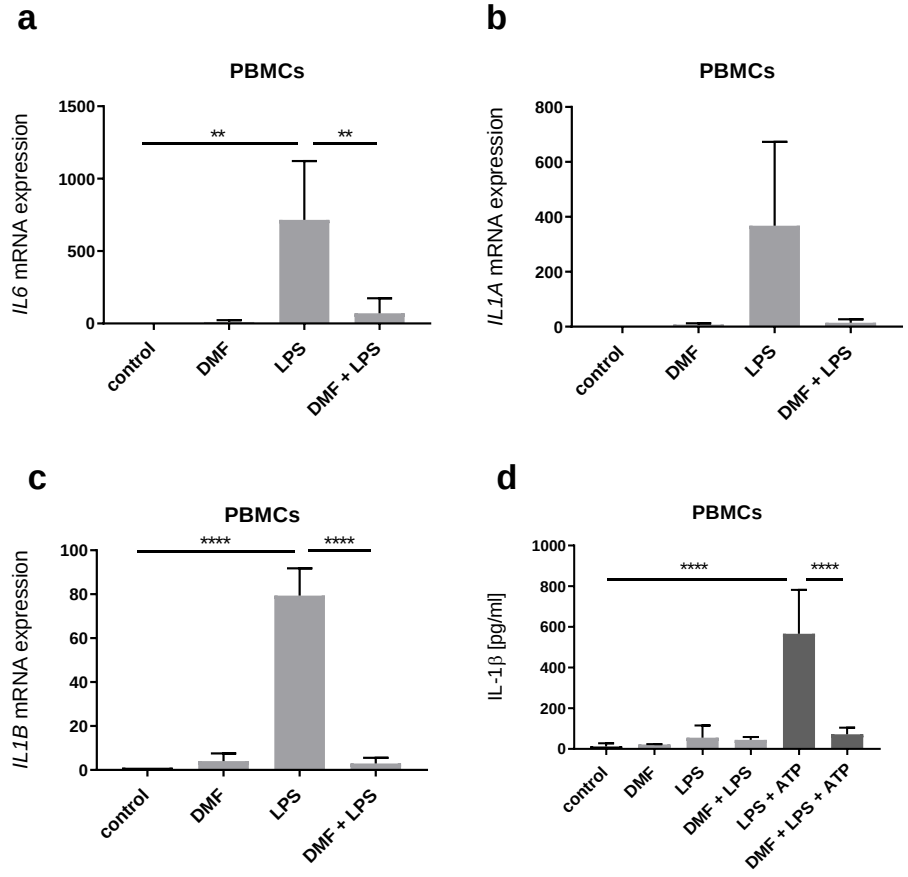

Figure 17: DMF suppresses *IL1* and *IL6* transcription. a-c PBMCs were treated with 70µM DMF (4h), 100ng/ml LPS (2h) and a combination of both. **a** *IL6*, **b** *IL1A* and **c** *IL1B* mRNA expression was measured by qRT-PCR. To activate the inflammasome PBMCs were additionally treated with 5mM ATP for 0.5 hours and **d** IL-1β secretion was measured by ELISA. Significance is implicated by stars *: p<0.05; **: p<0.01; ***: p<0.001.

5.2 Differential induction of cytokines in *Atf3*$^{-/-}$ and *Il6*$^{-/-}$ in mouse derived BMDCs after treatment with TLR ligands

5.2.1 Different regulation of IL-6 transcription and secretion in *Atf3*$^{-/-}$ BMDCs

For analyzing the influence of ATF3 and IL-6 on cell cycle and cytokine secretion by mouse derived BMDCs were generated from *wt*, *Atf3*$^{-/-}$ and *Il6*$^{-/-}$ mice. Cells were treated with different TLR ligands: R837 a TLR7 agonist, CPG a TLR9 agonist and LPS a TLR4 agonist. Cytokines were analyzed on protein as well as on transcriptional level (Figure 18 and Figure 19).

Il6 mRNA was increased after treatment with different TLR ligands in *Atf3*$^{-/-}$ compared to *wt* BMDCs (Figure 18a), however, no difference could be observed on protein level (Figure 18b). BMDCs generated out of *Il6*$^{-/-}$ mice showed no *Il6* on mRNA as well as on protein level as IL-6 was missing here.

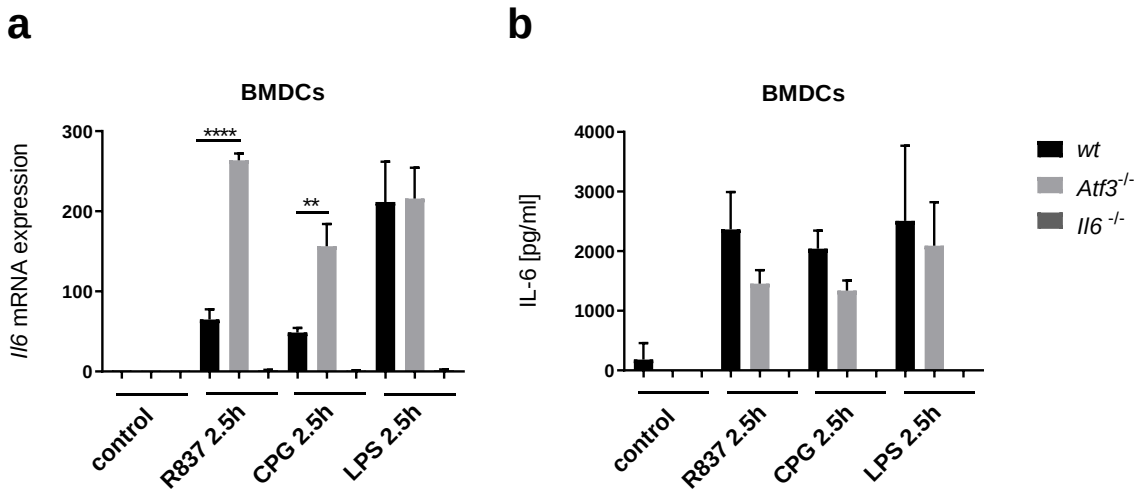

Figure 18: Differential induction of *Il6* on mRNA in *Atf3*$^{-/-}$ BMDCs. BMDCs out of *wt*, *Atf3*$^{-/-}$ and *Il6*$^{-/-}$ mice were treated with R837 (20µg/m), CPG (1µM) or LPS (100ng/ml) for 2.5 hours. Quantitative mRNA expression of **a** *Il6* was measured by qRT-PCR **b** IL-6 secretion was measured by ELISA. Significance is implicated by stars *: p<0.05; **: p<0.01; ***: p<0.001.

5.2.2 *Il1* and *Nlrp3* are significantly increased in *Il6* $^{-/-}$ BMDCs

IL-6 is conventionally secreted via the Golgi pathway, independent of Nod-like receptors. The secretion of IL-1β is controlled by the transcription or the secretion of the cytokine which are independently regulated. For transcription a TLR or cytokine signal via NF-κB is needed, while the secretion is mediated by Nod-like receptors such as NLRP3.

NLRP3 itself is also regulated similarly to *pro-Il1b* and therefore ATF3 as a transcription factor can either directly influence IL-1 transcription or indirectly via NLRP3 its secretion. Therefore, cytokine levels of IL-1β were analyzed, as well as transcription of *Atf3* and *Nlrp3* (Figure 19).

Treatment with TLR agonists resulted in an increase of *Il1b* mRNA (Figure 19a), while only a low amount of IL-1β was secreted (Figure 19b). Here a significant increase in BMDCs from *Il6* $^{-/-}$ mice compared to *wt* mice could be observed on both levels, even more pronounced on protein level.

ATF3 which might influence IL-1 transcription directly or via NLRP3 its secretion, showed no difference in the investigated knockout BMDCs (Figure 19c) only treatment with TLR agonists led to an increase of *Atf3* on transcriptional level. In contrast *Nlrp3* was differently regulated in the *Il6*$^{-/-}$ BMDCs, here a significant increase after treatment with LPS could be observed compared to *wt* BMDCs (Figure 19d).

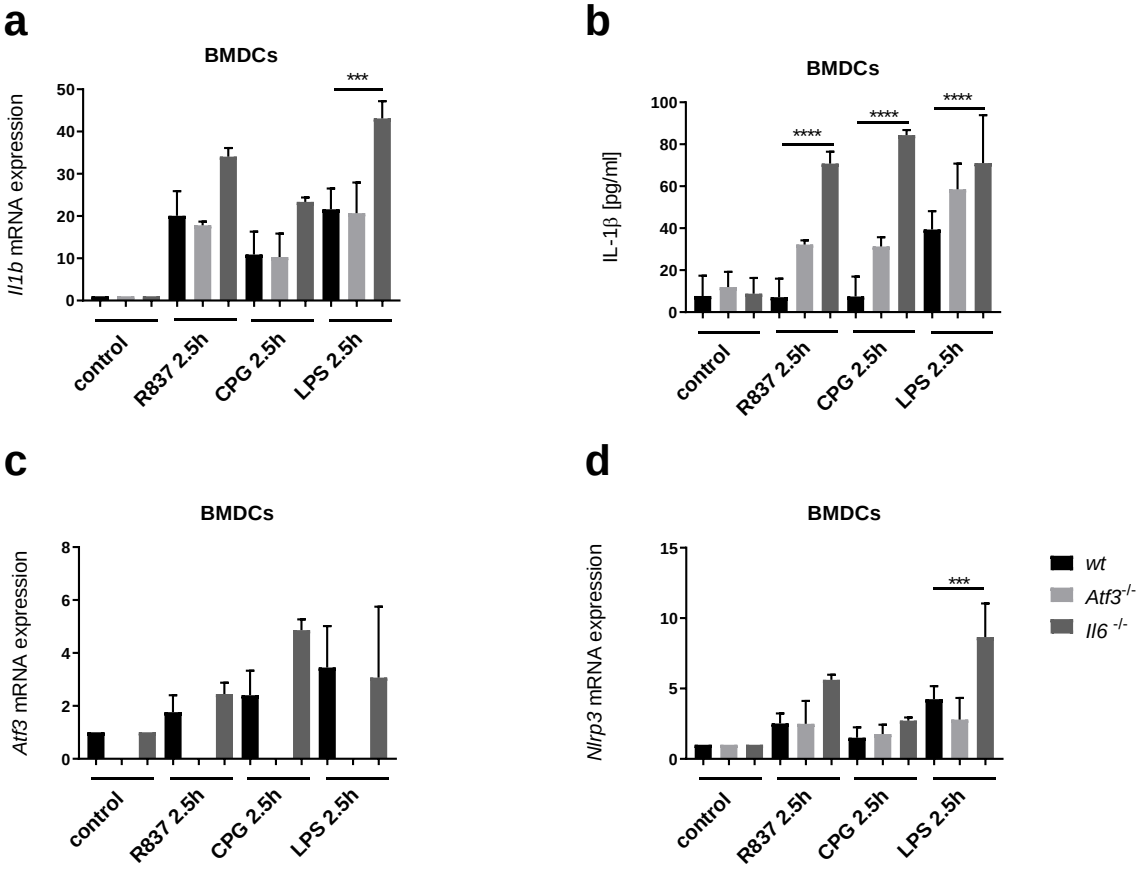

Figure 19: Differential induction of *Il1b* and *Nlrp3* in *Il6* $^{-/-}$ BMDCs. BMDCs out of *wt*, *Atf3*$^{-/-}$ and *Il6*$^{-/-}$ mice were treated with R837 (20µg/m), CPG (1µM) or LPS (100ng/ml) for 2.5 hours. Quantitative mRNA expression of **a** *Il1b*, **c** *Atf3* and **d** *Nlrp3* was measured by qRT-PCR. Secretion of **b** IL-1β was measured by ELISA. Significance is implicated by stars *: p<0.05; **: p<0.01; ***: p<0.001.

5.2.3 DMF-mediated suppression of IL-1β and IL-6 independently of ATF3 and IL-6

In human myeloid cells a DMF mediated suppression of IL-1β could be observed. To check whether this inhibition is dependent on ATF3 or IL-6 BMDCs were isolated form *wt*, *Atf3*$^{-/-}$ and *Il6*$^{-/-}$ mice and treated with LPS and ATP to activate inflammasome which results in a secretion of IL-1 and IL-6, shown in Figure 20.

Again *Il1b* and related *Nlrp3* were significantly increased in *Il6*$^{-/-}$ mice (Figure 20d-e). BMDCs were also pretreated with DMF and as seen before in human myeloid cells, DMF suppresses IL-1β and IL-6 on protein level (Figure 20d-e), as well as *Il6*, *Il1b* and *Nlrp3* on transcriptional level (Figure 20a-c). Therefore the effect seems to be independent of ATF3 and IL-6.

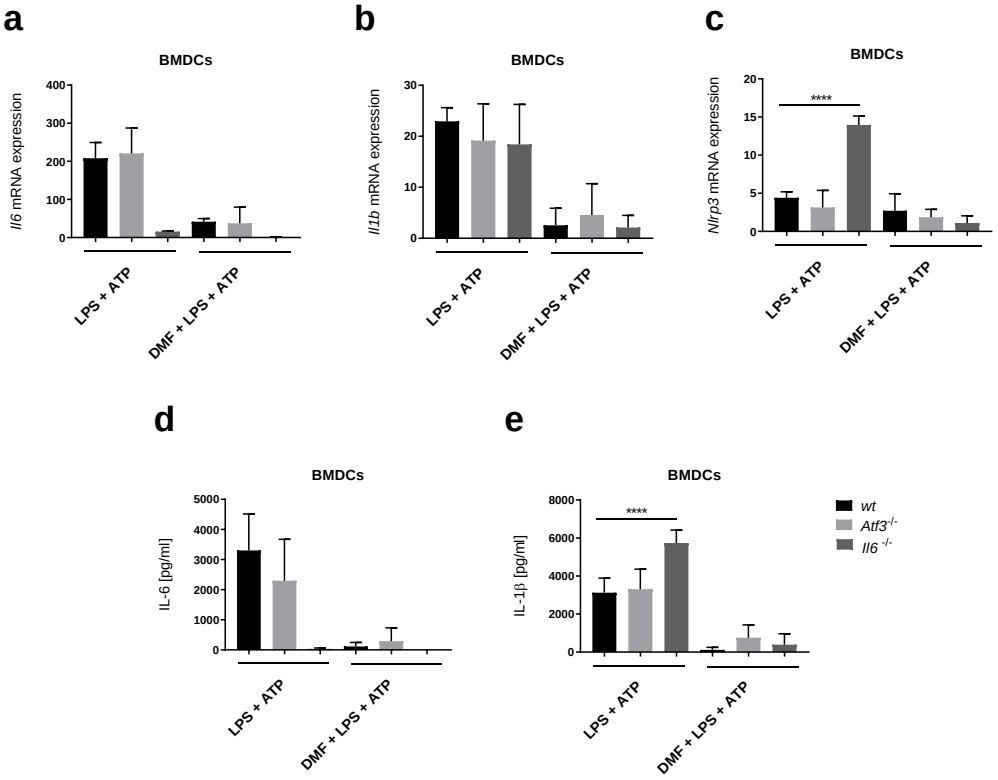

Figure 20: DMF-mediated suppression of IL-1β and IL-6 independently of ATF3 and IL-6. BMDCs were treated with 100ng/ml LPS (2h) and to activate the inflammasome additionally treated with 5mM ATP for 0.5 hours. Some cells were preincubated with 70µM DMF (2h). Quantitative mRNA expression of **a** *Il6*, **b** *Il1β* and **c** *Nlrp3* was measured by qRT-PCR. Protein secretion of **d** IL-6 and **e** IL-1β was measured by ELISA. Significance is implicated by stars *: p<0.05; **: p<0.01; ***: p<0.001.

5.3 Blocking of IL-1 receptor with Anakinra in BMDCs

5.3.1 Anakinra titration showed no effects on IL-1 in BMDCs

Because of the increased expression and secretion of IL-1 in *Atf3*$^{-/-}$ and *Il6*$^{-/-}$ BMDCs compared to *wt* BMDCs after treatment with different TLR ligands, Anakinra was used to block the IL-1α and IL-1β receptor. IL-1 is able to bind after its production to the IL-1 receptor where it then enhances again the production of IL-1. This feedback loop can be blocked by the IL-1 receptor agonist Anakinra.

BMDCs out of *wt*, *Atf3*$^{-/-}$ and *Il6*$^{-/-}$ mice were treated with different concentrations of Anakinra and cytokine expression and secretion was analyzed (Figure 21 - Figure 23).

Treatment with LPS as well as with LPS and ATP led to a slight induction of *Atf3* on mRNA level in *wt* as well as in *Il6*$^{-/-}$ BMDCs. While Anakinra showed no effect on *Atf3* (Figure 21a), as expected. *Il6* was only increased after treatment with LPS or a combination of LPS and ATP in *wt* and *Atf3*$^{-/-}$ BMDCs and Anakinra showed also no effects on *Il6* expression (Figure 21b). *Cxcl-1* was also increased after

treatment with the TLR ligands and no difference between the knockout and *wt* mice could be observed (Figure 21c).

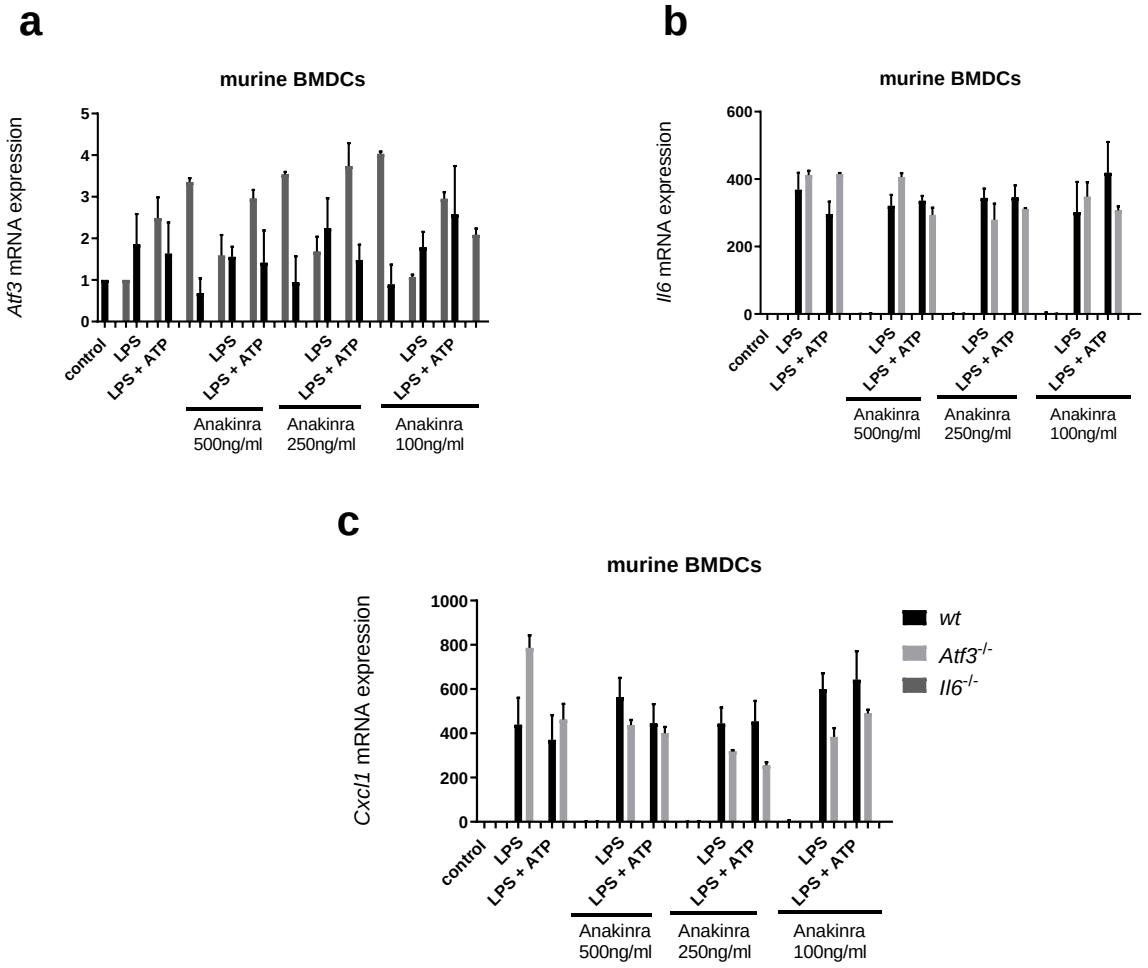

Figure 21: Blocking of IL-1 receptor with Anakinra showed no difference in *Atf3*, *Il6* and *Cxcl1* on mRNA expression. BMDCs were treated with 100ng/ml LPS (2h) and to activate the inflammasome additionally treated with 5mM ATP for 0.5 hours. Some cells were preincubated with Anakinra (500ng/ml, 250ng/ml or 100ng/ml) for 1 hour. Quantitative mRNA expression of **a** *Atf3*, **b** *Il6* and **c** *Cxcl1* was measured by qRT-PCR.

Treatment with LPS as well as with LPS and ATP led to an induction of *Il1a* on mRNA level in BMDCs that was not effected by Anakinra (Figure 22a). *Il1b* and *Nlrp3* were increased after treatment with LPS or a combination of LPS and ATP in BMDCs especially in *Il6*$^{-/-}$ BMDCs while Anakinra again showed no effect (Figure 22b-c).

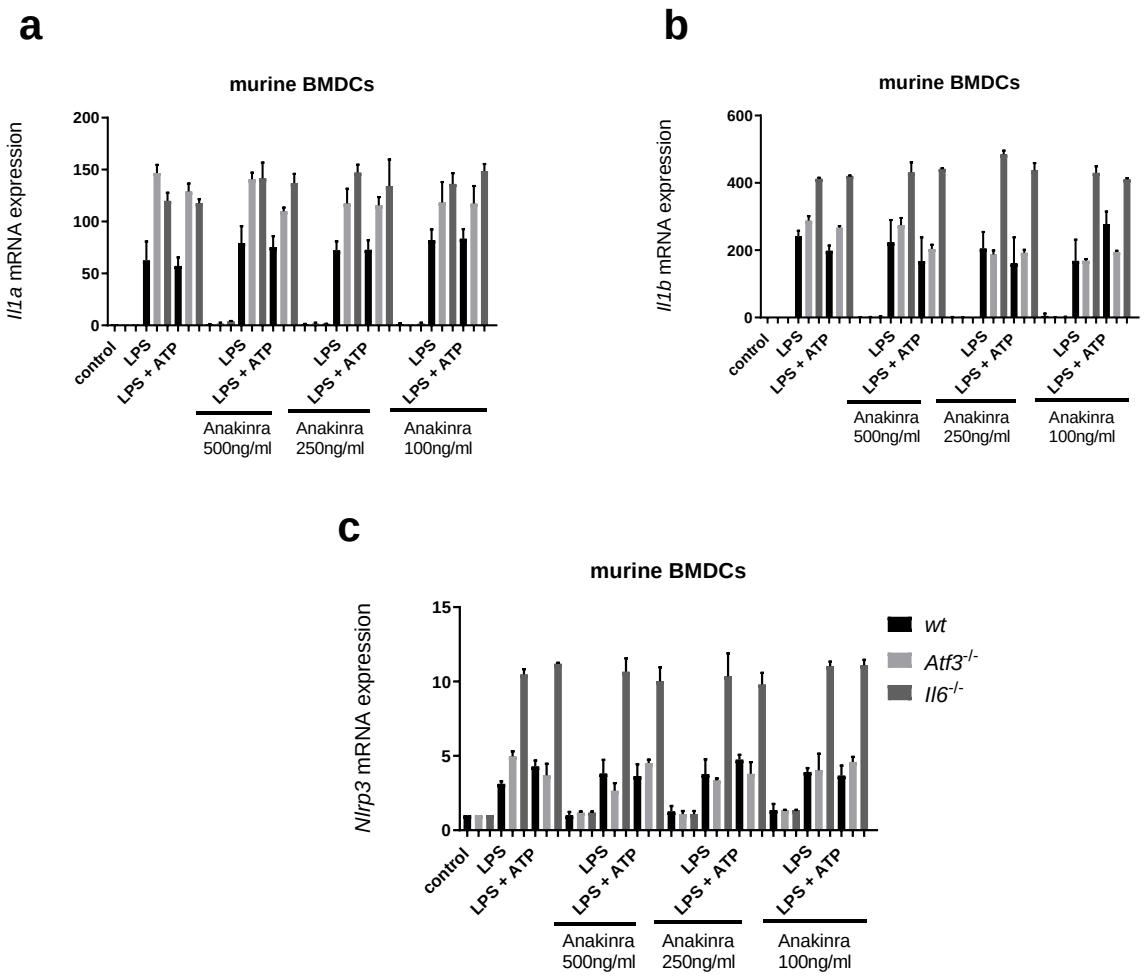

Figure 22: Blocking of IL-1 receptor with Anakinra showed no difference in *Il1* and *Nlrp3* on mRNA expression. BMDCs were treated with 100ng/ml LPS (2h) and to activate the inflammasome additionally treated with 5mM ATP for 0.5 hours. Some cells were preincubated with Anakinra (500ng/ml, 250ng/ml or 100ng/ml) for 1 hour. Quantitative mRNA expression of **a** *Il1a*, **b** *Il1b* and **c** *Nlrp3* was measured by qRT-PCR.

Analyzing the influence of Anakinra on protein level showed an induction of IL-1β and IL-6 after treatment with LPS and ATP like expected in BMDCs. While *Il6*$^{-/-}$ BMDCs showed a significant increase compared to *wt* BMDCs, but no influence of Anakinra on IL-1β or IL-6 protein production could be observed (Figure 23 a -b).

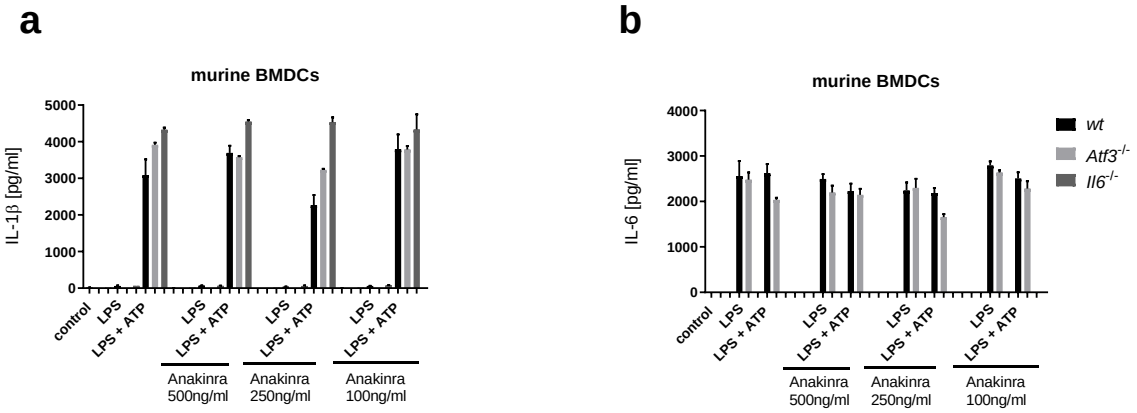

Figure 23: Blocking of IL-1 receptor with Anakinra showed no difference on IL-1β and IL-6 protein production. BMDCs were treated with 100ng/ml LPS (2h) and to activate the inflammasome additionally treated with 5mM ATP for 0.5 hours. Some cells were preincubated with Anakinra (500ng/ml, 250ng/ml or 100ng/ml) for 1 hour. Protein level of **a** IL-1β and **b** IL-6 was measured by ELISA.

5.3.2 Effect of LPS titration in combination with Anakinra

The missing effect of IL-1 receptor blocking may be due to an overload of LPS mediated IL-1. To evaluate a dose dependency, a titration of LPS was performed in *wt*, *Atf3*$^{-/-}$ and *Il6*$^{-/-}$ BMDCs.

BMDCs were treated with different concentrations of LPS in combination with ATP after treatment with Anakinra for one hour, shown in Figure 24-Figure 26.

mRNA expression of BMDCs treated with different concentrations of LPS, showed an increase of *Atf3* after treatment with LPS and ATP in *wt* BMDCs with also a slight increase of *Atf3* after treatment with Anakinra (Figure 24a). A dose dependent increase in *Il6* on mRNA level could be observed in *wt* and *Atf3*$^{-/-}$ BMDCs without any effects of Anakinra (Figure 24b). An increase of *Il6* in *Atf3*$^{-/-}$ BMDCs is due to the lack of *Atf3*. Having a look at the *Il1b* level an also dose dependent increase of *Il1* could be observed in all mice strains with a higher induction in *Atf3*$^{-/-}$ and *Il6* $^{-/-}$ BMDCs, but here no significant effect of Anakinra could be observed (Figure 24c).

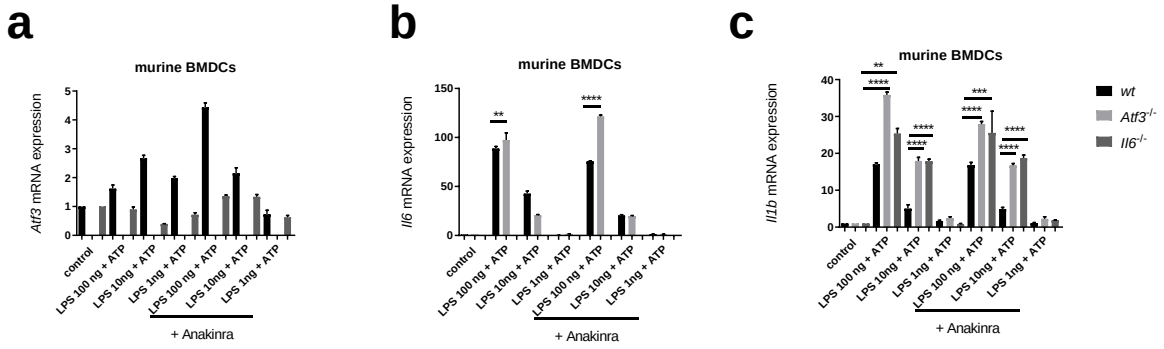

Figure 24: Titration of LPS and blocking of IL-1 receptor with Anakinra showed no difference in *Atf3*, *Il6* and *Il1* on mRNA expression. BMDCs were treated with 100ng/ml, 10ng/ml or 1ng/ml LPS (2h) and to activate the inflammasome additionally treated with 5mM ATP for 0.5 hours. Some cells were preincubated with Anakinra (250ng/ml) for 1 hour. Quantitative mRNA expression of **a** *Atf3*, **b** *Il6* and **c** *Il1b* was measured by qRT-PCR. Significance is implicated by stars *: p<0.05; **: p<0.01; ***: p<0.001.

IL-6 secretion was also dose dependently increased after the described treatment, both in *wt* and *Atf3*$^{-/-}$ BMDCs, which was not influenced by prior Anakinra exposure in *Atf3*$^{-/-}$ BMDCs (Figure 25). *Wt* BMDCs showed a slight decrease of IL-6 after Anakinra treatment.

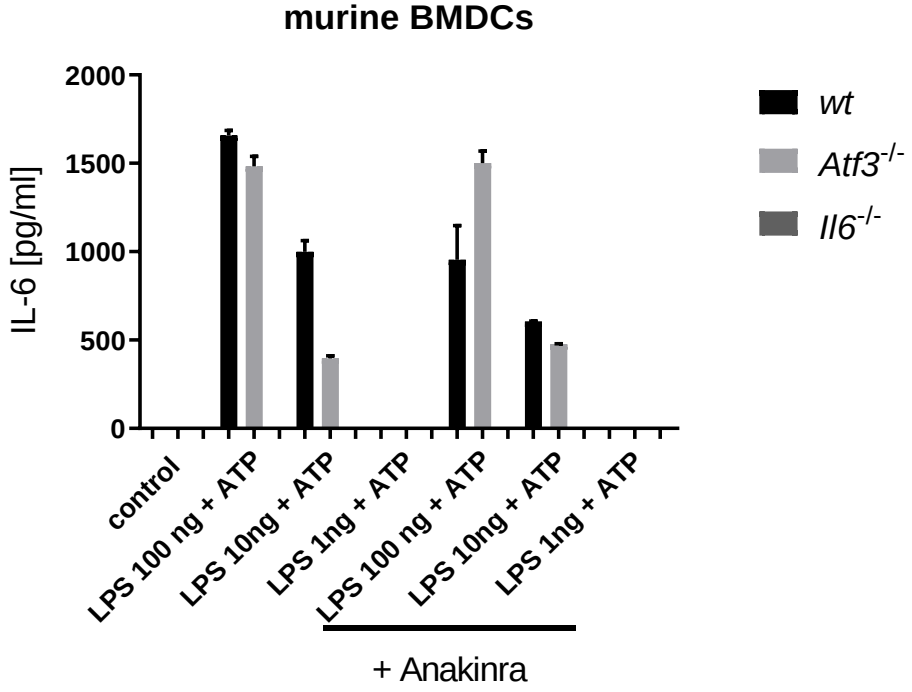

Figure 25: Titration of LPS and blocking of IL-1 receptor with Anakinra showed no difference in IL-6 secretion. BMDCs were treated with 100ng/ml, 10ng/ml or 1ng/ml LPS (2h) and to activate the inflammasome additionally treated with 5mM ATP for 0.5 hours. Some cells were preincubated with Anakinra (250ng/ml) for 1 hour. Protein level of IL-6 was measured by ELISA.

The titration of LPS showed first of all a dose dependent increase of IL-1β secretion in all BMDCs. This increase due to LPS treatment was significantly higher in *Atf3*$^{-/-}$ and *Il6*$^{-/-}$ BMDCs. Pretreatment with Anakinra showed only an effect in combination with LPS (10ng/ml), observing here a slight reduction of IL-1β secretion (Figure 26). This reduction could be observed in all BMDCs, suggesting that ATF3 and IL-6 have no influence on the effect of Anakinra.

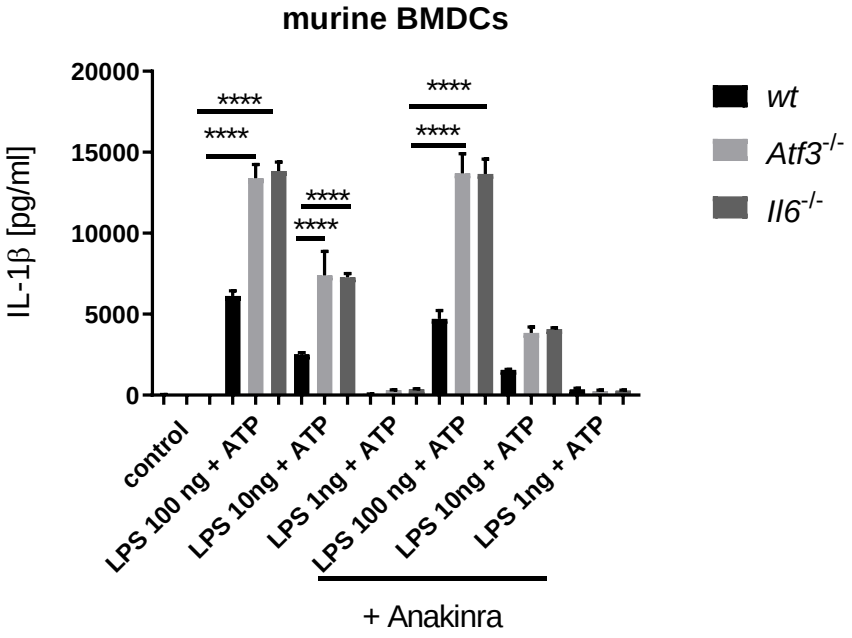

Figure 26: Dose dependent decrease of LPS-ATP-induced IL-1 secretion by Anakinra. BMDCs were treated with 100ng/ml, 10ng/ml or 1ng/ml LPS (2h) and to activate the inflammasome additionally treated with 5mM ATP for 0.5 hours. Some cells were preincubated with Anakinra (250ng/ml) for 1 hour. Protein level of IL-1β was measured by ELISA.

5.4 Differential induction of cytokines in *Atf3*$^{-/-}$ and *Il6*$^{-/-}$ keratinocytes

5.4.1 No difference of cytokine level in murine keratinocytes of *Il6* $^{-/-}$ mice after treatment with TLR ligands

In inflammatory skin diseases diverse cell types can be involved in the response of the immune system and its regulation. Therefore, beside BMDCs murine keratinocytes were investigated. To check

whether keratinocytes show the same behavior as BMDCs, keratinocytes were treated with different TLR ligands (Figure 27).

Wt and *Il6* $^{-/-}$ murine keratinocytes were treated with PMA for 4 and 16 hours to activate protein kinase C, with R837 for 2 and 4 hours to activate TLR7 and Poly (I:C) for 4 and 18 hours to activate TLR3.

The treatment with TLR agonists led to an increase of *Atf3* and *Cxcl1* on mRNA level in *wt* as well as in *Il6*$^{-/-}$ keratinocytes (Figure 27a, c). *Il6* was also induced after TLR treatment but as expected only in *wt* keratinocytes (Figure 27b). *Il1* and *Nlrp3* showed a slight increase after TLR treatment without any significant difference between the knockout strains (Figure 27d-f).

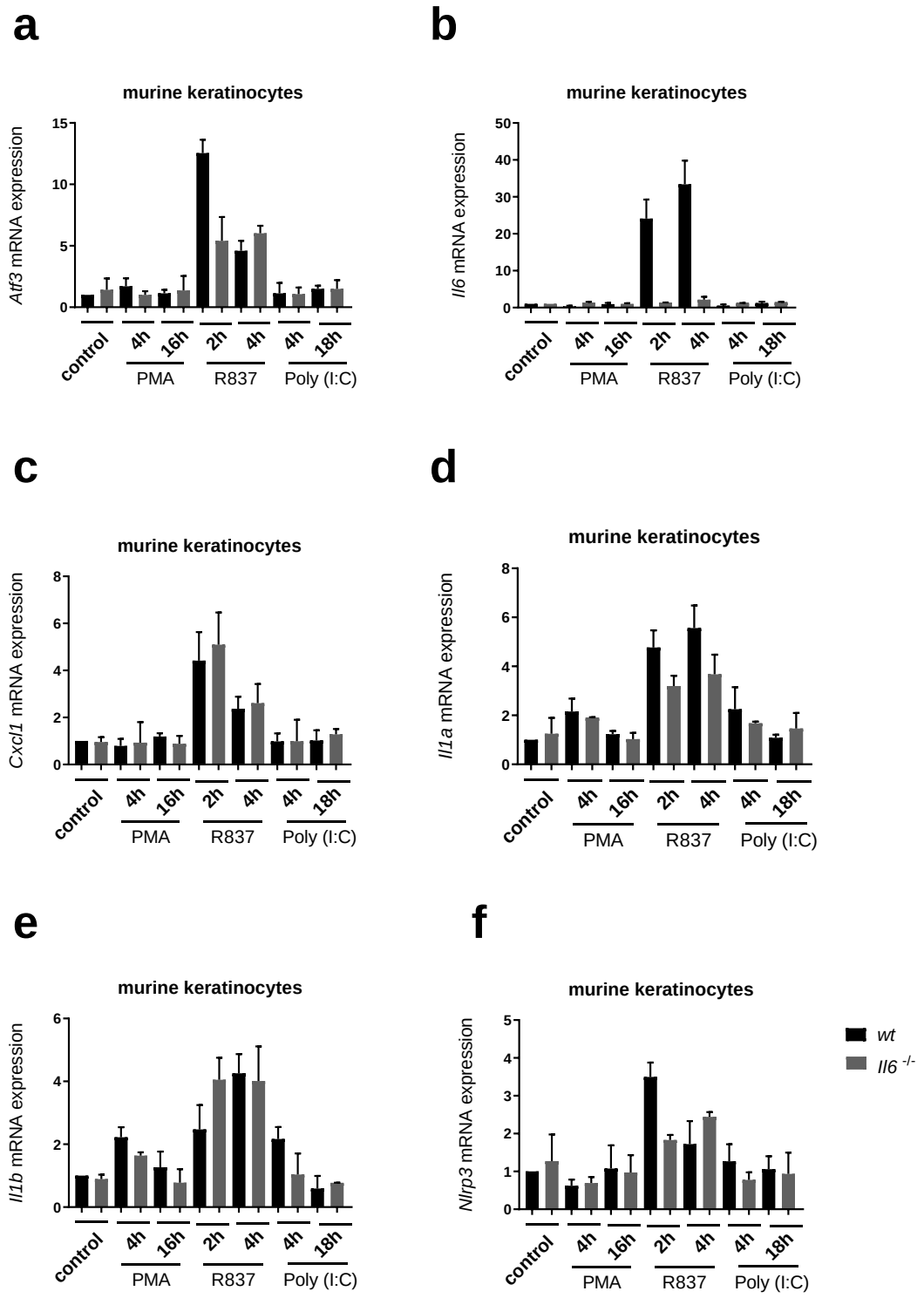

Figure 27: No impact of *Il6*-deficiency of *Atf3*, *Cxcl1*, *Il1a*, *Il1b* and f *Nlrp3* in keratinocytes after treatment with different TLR ligands. Murine keratinocytes out of *wt* and *Il6*$^{-/-}$ mice were treated with PMA (5µg/ml) for 4 and 16 hours, R837 (20µg/ml) for 2 and 4 hours and Poly (I:C) (10µg/ml) for 4 and 18 hours. Quantitative mRNA expression was measured by qRT-PCR for **a** *Atf3*, **b** *Il6*, **c** *Cxcl1*, **d** *Il1a*, **e** *Il1b* and **f** *Nlrp3*.

5.4.2 Different regulation of cytokines in murine *Atf3*$^{-/-}$ and *Il6*$^{-/-}$ keratinocytes after irradiation

As TLR activation showed no effect in murine keratinocytes, cells were activated with UVA and UVB irradiation. To check the viability of the cells after irradiation, an MTT assay was performed (Figure 28).

Cells were irradiated with UVA or UVB and then cultured for 4 or 24 hours. Murine keratinocytes were less viable after irradiation with UVB compared to exposure with UVA. After UVA irradiation viability was not altered between 4 or 24 hours, while cells were more sensitive to UVB treatment resulting in significant cell death.

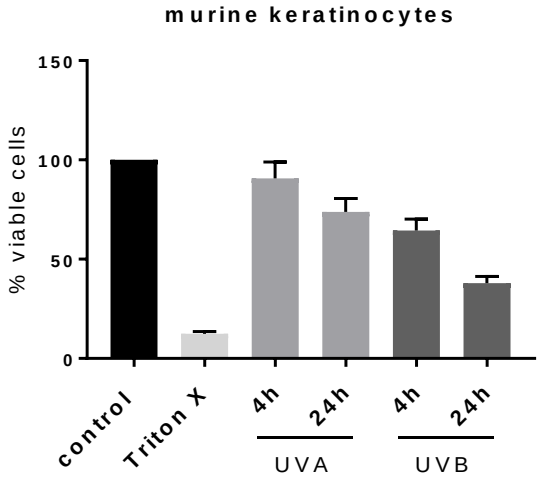

Figure 28: Viability of murine keratinocytes after irradiation. Murine keratinocytes were treated with UVA (5J/cm^2) or UVB (50mJ/cm^2) and further cultivated for 4 or 24 hours. As a positive control cells were treated with Triton X for 15 minutes. Viability was measured by MTT assay.

Because of the low viability of murine keratinocytes after treatment with UVB, cells were only treated with UVA and then analyzed after 4, 8 and 16 hours (Figure 29).

Treatment with UVA led to a slight increase of *Atf3* after 4 hours, with no difference between *Il6*$^{-/-}$ keratinocytes and *wt* keratinocytes (Figure 29a). Irradiation did not enhance *Il6* transcription, but the increase in *Atf3*$^{-/-}$ keratinocytes reached significance compared to *wt* (Figure 29b). UVA irradiation led to an increase of *Cxcl1*, *Il1a, Il1b* and related *Nlrp3* that peaked at 4 hours, which was significantly increased in *Atf3*$^{-/-}$ as well as *Il6*$^{-/-}$ keratinocytes compared to *wt* (Figure 29c-f).

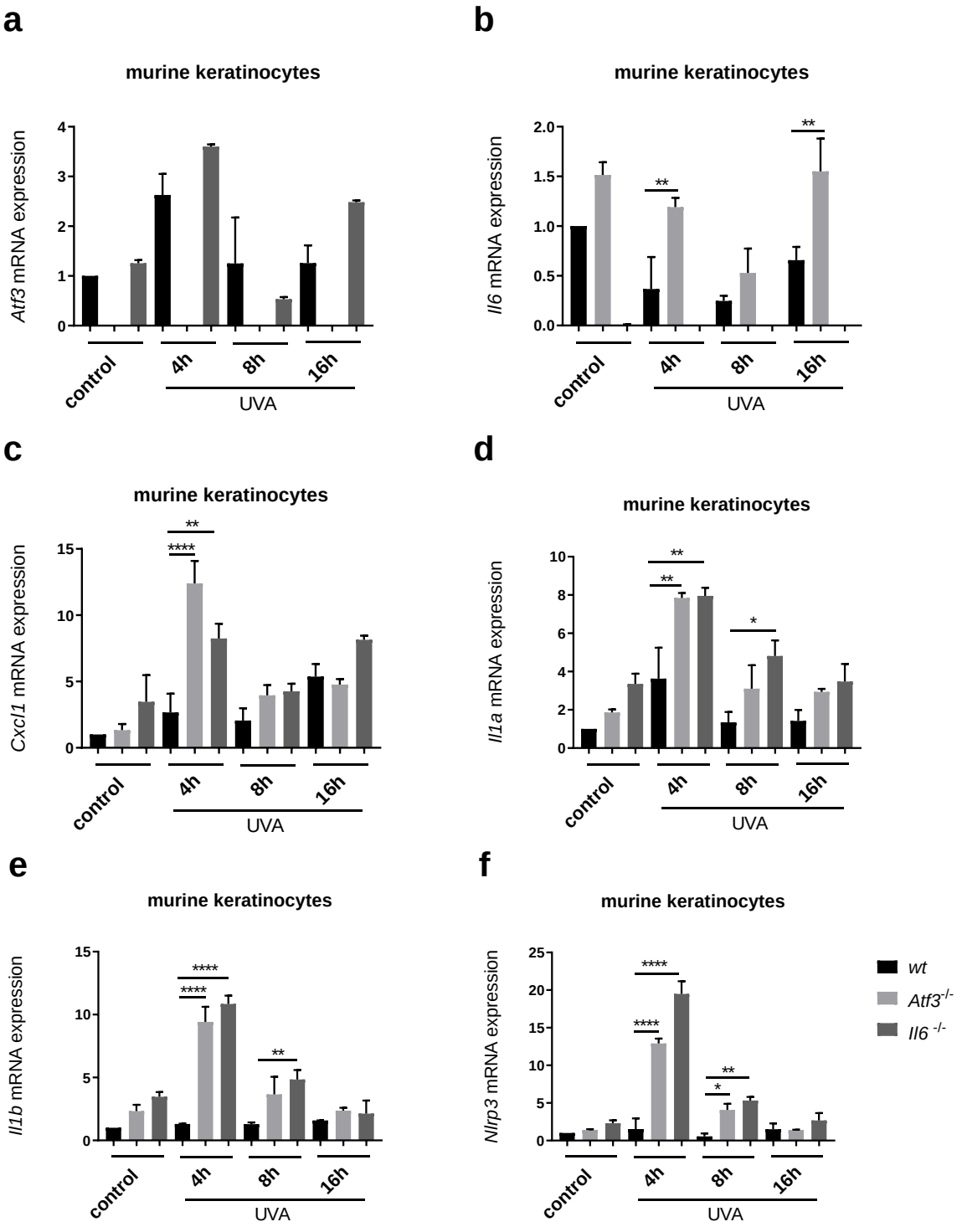

Figure 29: Differential regulation of cytokines and related genes in *Atf3*$^{-/-}$ and *Il6*$^{-/-}$ keratinocytes after irradiation. Murine *wt*, *Atf3*$^{-/-}$ and *Il6*$^{-/-}$ keratinocytes were treated with UVA (5J/cm^2) for the indicated time points. Quantitative mRNA expression was measured by qRT-PCR for **a** *Atf3*, **b** *Il6*, **c** *Cxcl1*, **d** *Il1a*, **e** *Il1b* and **f** *Nlrp3*. Significance is implicated by stars *: p<0.05; **: p<0.01; ***: p<0.001.

Evaluating the effect of UVA irradiation on protein secretion in murine keratinocytes, cells were treated as mentioned above (Figure 30).

UVA resulted in IL-1α secretion peaking at 8 hours. For each time point IL-1α was significantly increased in both *Atf3*$^{-/-}$ and *Il6*$^{-/-}$ keratinocytes compared to *wt* cells.

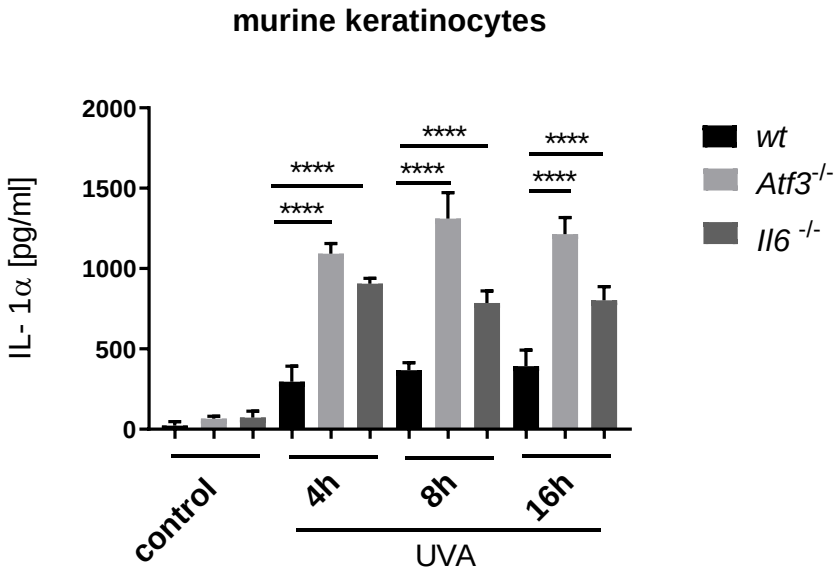

Figure 30: Differential protein production of IL-1α in *Atf3*$^{-/-}$ and *Il6*$^{-/-}$ keratinocytes after irradiation. Murine *wt*, *Atf3*$^{-/-}$ and *Il6*$^{-/-}$ keratinocytes were treated with UVA (5J/cm^2). After the indicated time points, the IL-1α protein level was detected by ELISA. Significance is implicated by stars *: p<0.05; **: p<0.01; ***: p<0.001.

Cells were pretreated with PMA to induce ATF3 and afterwards irradiated with UVA to activate the inflammasome (Figure 31).

To induce ATF3, cells were treated with PMA or irradiated with UVA or a combination of both. For *Atf3* an induction after UVA irradiation could be observed after 6 hours of about 2 fold, which was further increased after combined treatment, most prominently induced in *Il6*$^{-/-}$ keratinocytes about 5 fold (Figure 31a). *Il6* was super induced after a combined treatment, which was significantly increased in the *Atf3*$^{-/-}$ keratinocytes (Figure 31b). *Cxcl1*, *Il1a* and *Il1b* as well as *Nlrp3* induction after the combined treatment which was again significantly more prominent in the knockout keratinocytes compared to the *wt* keratinocytes (Figure 31c-f).

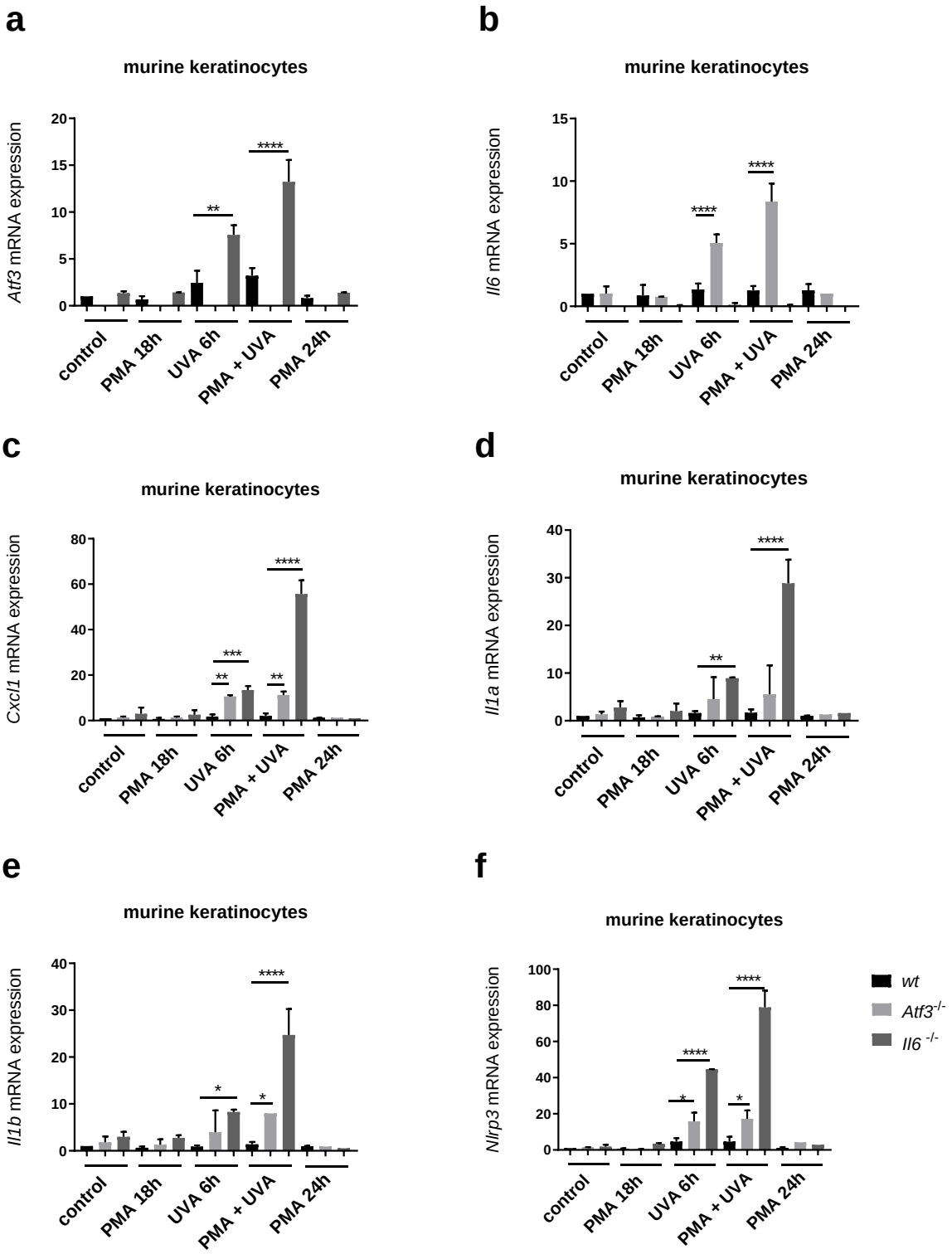

Figure 31: Stronger induction of *Atf3* after UVA irradiation in *Atf3*$^{-/-}$ and *Il6*$^{-/-}$ keratinocytes. Murine *wt*, *Atf3*$^{-/-}$ and *Il6*$^{-/-}$ keratinocytes were treated with PMA (10µg/ml) for 18/24 hours UVA light (5J/cm^2) for 6 hours or a combination of both (18 hours PMA + 6 hours UVA). Quantitative mRNA expression was measured by qRT-PCR

for **a** *Atf3*, **b** *Il6*, **c** *Cxcl1*, **d** *Il1a*, **e** *Il1b* and **f** *Nlrp3*. Significance is implicated by stars *: p<0.05; **: p<0.01; ***: p<0.001.

Regarding protein secretion after a combined treatment of PMA and UVA (Figure 32), IL-1α secretion was significantly stronger in the Atf3$^{-/-}$ keratinocytes compared to the *wt* cells.

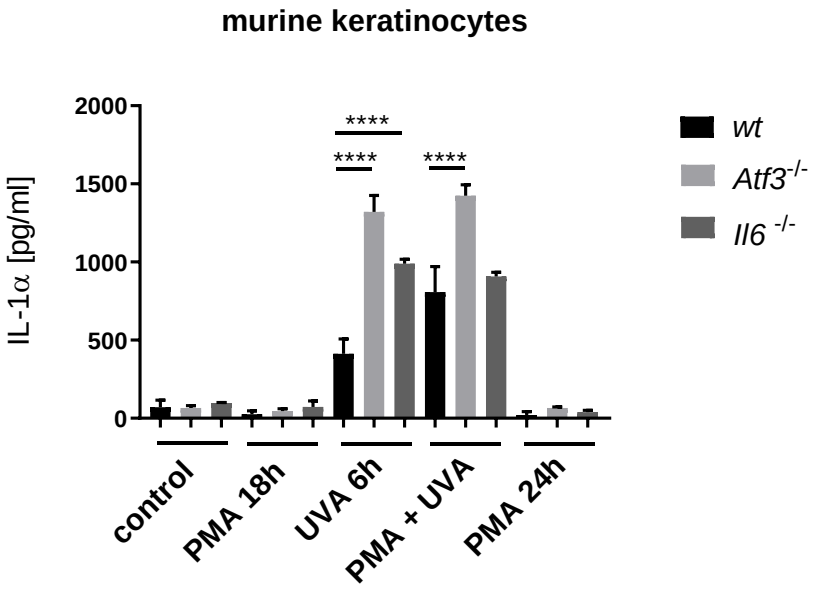

Figure 32: Increased IL-1α secretion after UVA irradiation in *Atf3*$^{-/-}$ and *Il6*$^{-/-}$ keratinocytes. *wt*, *Atf3*$^{-/-}$ and *Il6*$^{-/-}$ keratinocytes were treated with PMA (10µg/ml) for 18/24 hours UVA light (5J/cm^2) for 6 hours or a combination of both (18 hours PMA and after that 6 hours with UVA). Protein secretion was detected by ELISA for IL-1α. Significance is implicated by stars *: p<0.05; **: p<0.01; ***: p<0.001.

5.5 Response of human keratinocytes to UV irradiation

To check whether the effects after UV irradiation could also be observed in human keratinocytes, cells were treated with UVA or UVB light for 4 and 24 hours (Figure 33).

The viability of human keratinocytes was investigated by an MTT assay, here human keratinocytes showed a reduced viability after 24 hours of UVA or UVB irradiation (Figure 33a). The same effect could be observed by microscopy (Figure 33b), as half of the cells were dead after 24 hours of UVA treatment.

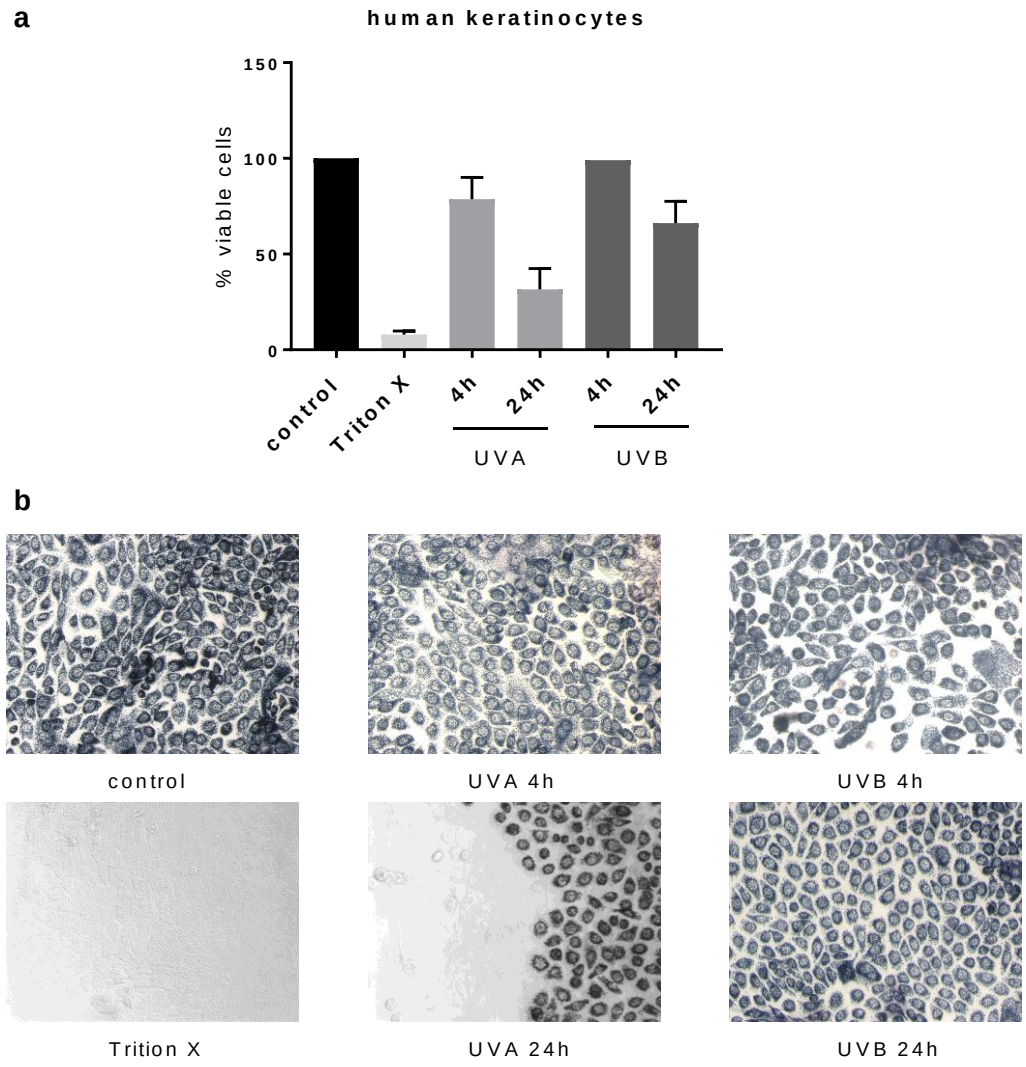

Figure 33: Viability of human keratinocytes after irradiation. Human keratinocytes were treated with UVA (5J/cm^2) or UVB (50mJ/cm^2) for 4 and 24 hours. As a positive control cells were treated with Triton X for 15 minutes. Viability was measured/analyzed by **a** MTT assay and **b** microscopically image.

Human keratinocytes showed a slight increase of *ATF3* after treatment with UVA irradiation which peaked at 4 hours, while response to UVB light was most pronounced at 8 hours (Figure 34a). UVA and less UVB irradiation increased *IL6* transcription (Figure 34b), similar to *CXCL8* (Figure 34c). *IL1A* and *IL1B* responded to both types of irradiation peaking after 4 and 8 hours (Figure 34d-e).

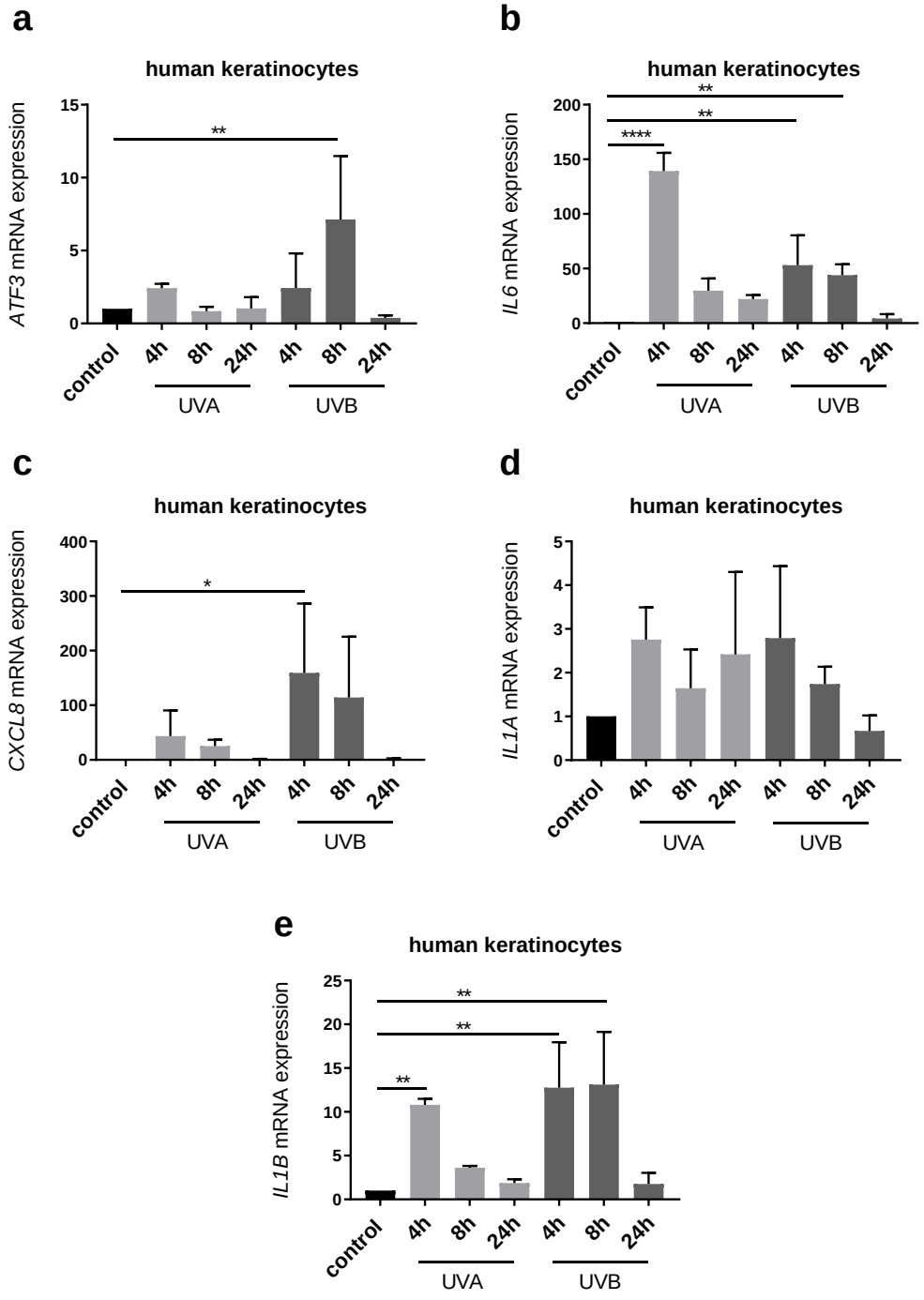

Figure 34: Response of human keratinocytes to irradiation. Human keratinocytes were treated with UVA (5J/cm^2) and UVB light (50mJ/cm^2) for the indicated time points. Quantitative mRNA expression was measured by qRT-PCR for **a** *ATF3*, **b** *IL6*, **c** *CXCL8*, **d** *IL1A* and **e** *IL1B*. Significance is implicated by stars *: p<0.05; **: p<0.01; ***: p<0.001.

Regarding protein secretion (Figure 35), human keratinocytes secreted high amounts of IL-1α after irradiation of UVA or UVB irradiation at all indicated time points (Figure 35a). A lower amount of IL-1β as well as IL-6 was secreted after irradiation with UVA or UVB light (Figure 35b-c).

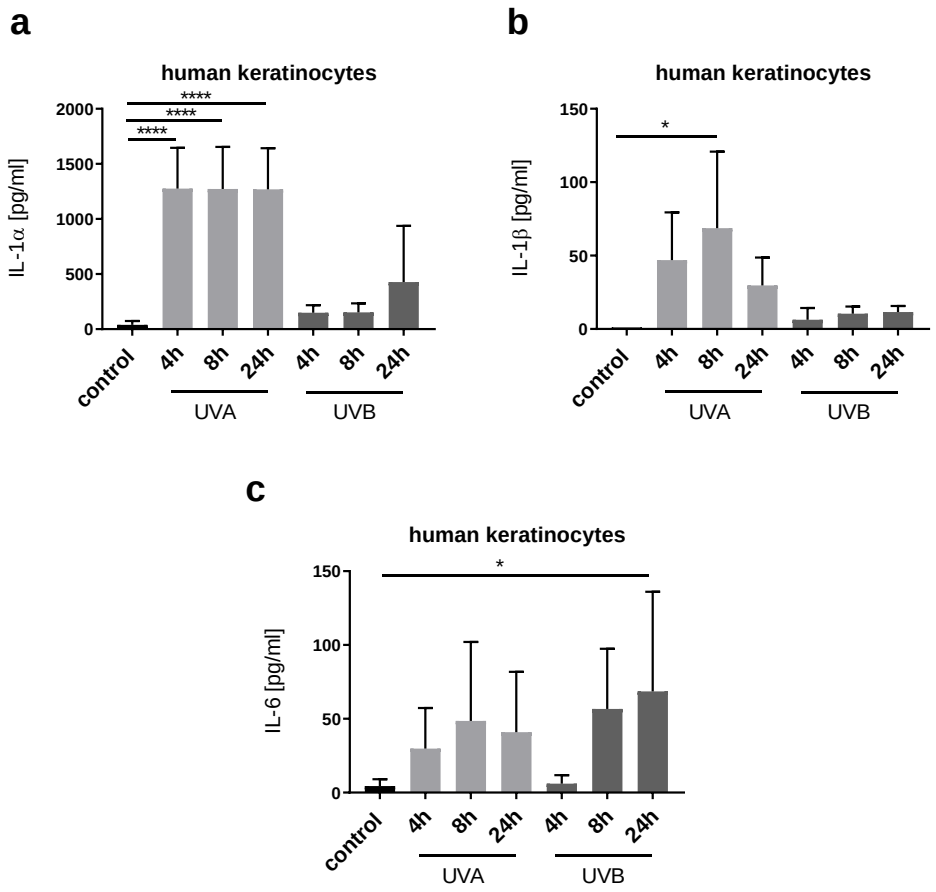

Figure 35: Protein secretion of human keratinocytes after irradiation. Human keratinocytes were treated with UVA (5J/cm^2) and UVB (50mJ/cm^2) for the indicated time points. Protein level was detected by ELISA for **a** IL-1α, **b** IL-1β and **c** IL-6. Significance is implicated by stars *: p<0.05; **: p<0.01; ***: p<0.001.

5.6 Silencing of ATF3 with siRNA in human keratinocytes

After treatment of murine *Atf3*$^{-/-}$ keratinocytes with UVA irradiation a different response compared to *wt* keratinocytes could be observed. To check whether the same effect of murine knockout keratinocytes can be observed in human cells, keratinocytes were transfected with siRNA targeting ATF3 and after 24 hours cells were activated with two different stimuli, as shown in Figure 36.

Transfecting the cells with siRNA and subsequent activating with either CsA or UVA irradiation led to an increase of *ATF3* in the control transfected cells, while the amount of *ATF3* in the *ATF3* knockdown cells was stronger reduced (Figure 36a). *IL6* was upregulated in cells treated with *ATF3* siRNA like expected and observed before in murine keratinocytes (Figure 36b). The basal level of *CXCL8* was

also increased after treatment with siRNA targeting *ATF3* (Figure 36c). The basal level of *IL1B* as well as related *NLRP1* and *NLRP3* are upregulated in the *ATF3* knockdown cells (Figure 36d-g). *IL1A* was increased in the knockdown cells compared to the control transfected cells after 4 hour of UVA irradiation. The same was observed for *IL1B, NLRP1* and *NLRP3* after UV irradiation, while here also the basal level of *IL1B, NLRP1* and *NLRP3* was higher in cells lacking *ATF3.*

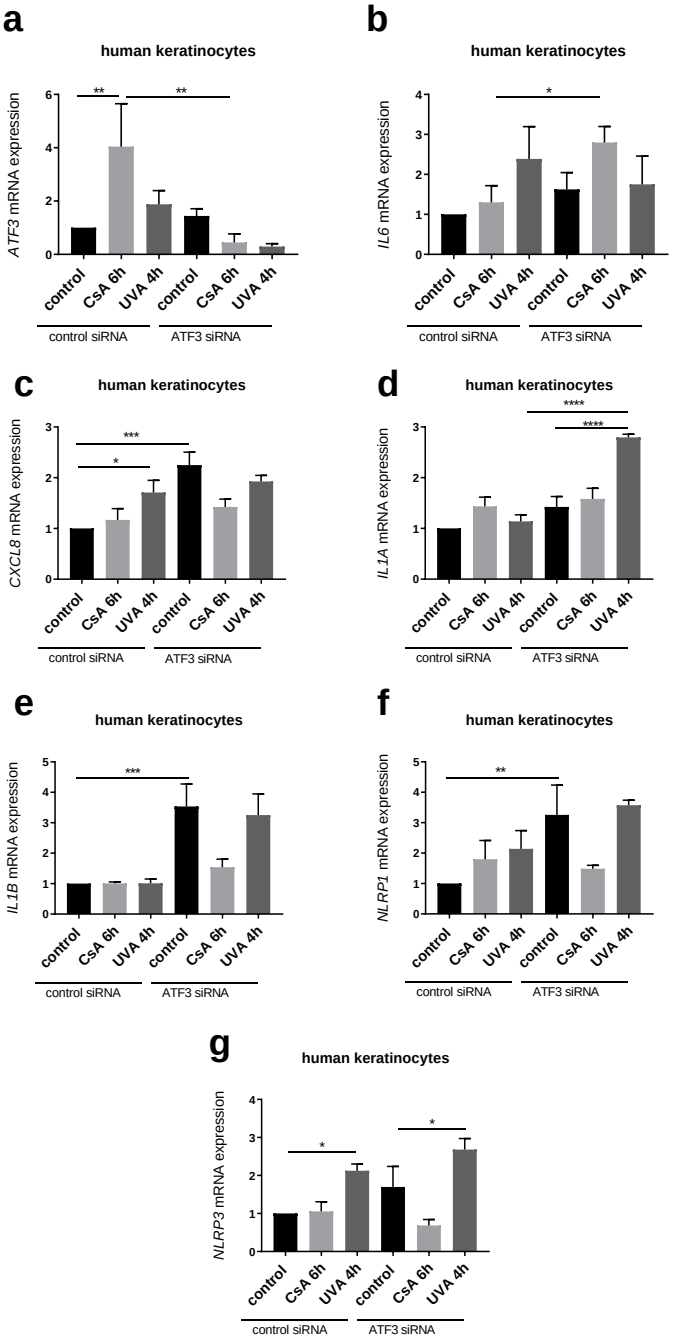

Figure 36: Different regulation after knockdown of *ATF3* with siRNA in human keratinocytes. Human keratinocytes were transfected with siRNA targeting *ATF3* or control transfection for 24 hours and then treated with CsA (10µM) for 6 hours or UVA (5J/cm^2) for 4 hours prior the RNA Isolation. Quantitative mRNA expression

was measured by qRT-PCR for **a** *ATF3*, **b** *IL6*, **c** *CXCL8*, **d** *IL1A*, **e** *IL1B*, **f** *NLRP1* and **g** *NLRP3*. Significance is implicated by stars *: p<0.05; **: p<0.01; ***: p<0.001.

Regarding protein secretion of the siRNA treated cells, differences could be observed, shown in Figure 37. Irradiation with UVA lead to an increase of IL-1α and IL-1β in the supernatant of the control as well as the *ATF3* knockdown cells, treatment with CsA showed no effect on IL-1 secretion. An increase of the IL-6 protein level was observed after CsA and UVA treatment.

SiRNA targeting *ATF3* showed an effect for IL-6 after irradiation with UVA, here a significant increase in the knockdown cells could be observed compared to control transfected cells (Figure 37c) also the basal level of IL-6 was higher in the *ATF3* transfected cells. While IL-1α and IL-1β showed no difference between the control and the siRNA *ATF3* keratinocytes (Figure 37a-b).

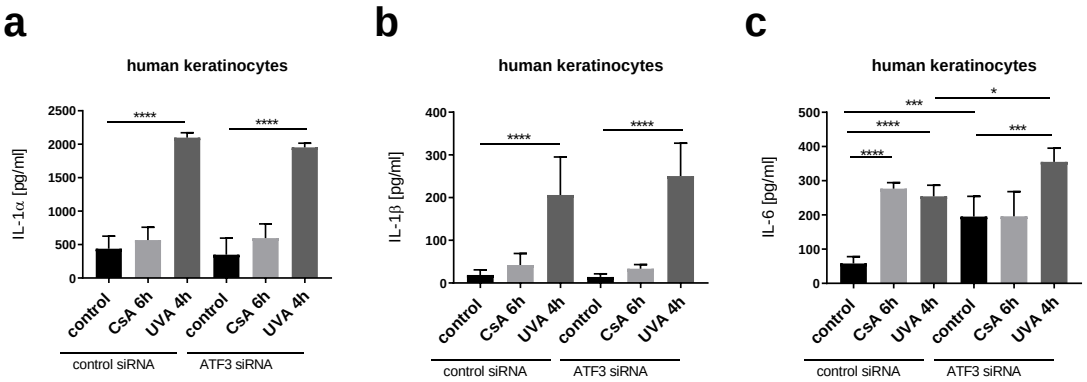

Figure 37: Differential induction after knockdown of ATF3 in keratinocytes only for IL-6 secretion. Human keratinocytes were transfected with siRNA for 24 hours and then treated with CsA (10µM) for 6 hours or UVA (5J/cm^2) for 4 hours prior the RNA isolation. Protein level was measured by ELISA **a** IL-1α, **b** IL-1β and **c** IL-6. Significance is implicated by stars *: p<0.05; **: p<0.01; ***: p<0.001.

5.7 TPA mouse model

5.7.1 Application of TPA

Application of TPA which activates protein kinase C (PKC) leads to an inflammatory hyperplasia in mice. Therefore *wt*, *Atf3*$^{-/-}$, *Il6*$^{-/-}$ and *Atf3*$^{-/-}$ x *Il6*$^{-/-}$ mice were treated with TPA or ethanol as a control on the ears for 5 days. At day 7 the mice were sacrificed and the samples for histology, RNA analysis and western blot analysis were taken.

Treatment with TPA for 5 days did not influence the weight of the animals in *wt*, *Atf3*$^{-/-}$ or *Il6*$^{-/-}$ or *Atf3*$^{-/-}$ x *Il6*$^{-/-}$ mice. Weight curves are shown in Figure 38.

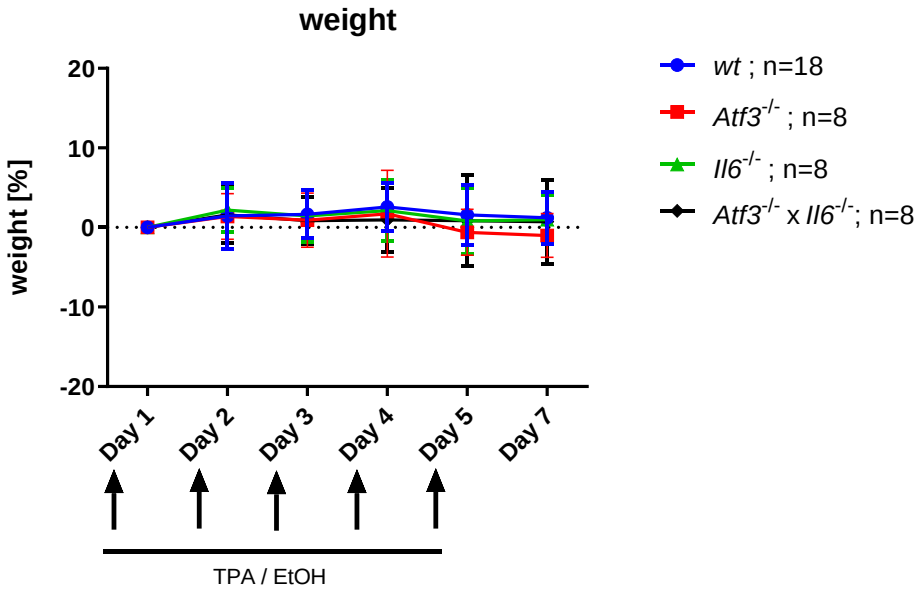

Figure 38: Weight curve during TPA application. *wt*, *Atf3*$^{-/-}$, *Il6*$^{-/-}$ and *Atf3*$^{-/-}$ x *Il6*$^{-/-}$ mice were treated with TPA (25µg/ml) on the right ear and Ethanol on the left ear for 5 days. Endpoint was on day 7. Shown is the change of the weight in percent over time.

The ear swelling of the animals, representing the level of inflammation, is shown in Figure 39. TPA led to an ear swelling which was most prominent in *wt* mice. While *Il6*$^{-/-}$, *Atf3* $^{-/-}$ and the *Atf3*$^{-/-}$ x *Il6* $^{-/-}$ mice showed strength of ear swelling after TPA treatment at the end of the experiment, ethanol treatment did not influence the ear swelling over the experiment.

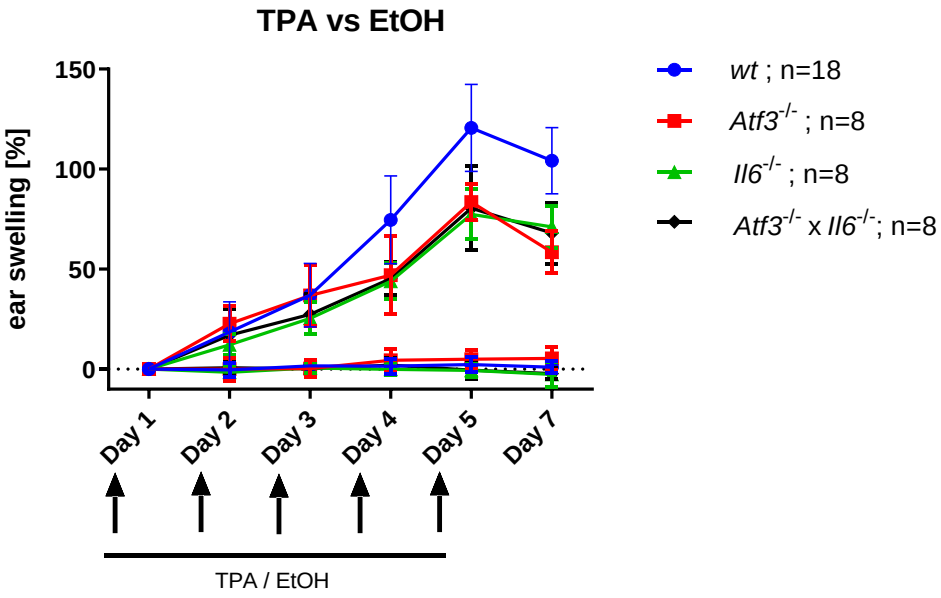

Figure 39: Ear swelling of *wt*, *Atf3* $^{-/-}$, *Il6*$^{-/-}$ and *Atf3*$^{-/-}$x*Il6*$^{-/-}$ mice after TPA application. *wt*, *Atf3*$^{-/-}$, *Il6*$^{-/-}$ and *Atf3*$^{-/-}$ x*Il6*$^{-/-}$ mice were treated with TPA (25µg/ml) on the right ear and ethanol on the left ear for 5 days. Endpoint was on day 7. Shown is the change of the ear swelling in percent over time.

For the analysis of the morphology and the characterization of the infiltrate histological stainings for HE (Figure 40), Ki67 (Figure 41), p53 (Figure 42) and Il1-β (Figure 43) were performed.

All genotypes showed no inflammation upon treatment with ethanol, while TPA treatment induced an inflammatory infiltrate and thickening of the epidermis in all mice. Differences between the manifestation of inflammation could be observed in the different genotypes. The most prominent thickening of the epidermis as well as the largest amount of inflammatory infiltrate was observed in *wt* mice. *Il6*$^{-/-}$ and *Atf3*$^{-/-}$ mice showed less thickening of the epidermis and a less pronounced inflammatory infiltrate. The epidermis of *Atf3*$^{-/-}$ x *Il6*$^{-/-}$ mice was thinner compared to the *wt* mice but infiltrate was observed more prominent than in *Il6*$^{-/-}$ and *Atf3*$^{-/-}$ mice (Figure 40).

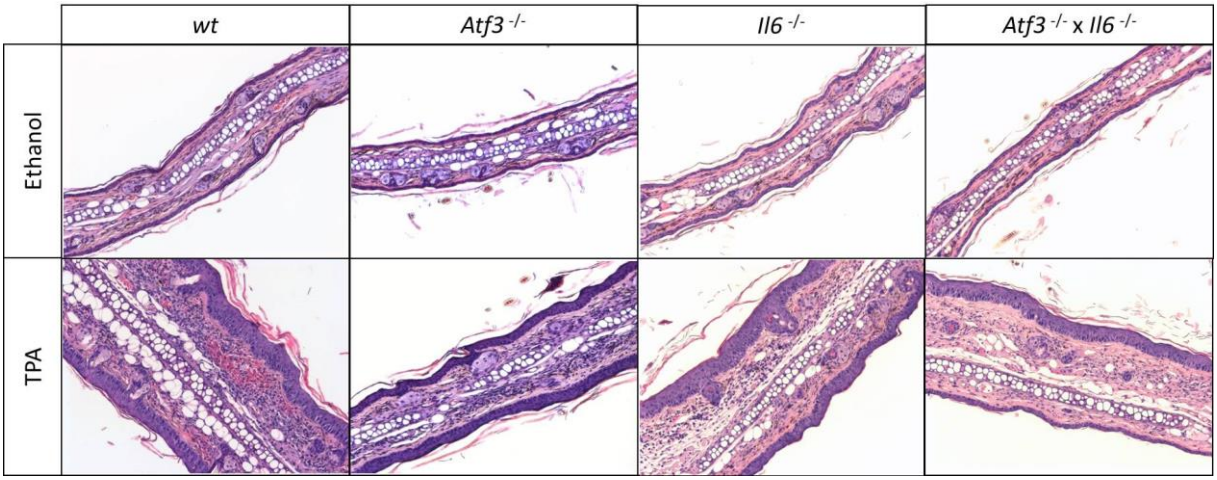

Figure 40: HE-staining of *wt*, *Atf3*$^{-/-}$, *Il6*$^{-/-}$ and *Atf3*$^{-/-}$x *Il6*$^{-/-}$ mice after TPA application.

The proliferation marker did not stain many cells in *Atf3*$^{-/-}$ mice treated with ethanol but TPA treatment increase the staining for Ki67 strongly. While *wt*, *Il6*$^{-/-}$ and *Atf3*$^{-/-}$x *Il6*$^{-/-}$ mice showed Ki67 labeled cells in ethanol as well as in TPA treated ears (Figure 41). Ki67 was strongly present in the infiltrate of all mice strains while no Ki67 was found in the epidermis.

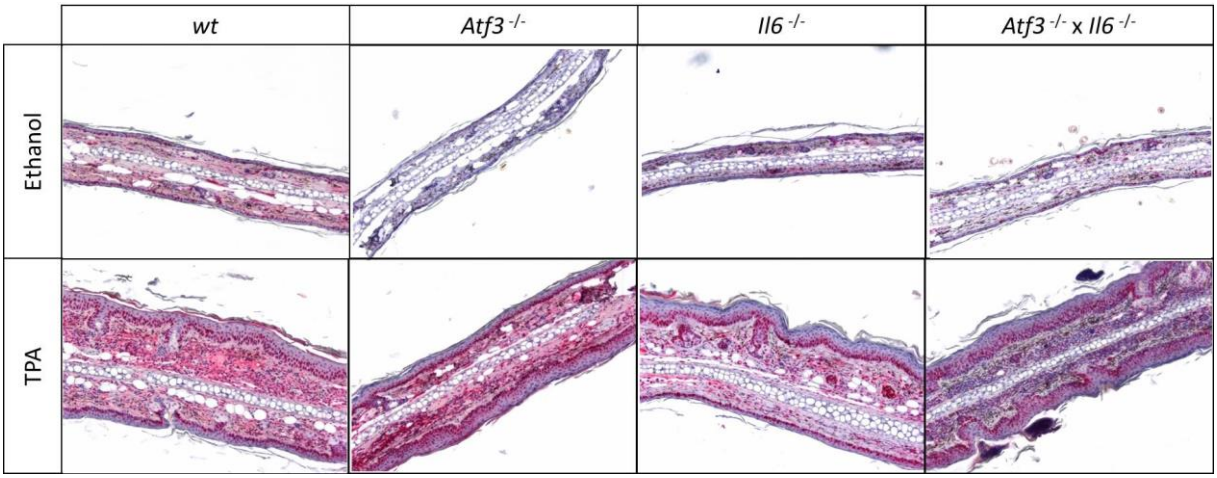

Figure 41: Ki67-staining of *wt*, *Atf3*$^{-/-}$, *Il6*$^{-/-}$ and *Atf3*$^{-/-}$x *Il6*$^{-/-}$ mice after TPA application.

Immunohistochemical staining for p53 is used as a surrogate for mutational analysis in the diagnostic workup of carcinomas of multiple sites including ovarian cancers (113). Strong and diffuse immune expression of p53 is generally interpreted as likely indicating a TP53 gene mutation (113). The amount of p53 was almost the same in *wt*, *Atf3*$^{-/-}$, *Il6*$^{-/-}$ and *Atf3*$^{-/-}$ x *Il6*$^{-/-}$ mice (Figure 42).

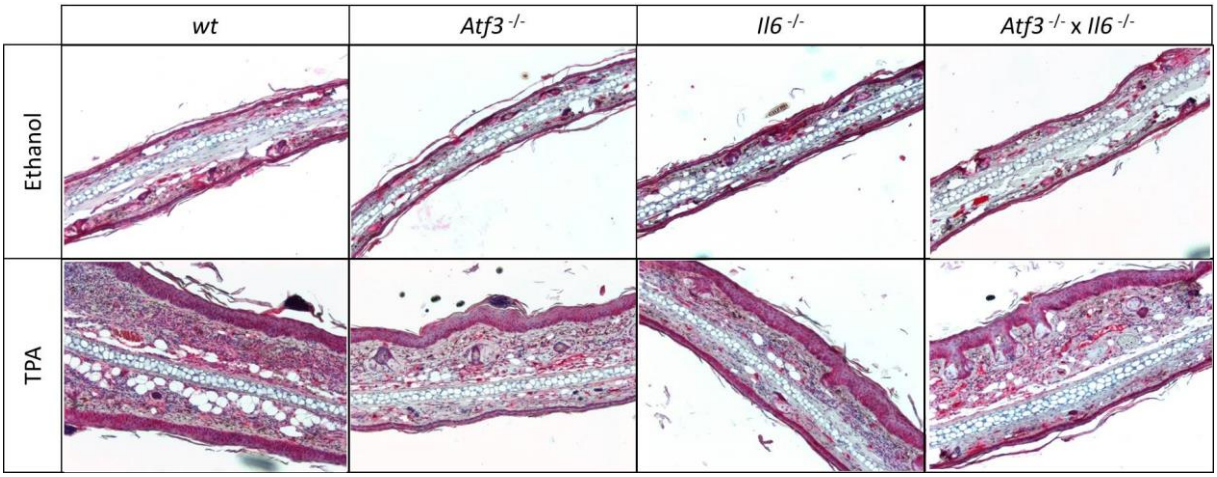

Figure 42: p53-staining of *wt*, *Atf3*$^{-/-}$, *Il6*$^{-/-}$ and *Atf3*$^{-/-}$x *Il6*$^{-/-}$ mice after TPA application.

An immunohistochemically staining for IL-1β was also performed (Figure 43). It showed that the amount of IL-1β in the tissue slices of the ears was increased in *Atf3* $^{-/-}$ and *Atf3*$^{-/-}$ x *Il6*$^{-/-}$ mice compared to *wt* mice. The *Il6* $^{-/-}$ showed almost the same amount of IL-1 like the *wt* mice.

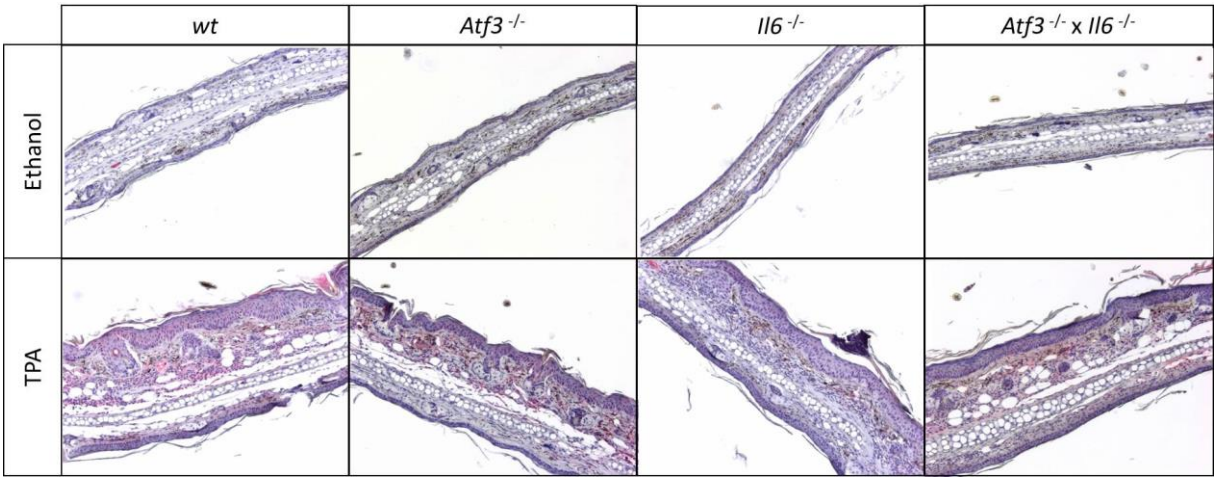

Figure 43: IL-1β-staining of *wt*, *Atf3*$^{-/-}$, *Il6*$^{-/-}$ and *Atf3*$^{-/-}$x *Il6*$^{-/-}$ mice after TPA application.

The mRNA profile of the ears after treatment with TPA is shown in Figure 44 - Figure 47 differences between the *wt* and knockout mice could be observed.

The activation of the protein kinase C after treatment with TPA did not impair *Atf3*-expression in *wt* and *Il6*$^{-/-}$ mice. As expected, no *Atf3* expression was detected in *Atf3*$^{-/-}$ and *Atf3*$^{-/-}$ x*Il6*$^{-/-}$ mice (Figure 44a). *Il6* was increased after treatment with TPA showing an inflammatory response in *wt* and significantly more in *Atf3*$^{-/-}$ mice (Figure 44b). *Cxcl1* was also induced by TPA significantly in *Atf3*$^{-/-}$ and *Atf3*$^{-/-}$x*Il6*$^{-/-}$ mice (Figure 44c).

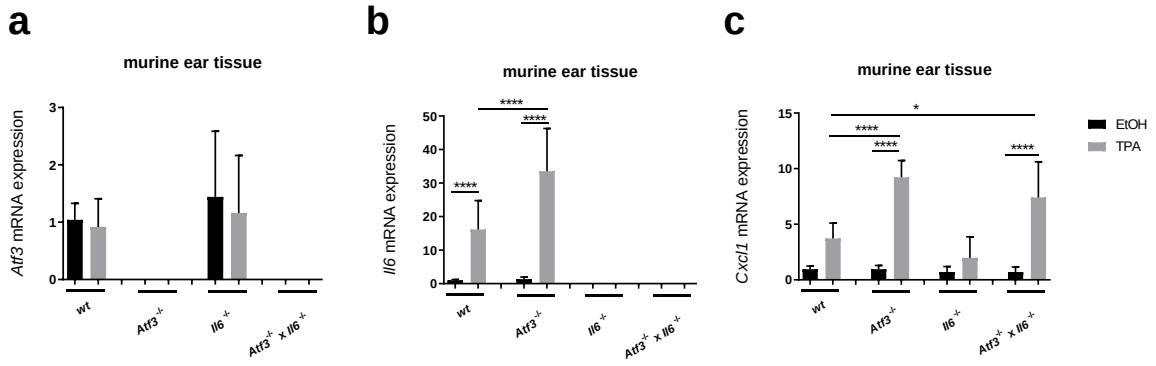

Figure 44: *Atf3*, *Il6* and *Cxcl*1 mRNA level of *wt*, *Atf3*$^{-/-}$, *Il6*$^{-/-}$ and *Atf3*$^{-/-}$x *Il6*$^{-/-}$ mice after TPA application. *wt*, *Atf3*$^{-/-}$, *Il6*$^{-/-}$ and *Atf3*$^{-/-}$x*Il6*$^{-/-}$ mice were treated with TPA (25µg/ml) on the right ear and ethanol on the left ear for 5 days. Endpoint was on day 7. Quantitative mRNA expression was measured by qRT-PCR for **a** *Atf3*, **b** *Il6* and **c** *Cxcl1*. Significance is given by stars *: p<0.05; **: p<0.01; ***: p<0.001.

Il1a and *Nlrp1* were not affected by TPA treatment (Figure 45a, c) while *Il1b* and *Nlrp3* were stronger augmented after treatment with TPA in all mice, while the *Atf3*$^{-/-}$ and *Atf3*$^{-/-}$x*Il6*$^{-/-}$ mice showed about 10 fold higher amounts of *Il1b*, like seen before also in the immunohistochemically staining, and *Nlrp3* was 2 fold induced (Figure 45b+d).

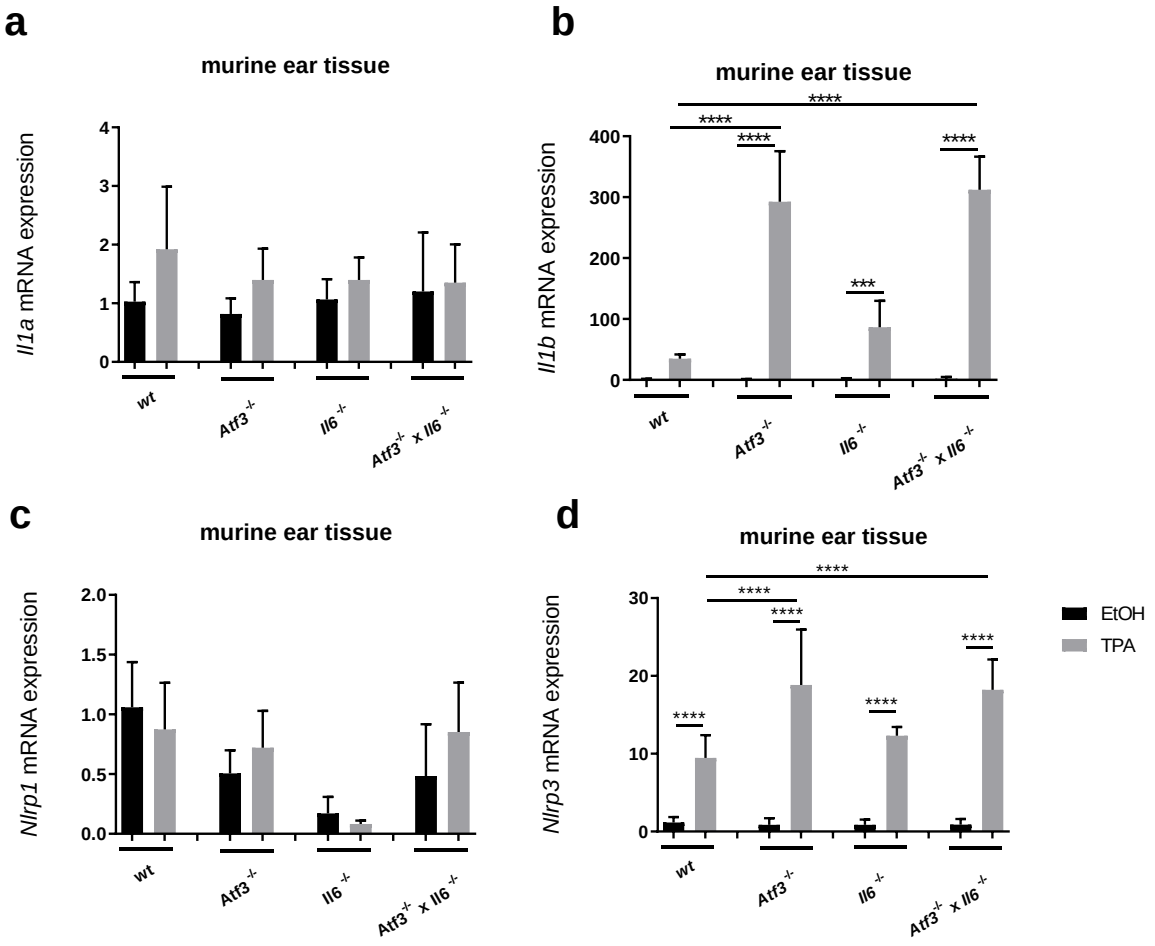

Figure 45: Cytokine profile *wt*, *Atf3*$^{-/-}$, *Il6*$^{-/-}$ and *Atf3*$^{-/-}$x *Il6*$^{-/-}$ mice after TPA application. *wt*, *Atf3*$^{-/-}$, *Il6*$^{-/-}$ and *Atf3*$^{-/-}$ x*Il6*$^{-/-}$ mice were treated with TPA (25µg/ml) on the right ear and ethanol on the left ear for 5 days. Endpoint was on day 7. Quantitative mRNA expression was measured by qRT-PCR for **a** *Il1a*, **b** *Il1b*, **c** *Nlrp1* and **d** *Nlrp3*. Significance is implicated by stars *: p<0.05; **: p<0.01; ***: p<0.001.

Because of the fact that besides pro- and anti-inflammatory cytokines also interferons are crucial for appropriate response to pathogens, damaged cells or irritants, we were also interested in Ifng and the related cytokines (114). However, *Ifng* and related cytokines *Cxcl9* and *Cxcl10* were not enhanced by treatment with TPA in any of the mice (Figure 46a-c).

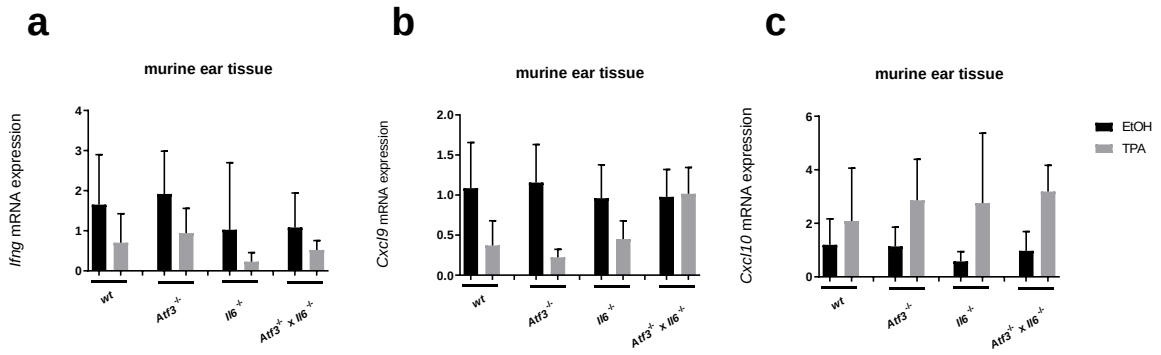

Figure 46: Interferon related genes in *wt*, *Atf3*$^{-/-}$, *Il6*$^{-/-}$ and *Atf3*$^{-/-}$x *Il6*$^{-/-}$ mice after TPA application. *wt*, *Atf3*$^{-/-}$, Il6$^{-/-}$ and *Atf3*$^{-/-}$x*Il6*$^{-/-}$ mice were treated with TPA (25µg/ml) on the right ear and ethanol on the left ear for 5 days. Endpoint was on day 7. Quantitative mRNA expression was measured by qRT-PCR for **a** *Ifng*, **b** *Cxcl9* and **c** *Cxcl10*.

As *Ifng* and related cytokines *Cxcl9* and *Cxcl10* showed no regulation between the *wt* and knockout mice, *Il2* and *Il4* were investigated after treatment with TPA. *wt* mice showed an increase of 10 fold after treatment with TPA for in *Il2* and *Il4.* All other knockout mice showed a significantly decrease in especially *Il2* and *Il4* about 10 fold for *Il2* compared to *wt* mice (Figure 47a+b).

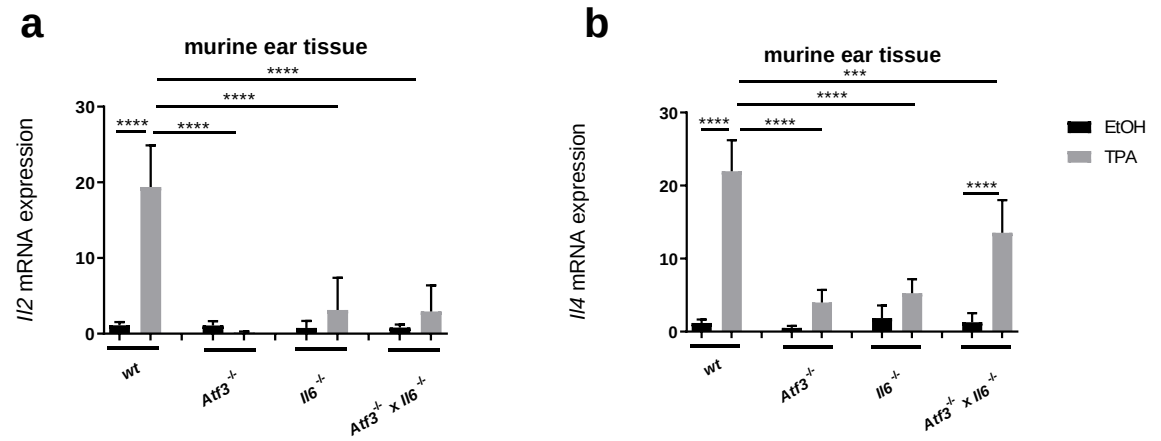

Figure 47: *Il2* and *Il4* level of *wt*, *Atf3*$^{-/-}$, *Il6*$^{-/-}$ and *Atf3*$^{-/-}$x *Il6*$^{-/-}$ mice after TPA application. *wt*, *Atf3*$^{-/-}$, *Il6*$^{-/-}$ and *Atf3*$^{-/-}$x*Il6*$^{-/-}$ mice were treated with TPA (25µg/ml) on the right ear and ethanol on the left ear for 5 days. Endpoint was on day 7. Quantitative mRNA expression was measured by qRT-PCR for **a** *Il2* and **b** *Il4*. Significance is implicated by stars *: p<0.05; **: p<0.01; ***: p<0.001.

In contrast to the T-cell associated cytokines, Nlrp3 and IL-1β were increased in wt, Atf3$^{-/-}$, Il6$^{-/-}$ and Atf3$^{-/-}$xIl6$^{-/-}$ mice, therefore a western blot for Nlrp3 and IL-1β was performed (Figure 48).

Here an increase of Nlrp3 protein after treatment with TPA could be observed in all mice stains. The western blot showed slightly more Nlrp3 on protein level in *Atf3*$^{-/-}$ and *Atf3*$^{-/-}$x*Il6*$^{-/-}$ mice. As a positive control BMDCs from *wt* mice were treated with LPS and ATP.

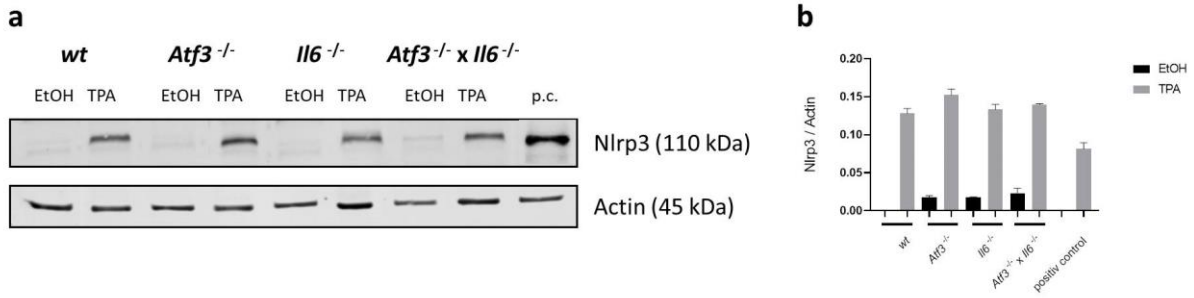

Figure 48: Nlrp3 western blot of *wt*, *Atf3*$^{-/-}$, *Il6*$^{-/-}$ and *Atf3*$^{-/-}$x *Il6*$^{-/-}$ mice after TPA application. *wt*, *Atf3*$^{-/-}$, *Il6*$^{-/-}$ and *Atf3*$^{-/-}$x*Il6*$^{-/-}$ mice were treated with TPA (25µg/ml) on the right ear and ethanol on the left ear for 5 days. Endpoint was on day 7. The same amount of protein from ear tissue of the mice was loaded into corresponding wells in each panel. Actin and Nlrp3 **a** detected and visualized by Western Blot and **b** quantitative analysis. As a positive control BMDCs from *wt* mice were treated with LPS (2h) and ATP (0.5h).

Also a western blot for IL-1β was performed shown in Figure 49. An increase on protein level of *pro-Il1b* after treatment with TPA in all mice strains could be observed. *Pro-Il1b* was super-induced in the *Atf3*$^{-/-}$ mice, confirming the results from the immunohistochemically staining and the mRNA expression level. The mature form of IL-1β could not be detected.

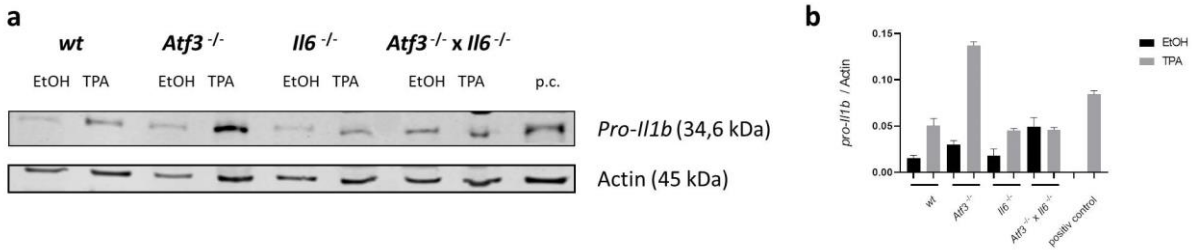

Figure 49: *Pro-Il1b* western blot of *wt*, *Atf3*$^{-/-}$, *Il6*$^{-/-}$ and *Atf3*$^{-/-}$x *Il6*$^{-/-}$ mice after TPA application. *wt*, *Atf3*$^{-/-}$, *Il6*$^{-/-}$ and *Atf3*$^{-/-}$x*Il6*$^{-/-}$ mice were treated with TPA (25µg/ml) on the right ear and ethanol on the left ear for 5 days. Endpoint was on day 7. The same amount of protein from ear tissue of the mice was loaded into corresponding wells in each panel. Actin and *pro-Il1b* were **a** detected and visualized by Western Blot and **b** quantitative analysis. As a positive control BMDCs from *wt* mice were treated with LPS (2h) and ATP (0.5h).

5.7.2 Application of TPA in IL-R1-antagonist (Anakinra) treated mice

As treatment with TPA implicated higher amounts or *Il1b* and *Nlrp3* RNA in *Atf3* $^{-/-}$, *Il6*$^{-/-}$ and *Atf3*$^{-/-}$x *Il6*$^{-/-}$ mice, we used Anakinra as an IL-1 receptor agonist to block IL-1 receptor signaling. *wt*, *Atf3* $^{-/-}$, *Il6*$^{-/-}$ and *Atf3*$^{-/-}$x *Il6*$^{-/-}$ mice were treated with TPA or ethanol on the ears for 5 days. On day 1, 3 and 5 a subgroup was additionally treated with Anakinra. At day 7 samples were taken for histology, RNA analysis and western blot analysis.

Treatment with TPA for 5 days upon IL-1R blockade again did not influence the weight of the animals in any genotype (Figure 50).

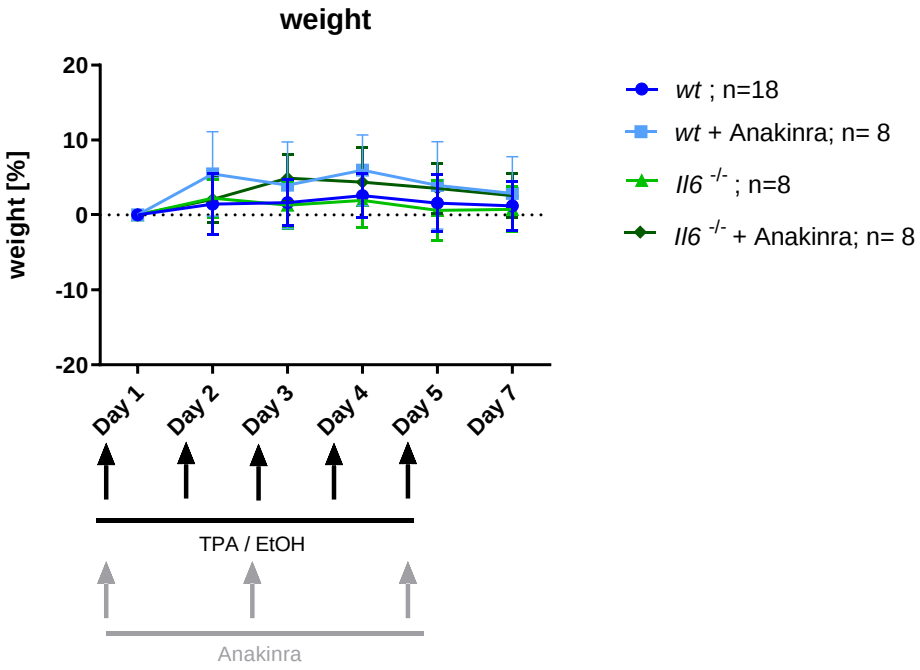

Figure 50: Weight curve over TPA application with additional treatment with Anakinra. *wt* and *Il6*$^{-/-}$ mice were treated with TPA (25µg/ml) on the right ear and ethanol on the left ear for 5 days. A subgroup was treated on day 1, 3 and 5 with Anakinra (i.p. 5mg/kg weight). Endpoint was day 7. Displayed is the change of the weight in percent over time.

The ear swelling of the animals, indicating the level of inflammation is shown in Figure 51.

TPA led to an ear swelling which was most prominent in *wt* mice. *Il6*$^{-/-}$ again showed less response to TPA treatment at the end of the experiment. Interestingly *wt* mice which were additionally treated with Anakinra showed less response to TPA treatment. While *Il6*$^{-/-}$ mice showed no change in the ear swelling response to treatment with Anakinra. Ethanol treated ears showed no change in the swelling over the experiment.

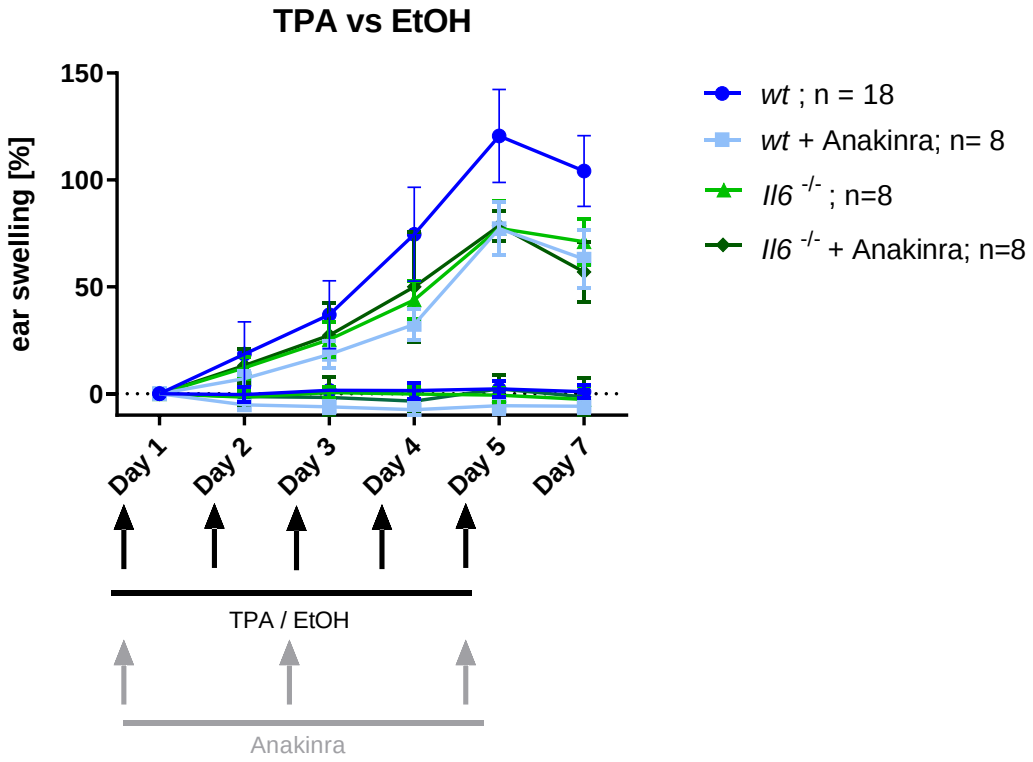

Figure 51: Ear swelling of *wt* and *Il6*$^{-/-}$ mice over TPA application with additional treatment with Anakinra. *wt* and *Il6*$^{-/-}$ mice were treated with TPA (25µg/ml) on the right ear and ethanol on the left ear for 5 days with or without additional treatment on day 1.3 and 5 with Anakinra (i.p. 5mg/kg weight). Endpoint was on day 7. Shown is the change of the ear swelling in percent over time.

To analyze this outcome closer, histological stainings were performed (Figure 52-Figure 55).

In the HE staining (Figure 52) all strains showed no inflammation upon treatment with ethanol, while TPA treatment leads to an inflammatory infiltrate and thickening of the epidermis in all mice. Differences between the levels of the inflammation could be observed in the different genotypes. The most prominent thickening of the epidermis as well as the highest amount of inflammatory infiltrate could be observed in *wt* mice as expected. Treatment with Anakinra led to less infiltrate in *wt* mice. Again, *Il6*$^{-/-}$ mice showed less thickening of the epidermis and less inflammatory infiltrate compared to *wt* mice but they showed no response to Anakinra treatment. Only the inflammatory infiltrate was slightly reduced in *Il6*$^{-/-}$ mice treated with Anakinra.

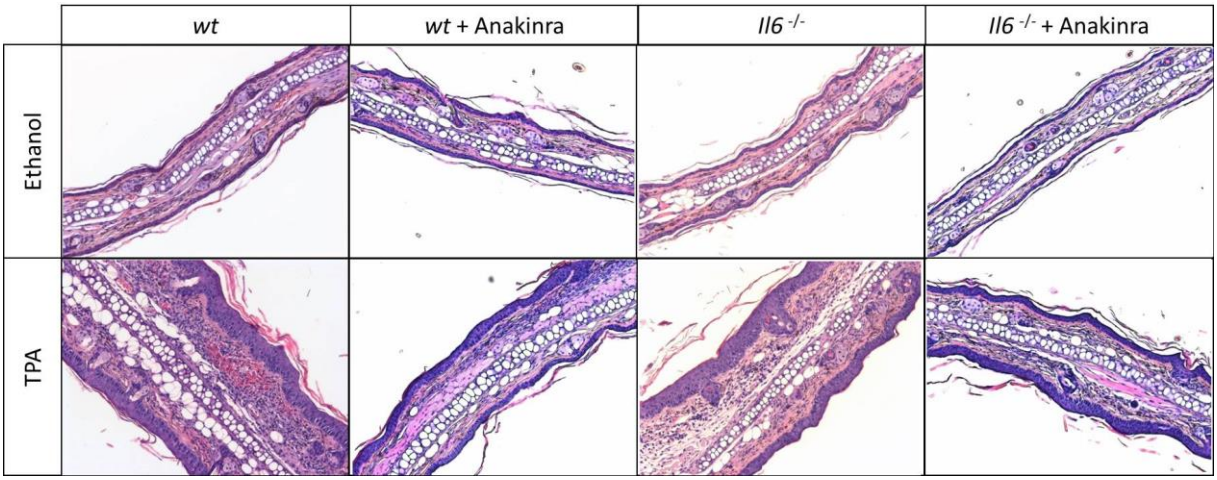

Figure 52: HE-staining of *wt* and *Il6*$^{-/-}$ mice after TPA application with additional treatment with Anakinra.

The proliferation marker Ki67 was not effected upon Anakinra treatment. In all mice strains the same amount of cells were labeled with Ki67 (Figure 53). Only *Il6*$^{-/-}$ mice treated with Anakinra showed slightly reduced Ki67 activity.

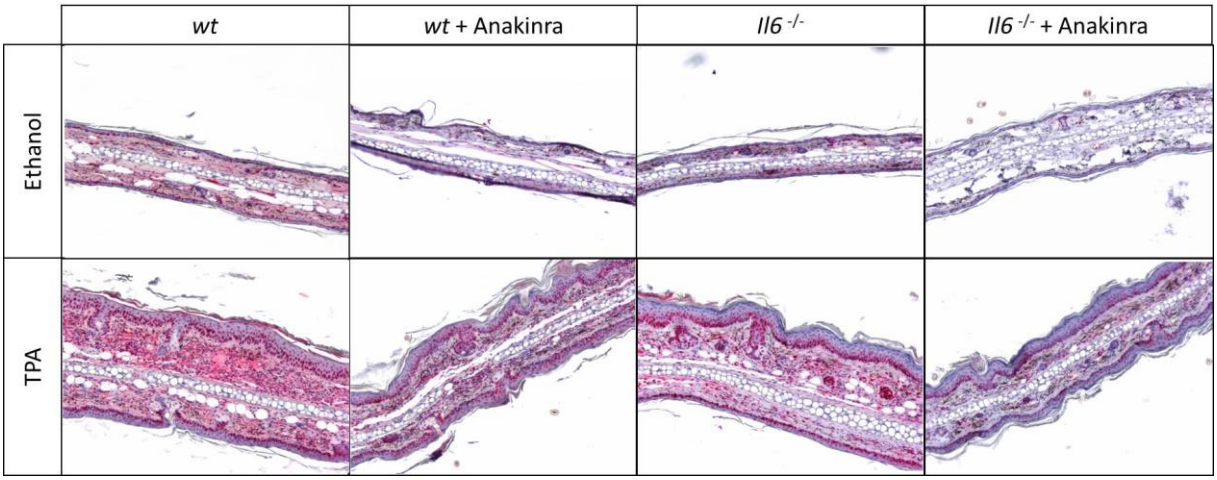

Figure 53: Ki67-staining of *wt* and *Il6*$^{-/-}$ mice after TPA application with additional treatment with Anakinra.

Immunohistochemical staining for p53 is used as a surrogate for mutational analysis in the diagnostic workup of carcinomas of multiple sites including ovarian cancers. Strong and diffuse immune expression of p53 is generally interpreted as likely indicating a TP53 gene mutation (113). The amount of p53 was the same in *wt* and *Il6*$^{-/-}$ mice after TPA treatment with or without Anakinra (Figure 54).

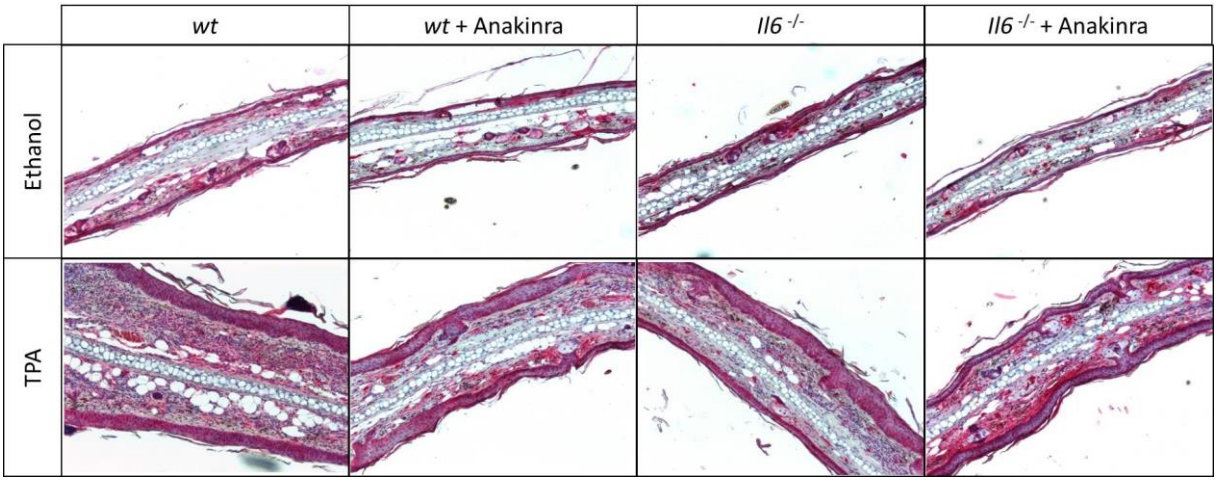

Figure 54: p53-staining of *wt* and *Il6*$^{-/-}$ mice after TPA application with additional treatment with Anakinra.

An immunohistochemically staining for IL-1β was also performed (Figure 55). Showing that the amount of IL-1β in the tissue slices of the ears was almost at the same level after the different treatments and in all mice strains.

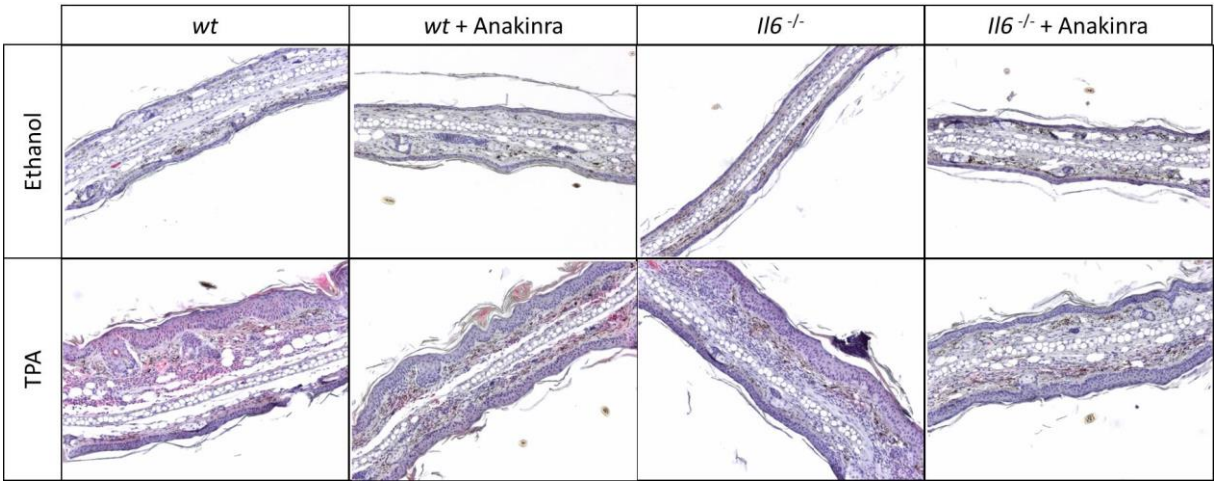

Figure 55: IL-1β-staining of *wt* and *Il6*$^{-/-}$ mice after TPA application with additional treatment with Anakinra.

The cytokine profile of the ears after treatment with TPA and Anakinra is shown in Figure 56-Figure 59.

The activation of the protein kinase C after treatment with TPA and the blocking of the IL1 receptor with Ankinra did not affect *Atf3* in *wt* or *Il6*$^{-/-}$ mice on mRNA level (Figure 56a). *Il6* was increased after treatment with TPA showing an inflammatory response in *wt* mice without additional Anakinra treatment. Interestingly *wt* mice which were treated with Anakinra showed a reduced expression of *Il6* mRNA after treatment with TPA, which was almost completely diminished (Figure 56b). *Cxcl1* was also increased after treatment with TPA but decreased in *wt* mice with were also treated with Anakinra, *Il6* mice$^{-/-}$ showed no effect to Anakinra (Figure 56c).

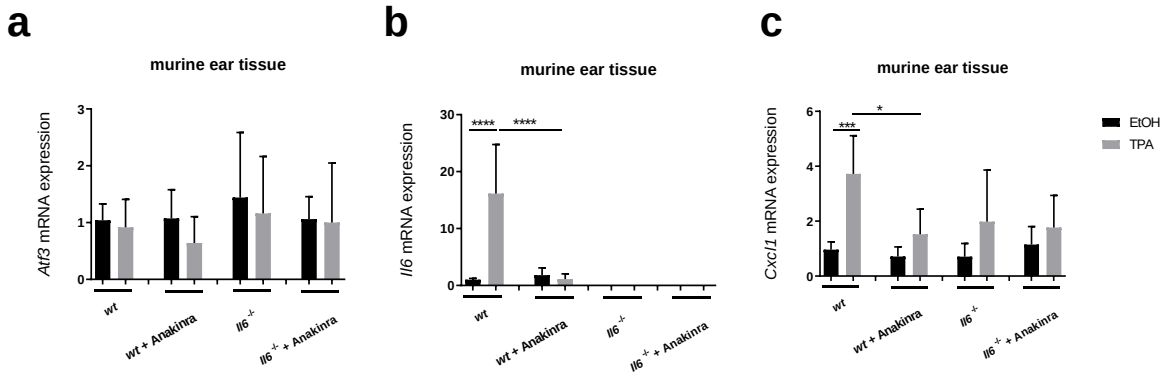

Figure 56: *Atf3*, *Il6* and *Cxcl1* level of *wt* and *Il6*$^{-/-}$ mice after TPA application with additional treatment with Anakinra. *wt* and *Il6*$^{-/-}$ mice were treated with TPA (25µg/ml) on the right ear and Ethanol on the left ear for 5 days, additional treatment on day 1.3 and 5 with Anakinra (i.p. 5mg/kg weight). Endpoint was on day 7. Quantitative mRNA expression was measured by qRT-PCR for **a** *Atf3*, **b** *Il6* and **c** *Cxcl1*. Significance is implicated by stars *: p<0.05; **: p<0.01; ***: p<0.001.

Il1a was not affected upon TPA or Anakinra treatment (Figure 57a) while *Il1b* and *Nlrp3* were stronger increased after treatment with TPA in all mice showing again an inflammatory response after TPA treatment. Again *Il6*$^{-/-}$ mice showed significantly higher amounts of *Il1b* and *Nlrp3* on mRNA compared to *wt* mice. Mice treated additionally with Anakinra showed less *Il1b* and *Nlrp3* in *wt* as well as in *Il6*$^{-/-}$ mice (Figure 57b+c).

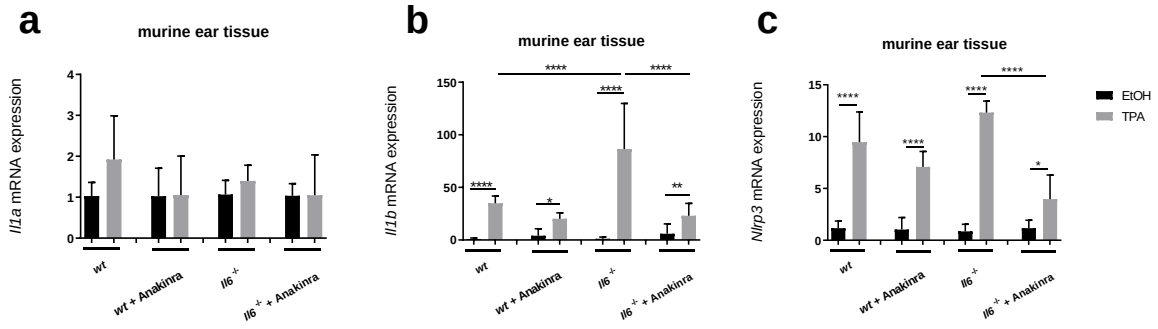

Figure 57: Cytokine profile of *wt* and *Il6*$^{-/-}$ mice after TPA application with additional treatment with Anakinra. *wt* and *Il6*$^{-/-}$ mice were treated with TPA (25µg/ml) on the right ear and Ethanol on the left ear for 5 days, additional treatment on day 1, 3 and 5 with Anakinra (i.p. 5mg/kg weight). Endpoint was on day 7. Quantitative mRNA expression was measured by qRT-PCR for **a** *Il1a*, **b** *Il1b* and **c** *Nlrp3*. Significance is implicated by stars *: p<0.05; **: p<0.01; ***: p<0.001.

Because of the fact that besides pro- and anti-inflammatory cytokines interferons are crucial for appropriate response to pathogens, damaged cells or irritants in inflammatory response, we were also

interested in Ifng and the related cytokines (114). But *Ifng* and related cytokines *Cxcl9* and *Cxcl10* were not affected after treatment with TPA or Anakinra in all mice (Figure 58a-c).

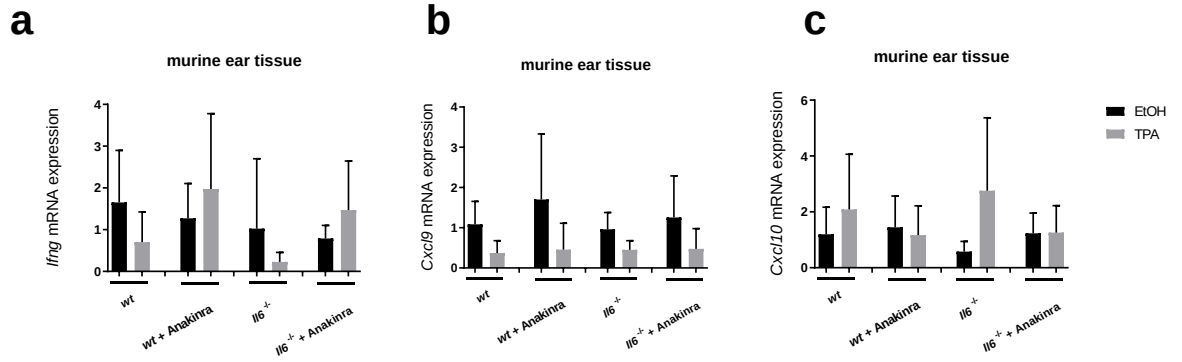

Figure 58: Interferon related genes of *wt* and *Il6*$^{-/-}$ mice after TPA application with additional treatment with Anakinra. *wt* and *Il6*$^{-/-}$ mice were treated with TPA (25µg/ml) on the right ear and Ethanol on the left ear for 5 days, additional treatment on day 1, 3 and 5 with Anakinra (i.p. 5mg/kg weight). Endpoint was on day 7. Quantitative mRNA expression was measured by qRT-PCR for **a** *Ifng*, **b** *Cxcl9* and **c** *Cxcl10*.

Analysis of the T-cell associated cytokines *Il2* and *Il4* after treatment with TPA showed an increase in most prominent in *wt* mice, in *Il6*$^{-/-}$ mice *Il2* and *Il4* were almost completely abolished. With additional Anakinra treatment a decrease of about 10 fold in *Il2* and *Il4* could also be observed in *wt* mice compared to treatment only with TPA (Figure 59a + Figure 59b).

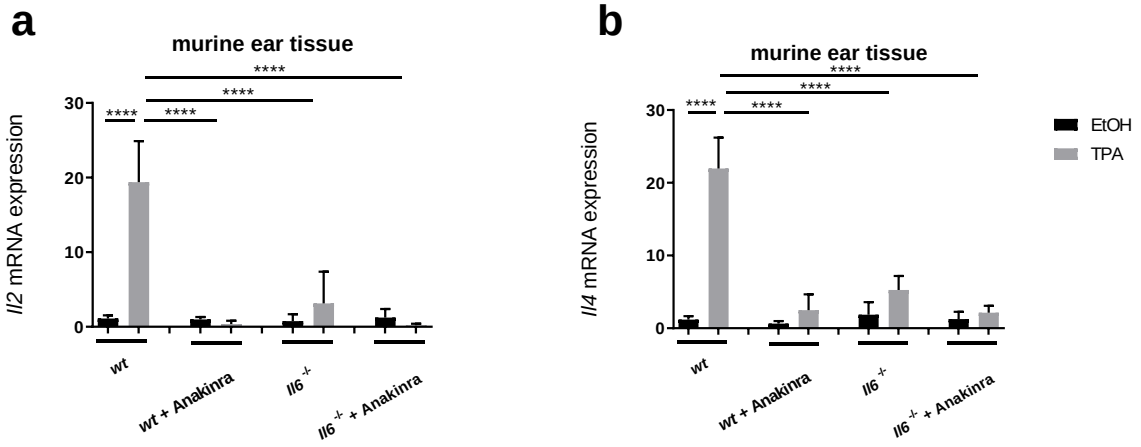

Figure 59: *Il2* and *Il4* level of *wt* and *Il6*$^{-/-}$ mice after TPA application with additional treatment with Anakinra. *wt* and *Il6*$^{-/-}$ mice were treated with TPA (25µg/ml) on the right ear and Ethanol on the left ear for 5 days with some additional treatment on day 1, 3 and 5 with Anakinra (i.p. 5mg/kg weight). Endpoint was on day 7. Quantitative mRNA expression was measured by qRT-PCR for **a** *Il2* and **b** *Il4*. Significance is implicated by stars *: p<0.05; **: p<0.01; ***: p<0.001.

To visualize the effects of Anakinra treatment on the IL-1β pathway a western blot for Nlrp3 was performed. The results are shown in Figure 60.

The western blot for Nlrp3 showed a slight increase of Nlrp3 after treatment with TPA. This effect was shown in each mouse and could be suppressed by treatment with Anakinra. Showing less Nlrp3 in Anakinra treated mice compared to only TPA treatment confirmed the results of the RT-PCR, showing less mRNA expression of *Nlrp3* in Anakinra treated animals.

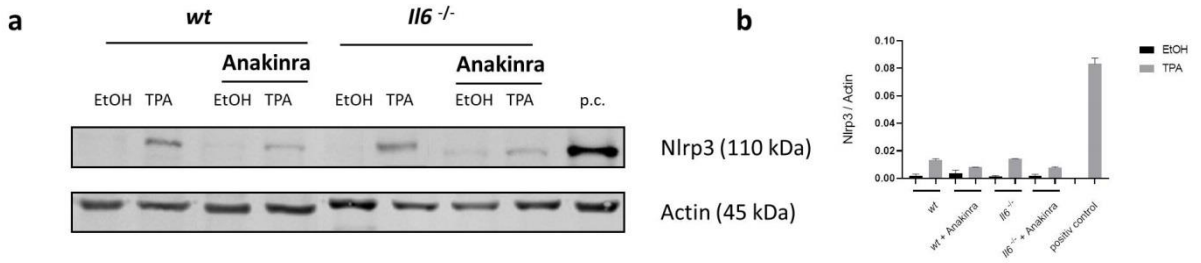

Figure 60: Nlrp3 western blot of *wt* and *Il6*$^{-/-}$ mice after TPA application with additional treatment with Anakinra. *wt* and *Il6*$^{-/-}$ mice were treated with TPA (25µg/ml) on the right ear and Ethanol on the left ear for 5 days, additional treatment on day 1, 3 and 5 with Anakinra (i.p. 5mg/kg weight). Endpoint was on day 7. The same amount of protein from ear tissue of the mice was loaded into corresponding wells in each panel. Actin and Nlrp3 **a** were detected and visualized by Western Blot and **b** quantitative analysis. As a positive control BMDCs from *wt* mice were treated with LPS (2h) and ATP (0.5h).

Also a western blot for IL-1β was performed shown in Figure 61. The increase of *Il1b* which was observed on mRNA level after TPA treatment was also present on protein level. An increase of *pro-Il1b* after treatment with TPA was observed in all mice strains especially in *Il6*$^{-/-}$ mice. But mice treated additionally with Anakinra showed less *pro-Il1b* confirming the RT-PCR results. The mature form of IL-1β could not be detected.

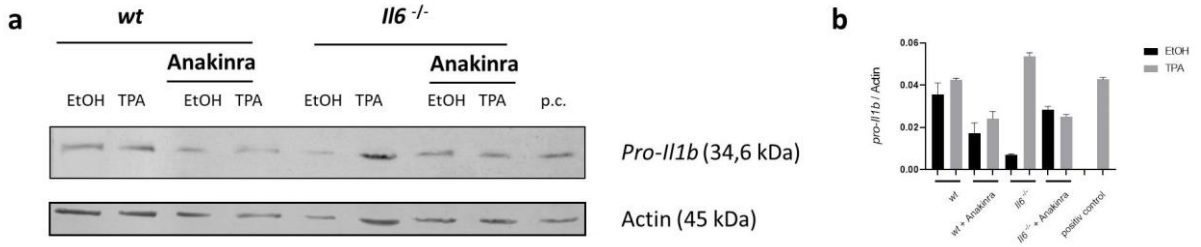

Figure 61: *Pro-Il1b* western blot of *wt* and *Il6*$^{-/-}$ mice TPA application with additional treatment with Anakinra. *wt* and *Il6*$^{-/-}$ mice were treated with TPA (25µg/ml) on the right ear and Ethanol on the left ear for 5 days, additional treatment on day 1, 3 and 5 with Anakinra (i.p. 5mg/kg weight). Endpoint was on day 7. The same amount of protein from ear tissue of the mice was loaded into corresponding wells in each panel. Actin and *pro-Il1b* **a** were detected and visualized by Western Blot and **b** quantitative analysis. As a positive control BMDCs from *wt* mice were treated with LPS (2h) and ATP (0.5h).

5.8 HPV-mouse model

5.8.1 HPV mouse model without additional treatment

HPV$^+$, HPV$^+$ x *Atf3*$^{-/-}$ and HPV$^+$ x *Il6*$^{-/-}$ mice should develop spontaneously papillomas. Therefore, the development of papillomas was controlled in the different knockout mice until the age of 30 weeks. In contrast to the reported data, none of the mice developed papilloma in this timeframe like described. Therefore the mice were irradiated with UV light to induce papilloma development as described by Deshmukh et al (115).

5.8.2 HPV mouse model with UV irradiation

HPV$^+$, HPV$^+$ x *Atf3*$^{-/-}$ and HPV$^+$ x *Il6*$^{-/-}$ mice were irradiated with 10J/cm^2 UVA and 1J/cm^2 UVB at an age of 6 weeks and then observed for 18 weeks. The samples for RNA analysis and histology were taken at an age of 18 weeks. The results are shown in Figure 62 - Figure 65.

The macroscopic observation of HPV$^+$ x *Il6*$^{-/-}$ mice is shown in Figure 62 representative for all three mice strains. All mice showed a sunburn after irradiation at day 4 which recovered completely without papilloma development.

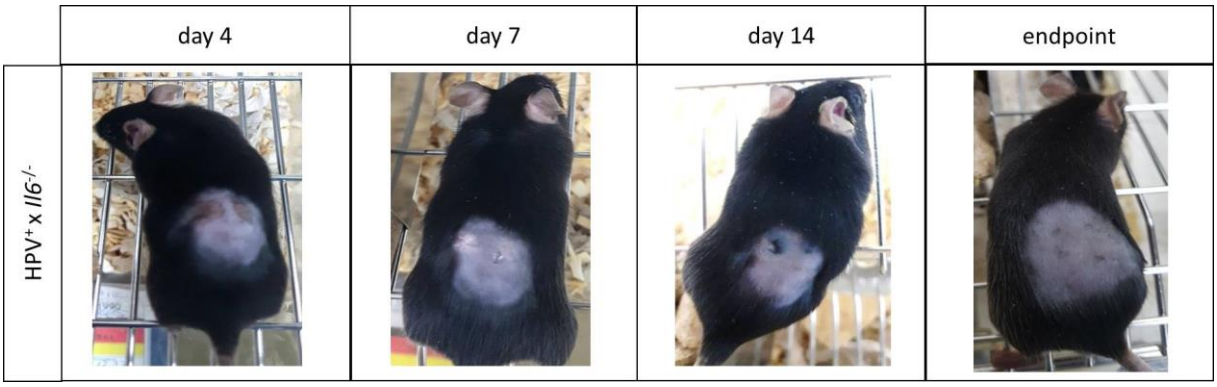

Figure 62: Clinical phenotype of irradiated HPV$^+$ x *Il6*$^{-/-}$ mice. Mice were irradiated at an age of 6 weeks with 10J/cm^2 UVA and 1J/cm^2 UVB light and mice were observed for 18 weeks.

After 18 weeks samples for histology were taken from the back skin of the mice shown in Figure 63. HE staining was performed showing no difference between untreated and irradiated mice in all four mice strains, there was no clinical indication for a development of papilloma features in none of the mouse strains.

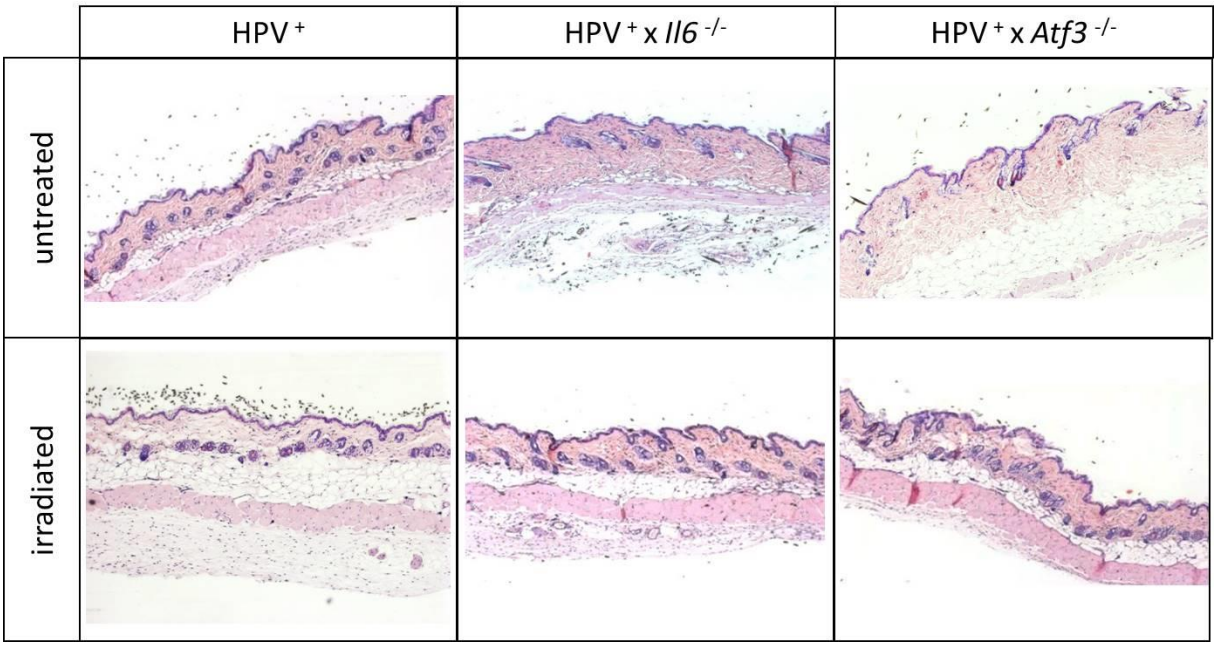

Figure 63: HE staining 18 weeks after irradiation of HPV genetic mice. Mice were irradiated at an age of 6 weeks with 10J/cm^2 UVA and 1J/cm^2 UVB light. HE staining was performed at week 18 after irradiation.

Samples for RNA analysis were taken after 18 weeks from the back skin of the mice and the cytokine profile was analyzed shown in Figure 64 - Figure 65.

Surprisingly 18 weeks after irradiation with UV light a slight increase for *Cxcl1* (Figure 64c) and *Nlrp3* (Figure 64d) was observed. *Il1a* (Figure 64e) and *Il1b* (Figure 64f) were not affected. Interestingly HPV$^+$ and HPV$^+$ x *Il6*$^{-/-}$ mice showed an increase of *Atf3* after irradiation (Figure 64a).

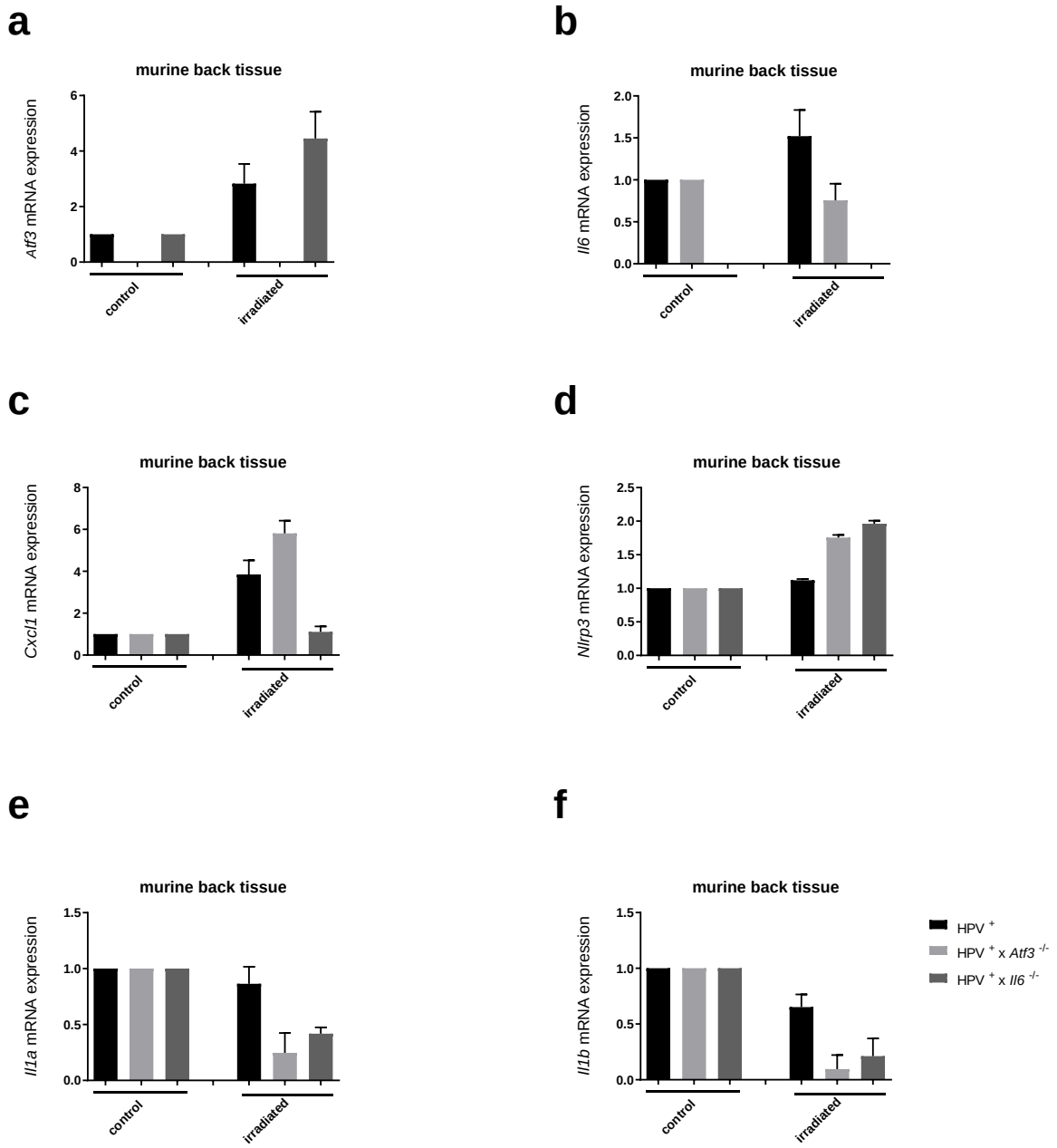

Figure 64: Cytokine profile of HPV positive genetic mice 18 weeks after irradiation. Mice were irradiated at an age of 6 weeks, endpoint of the experiment was after 18 weeks. Quantitative mRNA expression was measured by qRT-PCR for **a** *Atf3*, **b** *Il6*, **c** *Cxcl1*, **d** *Nlrp3*, **e** *Il1a* and **f** *Il1b*. Significance is implicated by stars *: p<0.05; **: p<0.01; ***: p<0.001.

Interestingly, slight increase of 2 to 4 fold of *Atf3* was observed even 18 weeks after UV-irradiation. This was then further investigated in more mice, showing that the majority of the HPV^{+} and HPV^{+} x *Il6*$^{-/-}$ mice showed no significant effect on *Atf3* after irradiation therefore this was not further evaluated (Figure 65).

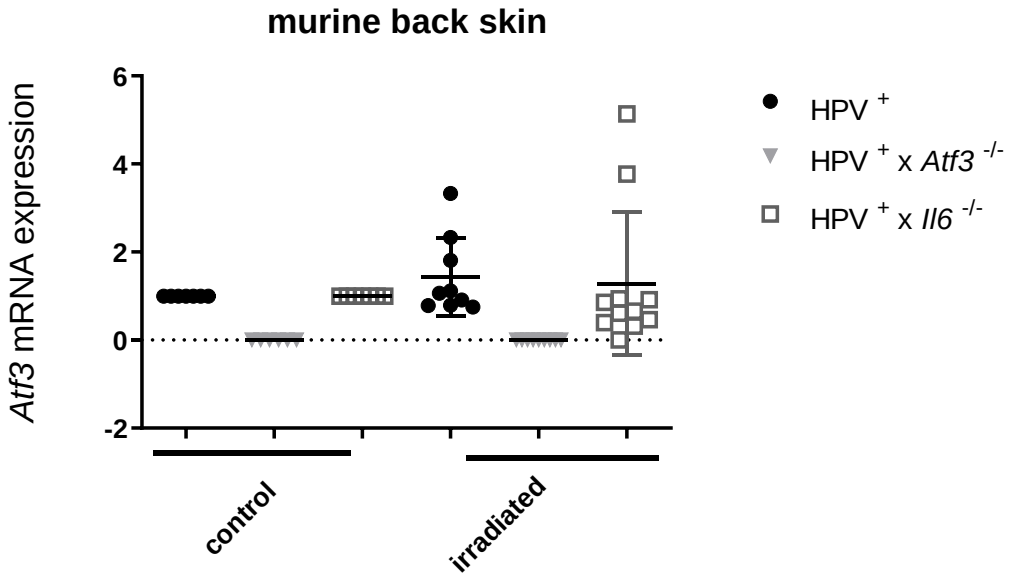

Figure 65: *Atf3* expression in HPV positive genetic mice. Mice were irradiated at an age of 6 weeks; endpoint of the experiment was after 18 weeks. Quantitative mRNA expression was measured by qRT-PCR for *Atf3*.

6 Discussion

Systemic treatment with CsA increases the susceptibility to UV-induced non-melanoma skin cancer (87, 93). Psoriasis can be treated with a high efficiency either with CsA or DMF, two drugs that both can induce ATF3 (87, 89). Interestingly increased SCC incidence and prevalence is only reported in patients which were treated with CsA (116), while patients treated with DMF, which is also known to induce ATF3 (89), do not show an increased tumor development (117). DMF is also experimentally used to impair tumor growth (118, 119). The promotion of pro-tumorigenic and inhibition of tumor-suppressive factors results in cancer. One factor which might control and regulate this imbalance is the transcription factor ATF3. It can directly bind p53 which leads to a downregulation and an acceleration of the cell cycle in keratinocytes (120). This may result in an increased risk of oncogene induced SCC formation. This CsA mediated cancer promotion through ATF3-induction is dominating and it seems to overcome the ATF3- mediated suppression of cancer promoting cytokines like IL-1, IL-6 (86) and IL-8 (87), similarly to IL-1 signaling (40, 121). Keratinocytes undergo malignant transformation to SCC cells and myeloid cells control or support the tumor growth; therefore, the hypothesis is that these cell types might respond differently to CsA or DMF treatment. If the regulation of ATF3 is different in the respective cell types, it could provide an explanation for the differential skin cancer induction of CsA as compared to DMF treatment.

The induction of *ATF3* is more prominent in keratinocytes by CsA then by Ebselen or DMF treatment, which are both utilizing GSH and ROS. But comparing myeloid cells with keratinocytes, CsA induces lower levels of *ATF3* than Ebselen or DMF.

CsA as well as DMF can both induce NRF2 by binding to the ATF3 promoter (76, 93), in keratinocytes UVA is also able to induce *ATF3* (93). Because of the fact, that the immunosuppressive effects of DMF are dependent on HO-1, the induction of *HMOX1* by DMF, Ebselen or CsA in keratinocytes as well as in monocytes were also investigated. *HMOX1* mRNA in myeloid cells was increased by both Ebselen and DMF and showed dose and time dependent increases, while CsA failed to induce *HMOX1* in these cells. The same could be observed in keratinocytes where CsA was not able to induce *HMOX1* while DMF and to a lesser extent Ebselen increased *HMOX1* levels (91).

It is known that *ATF3* is induced by cellular stress (122), which can be mediated via either TLR-activation or PKC activation. PKC activation is not only involved in the activation of immune cells (123), it is also involved in the development of SCC (124). Therefore, the induction of *ATF3* via PMA was analyzed in keratinocytes. In comparison to CsA or DMF, PMA or LPS treatment leads only to a small increase in *ATF3* expression with no relevant alterations in *HMOX1* level, confirming published data (89).

An increase of the *ATF3* level in keratinocytes and myeloid cells is based on CsA or DMF and not on immune activation through PKC or via LPS (109). The transcription of *IL6* and *IL1B* can be upregulated by TLR4 activation. This was shown in myeloid cells treated with LPS resulting in IL-6 after transcription on mRNA level. At the same time, only a slight release of IL-1β was observed, IL-1β is only secreted after a second additional signal via the inflammasome.

The transcription of *IL6*, which is a pro-inflammatory cytokine, is suppressed by DMF, but not by CsA treatment. A reason for this finding is the direct binding of ATF3 to the IL-6 promoter (76, 125) but this does not explain the suppression of *IL1* cytokines. Recently, DMF was reported to inhibit NFkB activation independently of NRF-2 (126), a putative explanation of the strong inhibition of all three pro-inflammatory cytokines investigated. A combined treatment of LPS and the NLRP3-agonist ATP induces only a stronger IL-1β secretion with no effects on mRNA level (113).

In summary, the different carcinogenic potential of CsA and DMF might be due to different targeting of ATF3 in myeloid cells or in keratinocytes. Keratinocytes seem to be more sensitive to CsA induced *ATF3*, whereas the DMF mediated anti-inflammatory potential is more prominent in myeloid cells. This could provide an explanation for the difference of the skin carcinogenesis between CsA or DMF treatment and the associated ATF3 induction.

The regulatory role of ATF3, which can either suppress an inflammatory response or prone to a tumor promoting environment, was then further investigated using different knockout mice strains. For a closer look at the influence of ATF3 and its regulatory role in inflammation, *wt*, *Atf3*$^{-/-}$ and *Il6*$^{-/-}$ BMDCs were generated. To dissect the influence of ATF3 and IL-6 on cytokine regulation, BMDCs were treated with different TLR ligands to ensure an activation of NFκB and the production of pro-inflammatory cytokines like *pro-Il1b*. The treatment with LPS is known to activate TLR4 (127), while R837 is an activator of TLR7 (128) and CpG of TLR9 (129).

The expression as well as the secretion of IL-6 was increased after treatment with the different TLR ligands, showing significantly more *Il6*-mRNA in the absence of *Atf3*. This confirms the previous finding that ATF3 is able to suppress the transcription of *Il6* (76, 130) and therefore has an anti-inflammatory potential. The secretion of IL-6 was differently regulated showing less IL-6 in the *Atf3*$^{-/-}$ BMDCs, expecting that this is due to a time delay of secretion. It was shown that IL-6 secretion peaks 4 hours after LPS treatment in human monocytes (131) and therefore the ideal time-point to investigate the secretion of IL-6 in murine dendritic cells might be later. This serves as a possible explanation for the difference in secreted IL-6 compared to its transcription.

Regarding IL-1β, treatment with the TLR ligands led to an increase of *Il1b*-mRNA as well as secreted protein, confirming published data (132). But interestingly, deficiency for *Atf3* and *Il6* augments IL-1 induction and secretion. In line with this finding that deficiency of *Il6* leads to a higher amount of IL-1 in dendritic cells, it was shown in *Il6*$^{-/-}$ macrophages that IL-6 plays a role in regulating the age-related defects in macrophages through alteration of pro inflammatory cytokines (133). Here aged *Il6*$^{-/-}$ macrophages showed higher levels of IL-1 after treatment with LPS (133), which would fit to the significant increase of IL-1β in the *Il6*$^{-/-}$ BMDCs.

Only small amounts of IL-1β were secreted showing that TLR-ligation alone is not sufficient for robust IL-1β secretion. The activation with a TLR ligand leads to the generation of the precursor *pro-Il1b*. To be secreted, a second signal is needed. This second signal is most of the time via a Nod-like-receptor like NLRP3. But NLRP3 and IL-1β are regulated similarly. Ttherefore, ATF3 as transcription factors can either directly influence the secretion of IL-1β or indirectly via NLRP3. As *Atf3* is not altered in *wt*

or *Il6*$^{-/-}$ BMDCs, it has no direct influence on IL-1β production, however, *Nlrp3* is significantly increased in the absence of *Il6*, explaining the increase of IL-1β in *Il6*$^{-/-}$ BMDCs after LPS treatment.

Taken together the significant increase of IL-1β and Nlrp3 in murine *Atf3*$^{-/-}$ and *Il6*$^{-/-}$ BMDCs compared to *wt* cells suggested that ATF3 and/or IL-6 are indirectly involved in the regulation of pro-inflammatory cytokines via NLRP3. Therefore, ATF3 and/or IL-6 may regulate factors of inflammation as they serve as anti-inflammatory regulators. The absence of ATF3 and/or IL-6 leads to the enhanced production of pro-inflammatory cytokines like IL-1 and can promote an inflammatory response.

In human monocytes DMF is able to suppress the LPS mediated secretion of IL-1β and IL-6 (91). To check whether this depends on ATF3 or IL-6, BMDCs (*wt*, *Atf3*$^{-/-}$ and *Il6*$^{-/-}$) were treated with LPS and ATP. The prior treatment with DMF inhibits the transcription via inhibition of NFkB (126). In murine BMDCs the prior treatment with DMF showed no differences between *wt*, *Atf3*$^{-/-}$ and *Il6*$^{-/-}$ BMDCs as a suppression of the inflammatory cytokines IL-1β and IL-6 occurred in all three strains.

The results exhibit that, the DMF mediated suppression of IL-1β and IL-6, shown in human myeloid cells and murine BMDS, is not regulated via ATF3 or IL-6, as deficiency of ATF3 or IL-6 had no effect on the DMF mediated inhibition.

As described, *in vitro* a compensatory increase of IL-1β in *Atf3*$^{-/-}$ and *Il6*$^{-/-}$ BMDCs after TLR treatment compared to *wt* mice was observed within the experiments of this work. To mechanistically address this increase, Anakinra (IL-1R1-antagonist) was used to block the IL-1 receptor signaling. Nowadays Anakinra is clinically used as a treatment for inflammatory disease such as rheumatoid arthritis (134), inborn fever syndromes and Schnitzler syndrome (135). Anakinra binds to the IL-1 receptor and blocks its function, therefore IL-1α and IL-1β are not able to bind to their own receptor again, which inhibits the production of IL-1 induced by the receptor. Therefore the feedback loop of IL-1 to its own receptor is blocked by the anti-inflammatory treatment with Anakinra (136).

To show whether this mechanism is involved in the increased production of IL-1β in *Atf3*$^{-/-}$ and *Il6*$^{-/-}$ BMDCs, cells were treated with Anakinra prior to LPS induced IL-1 production. LPS induced mRNA expression of *Atf3*, *Il6* and *Cxcl-1* were not affected by Anakinra treatment, pointing towards no direct involvement of *Atf3*, *Il6* and *Cxcl-1*. Comparing *Il1a, Il1b* and *Nlrp3* significant more *Il1a, Il1b* and *Nlrp3 were induced* in *Atf3*$^{-/-}$ and *Il6*$^{-/-}$ BMDCs as expected and seen before, but this effect could not be reversed by treatment with Anakinra neither in *wt* nor in *Atf3*$^{-/-}$ and *Il6*$^{-/-}$ BMDCs. The same results could be observed for IL-1β and IL-6 protein secretion, indicating that the enhanced production of pro-inflammatory cytokines in the absence of ATF3 and/or IL-6 are not mediated by IL-1 receptor 1-signalling.

The idea was now to vary the amount of LPS induced IL-1. The reason for the loss of function from Anakinra in this setting may be due to an overload of LPS mediated *pro IL-1*. If the IL-1 levels present after treatment with LPS are too high, Anakinra mediated blocking is maybe not sufficient anymore, as the system is already saturated. Therefore, a titration of LPS in combination with Anakinra was performed. But again, no effect of Anakinra for *Atf3*, *Il6* as well as *Il1b* mRNA was noted; and Anakinra treatment did not influence IL-6 protein secretion. Only IL-1β secretion after Anakirna treatment

showed a slight reduction of IL-1β after treatment with the lowest dose of LPS hinting to an impact of the IL-1 receptor mediated feedback loop in low stimulation conditions. This suppression was independent of ATF3 and/or IL-6 as it was also observed in *wt* BMDCs.

In summary, this feedback loop via the IL-1 receptor does not explain the higher amounts of IL-1β in *Atf3*$^{-/-}$ and *Il6*$^{-/-}$ BMDCs. So, IL-1 itself seems not to be the regulatory factor in this setting.

Not only myeloid cells are involved in early, non-T cell dependent skin inflammation, keratinocytes also play an important role in the regulation and the response of the immune system (137). Because of the higher amount of IL-1β most prominent in *Il6*$^{-/-}$ BMDCs after treatment with TLR ligands, seen in this work, the idea was to investigate the influence of IL-6 to TLR activation in keratinocytes.

Treatment with PMA which leads to the activation of the protein kinase C (138) resulted in an increase of the cytokine level. This increase was also observed when keratinocytes were treated with R837 and Poly (I:C) a TLR3 agonist (139).Treatment of keratinocytes with the different TLR ligands or the activation of the protein kinase C led to an increase of *Atf3*, *Il6*, *Cxcl1*, *Il1a* and *Il1b* most prominent after treatment with R837. But this increase could be observed in *wt* as well as in *Il6*$^{-/-}$ keratinocytes.

Observing no significant difference in the cytokine level of *wt* and *Il6*$^{-/-}$ keratinocytes after TLR ligation, led to the conclusion that the cytokine level triggered by TLRs in keratinocytes is not regulated via IL-6 in contrast to myeloid cells, were the cytokine level seemed to be regulated via ATF3 and/or IL-6

To investigate if keratinocytes response differently on TLR or PKC activation compared to other stimuli, NLRP1/NLRP3 activation by UV treatment was performed. UV increases pro-inflammatory cytokines in keratinocytes and leads to local and systemic inflammatory reactions and alterations of the immune response (140). First of all, the impact of the irradiation with UV on the viability of the cells was investigated. Here, in response to UVB irradiation murine keratinocytes were not viable anymore after 24 hours. Because of the low viability of the cells after UVB treatment, only the effects of UVA irradiation in murine keratinocytes were investigated.

UVA irradiation for 4, 8 and 16 hours in murine keratinocytes induced *Atf3* after 4 hours. This increase of ATF3 after irradiation with UVA was already shown in primary human keratinocytes (93). A significant increase was observed for *Il6* and *Cxcl1* in the *Atf3*$^{-/-}$ keratinocytes after irradiation with UVA, confirming that ATF3 is able to suppress the transcription of IL-6 even in keratinocytes. CXCL1, which is produced by keratinocytes to attract neutrophils, was reported to be regulated by ATF3 (141). This might explain the increase in transcription of *Cxcl1* in murine keratinocytes lacking ATF3. For *Il1a* and *Il1b* as well as *Nlrp3* a significant increase on mRNA level was observed most prominently in *Il6*$^{-/-}$ keratinocytes. IL-1α secretion was also enhanced in the absence of IL6, probably to compensate the lack of IL-6.

Furthermore, this indicates, similarly like what was shown before in DCs, a different regulation of the cytokine level in *Il6* deficient keratinocytes compared to *wt* keratinocytes as absence of ATF3 and/ or IL-6 led again to an enhanced production of pro-inflammatory cytokines.

To check whether this effect in the *Il6*$^{-/-}$ keratinocytes is due to NLRP3 or ATF3, cells were pretreated with PMA to induce ATF3 (142) before irradiating the cells. The irradiation with UVA showed again an increase of pro-inflammatory cytokines more prominent in *Il6* deficient keratinocytes. The prior induction of ATF3 via PMA before irradiation with UVA resulted in an even more pronounced amount of *Il1a, il1b* and *Nlrp3* on mRNA and IL-1α on protein level.

Taken together, the activation of ATF3 seems to be involved in the regulation of IL-1 via NLRP3, as induction of ATF3 is able to increase the amount of IL-1 which is produced.

Both ex vivo in murine skin explants as well as in keratinocytes a higher amount of IL-1 and NLRP3 after different stimuli could be observed in the absence of ATF3 or IL-6. We now wanted to investigate if this difference is also present in human skin by using primary human keratinocytes. As in murine keratinocytes the clearest differences between the knockout cells in comparison to *wt* cells were observed after UV-treatment, the induction of cytokines in human keratinocytes after irradiation with UV was analyzed.

Analyzing the viability of human keratinocytes to UVA and UVB irradiation the cells were more sensitive to UVA than UVB light after 24 hours. Nevertheless, the experiments were performed with both UVA and UVB irradiation. As expected, irradiation with UVA and UVB lead to an increase of *ATF3* with can be explained by reactive oxygen species-mediated nuclear factor erythroid 2-related factor 2 (NRF2) activation. ATF3 expression is induced by the direct binding of NRF2 to its promoter (143). At the same time irradiation with UV leads to an increase of *IL6*, *CXCL8* and *IL1B* mRNA. This increase of pro inflammatory cytokines is explained by the production of danger signals. Direct absorption of UV irradiation leads to the production of ROS. One of the first signals of viable keratinocytes to UV damage is the formation of the inflammasome resulting in production of pro-inflammatory cytokines (144). Additionally, a prominent increase of secreted IL-1α, IL-1β and IL-6 protein was observed, which is also a consequence of the inflammasome activation. This confirms data for UVB irradiation in HaCat cells, where an increase of various cytokines was shown before (145). To check also in the human system if the absence of ATF3 leads to an enhanced production of pro-inflammatory cytokines like IL-6 and IL-1, ATF3 was knocked down via siRNA in human keratinocytes. Then, keratinocytes were treated with CsA or irradiated with UVA to induce ATF3 as well as inflammatory cytokines. Loss of ATF3 in the siRNA transfected cells showed a sufficient knockdown of ATF3 in CsA or UV irradiated cells. Again, ATF3 was able to suppress the transcription of IL-6 also in human keratinocytes. Interestingly transfected cells showed a higher amount of IL1A and IL1B mRNA, but not secreted protein.

Again, ATF3 seems to regulate the production of pro-inflammatory cytokines also in human keratinocytes. This shows that ATF3 might regulate cytokine transcription in different cell types and different species, serving as a general conserved regulator of inflammation.

To investigate the interplay between myeloid cells and keratinocytes in inflammation and the regulatory effects of ATF3 and IL-6 an *in vivo* model was performed. Within this *in vivo* model it is possible to mimic the immune response for a better understanding of the complex interplay between

the different cell types and the function of ATF3 and IL-6 in inflammatory responses. The TPA mouse model was used to investigate inflammation in *wt*, *Atf3*$^{-/-}$, *Il6*$^{-/-}$ and *Atf3*$^{-/-}$ x *Il6*$^{-/-}$ mice. TPA leads to the activation of the protein kinase C, initiating an inflammatory response comparable to inflammatory skin diseases in human (97, 98). This treatment did not include a systemic effect as it did not cause weight loss.

Ear swelling can serve as an indicator for the level of inflammation in mice. Treatment with TPA leads to an ear swelling which is most prominent in *wt* mice, while *Atf3*$^{-/-}$, *Il6*$^{-/-}$ and *Atf3*$^{-/-}$ x *Il6*$^{-/-}$ mice showed less ear swelling. This indicates less inflammation within the tissue. The reduced level of inflammation in *Atf3*$^{-/-}$ mice was not expected before, as the loss of ATF3 should result in higher levels of IL-6. A high level of IL-6 should result in a high level of inflammation (146). But interestingly, in this setting, the *Atf3*$^{-/-}$ mice showed less ear swelling, indicating less inflammation. This was also confirmed by the HE staining, here again *wt* mice were more responsive to TPA treatment than *Atf3*$^{-/-}$, *Il6*$^{-/-}$ and *Atf3*$^{-/-}$ x *Il6*$^{-/-}$ mice, resulting in a pronounced inflammatory infiltrate and thickening of the epidermis. It was already shown that endogenous IL-6 plays a crucial anti-inflammatory role in both local and systemic acute inflammatory responses by controlling the level of pro-inflammatory, but not anti-inflammatory cytokines (143), (147). IL-6 can serve as bimodal cytokine with both anti- and pro-inflammatory properties (148, 149). As IL-6 is increased in the *Atf3*$^{-/-}$ mice, it is possible that in this setting the high level of IL-6 plays an anti-inflammatory role which might explain the lower level of inflammation in the absence of ATF3. For *Il6*$^{-/-}$ mice it was already shown that inflammatory infiltration and systemic inflammation are reduced, because of loss of IL-6 (150). This fits to the findings here, less ear swelling after TPA treatment as well as less inflammatory infiltrate in the HE staining for the *Il6*$^{-/-}$ mice.

Having a closer look at the tissue of the ears Ki67 and p53 stainings were performed. Ki67 is a marker for proliferation of the cells (151), in mice treated with ethanol or TPA no difference of the Ki67 level was observed in any genotype, arguing, that proliferation is not affected by loss of ATF3 or IL-6. P53 is a marker for mutational load (152), which is not affected by ATF3 as well as IL-6 in this experimental set-up. Indicating, that neither the proliferation nor the mutational load is affected by ATF3 or IL-6 after TPA activation.

An immunohistochemically staining for IL-1β was performed as a marker for innate inflammation. Surprisingly, more cells were labeled with *pro-Il1b* in *Atf3*$^{-/-}$ and *Atf3*$^{-/-}$ x *Il6*$^{-/-}$ mice, with at the same time less inflammatory infiltrate and thickening of the epidermis. This finding supports the in vitro findings of increased IL-1 in DCs and keratinocytes isolated from *Atf3*$^{-/-}$ and *Il6*$^{-/-}$ mice. As described before IL-6 is increased in the *Atf3*$^{-/-}$ mice and here the high level of IL-6 may be the reason for the higher amount of IL-1 in the tissue of the mice lacking ATF3, because IL-6 controls the level of pro-inflammatory cytokines. But this assumption has to be confirmed by having a look at the cytokine profile of the inflamed tissue.

To have a closer look at the inflammatory response upon TPA treatment the cytokine profile of the ears was investigated via RT-PCR. As expected, more *Il6* and *Cxcl1* were present in the *Atf3*$^{-/-}$ mice. Although the inflammatory response and ear swelling were reduced in *Atf3*$^{-/-}$, *Il6*$^{-/-}$ and *Atf3*$^{-/-}$ x *Il6*$^{-/-}$ mice, these mice carried higher amounts of *Il1b* and *Nlrp3 mRNA* after TPA treatment. Therefore, IL-1

and NLRP3 cannot be the reason for the lower inflammatory response as ear swelling and cytokine expression do not correlate. Additionally, IL-6 cannot be the reason for the higher levels of IL-1 like expected before as in the mice lacking *Il6* a high amount of IL-1 was found.

Besides pro- and anti-inflammatory cytokines interferons are crucial for appropriate response of pathogens or irritants in inflammatory response (153). In our system *Ifng* was not the regulatory factor responsible for less inflammation in the knockout mice. T cell regulating factors such as *Il2* and *Il4* were suppressed in TPA-treated *Atf3*$^{-/-}$, *Il6*$^{-/-}$ and *Atf3*$^{-/-}$ x *Il6*$^{-/-}$ mice. This might explain the divergence between innate pro-inflammatory cytokines and the inflammatory response in the tissue of the knockout mice compared to *wt* mice. It was shown that Interleukin (IL)-4 has anti-inflammatory properties, this anti-inflammatory properties are able to suppress the production of tumor necrosis factor (TNF)-α and IL-1β by lipopolysaccharide (LPS)-activated human monocytes (154), (155). Diminished IL-4 in the respective knockout mice induces IL-1β, as the inhibitory effect of IL-4 on IL-1β is missing.

Interleukin-2 (IL-2) is known to show many different functions during an inflammation, which are sometimes opposing. IL-2 is known to induce T-cell proliferation and T-helper 1 (Th1) and Th2 effector differentiation and it provides T cells with a long-lasting competitive advantage resulting in the optimal survival and function of memory cells (156). Therefore, loss of IL-2 in the knockout mice can provide an explanation for less inflammation, because of less T-cell activation.

To prove the higher amounts of *Nlrp3* and *Il1b* in the knockout mice after TPA treatment on mRNA level also on protein level a western blot was performed confirming higher amounts of Nlrp3 and *pro-Il1b* in the *Atf3*$^{-/-}$ mice compared to *wt* mice.

Taken together, this *in vivo* experiment showed an interesting connection between ATF3 and/or IL-6 and the level of inflammation. Mice lacking ATF3 and/or IL-6 showed on the one hand less inflammation due to less inflamed tissue of the ears, but on the other hand these mice showed also high amounts of pro-inflammatory IL-1β. What on the first look seems to be contrary, seems now to fit with the complete loss of IL-2 and IL-4 in mice lacking ATF3 and/or IL-6, this shows a connection between both findings. Mice lacking ATF3 and/or IL-6 seem to show an immune response with is innate with less inflamed tissue but high amounts of pro-inflammatory cytokines but almost no T-cell associated genes like IL-2 and IL-4. In contrast *wt* mice showed a typical adaptive phenotype of inflammation with high inflamed tissue, lower amounts of IL-1β and high amounts of T-cell associated genes like IL-2 and IL-4.

Finally, we aimed to investigate the effects of the IL-1 receptor blockade, which was not that functional *in vitro,* also *in vivo*. Therefore mice were additionally treated with Anakinra to TPA treatment. Anakinra had no influence on the weight of the animals and partially protected from ear swelling in *wt* mice as expected, showing the anti-inflammatory potential of Anakina. Interestingly, *Il6*$^{-/-}$ mice were not influenced by Anakinra in combination with TPA, suggesting that Anakinra can only lower the level of inflammation if IL-6 is present. The same was confirmed by the HE staining, showing less inflammation in *wt* mice treated with Anakinra but no differences in *Il6*$^{-/-}$ mice.

Analysis of the cytokine profile, no *Il6* was present in the *wt* mice treated with Anakinra. So treatment with Anakinra leads to a decrease of IL-6 which results in less inflammation, confirming published data (157). The fact that Anakinra shows no influence on mice lacking IL-6 leads to the assumption that the suppressive effect of Anakinra is mediated by IL-6, as if no IL-6 is present Anakinra is not able to lower the inflammation. We could furthermore observe a slight decrease of *Il1b* and *Nlrp3* in both mice treated with Anakinra, showing that Anakinra is able to lower the level of IL-1 also if IL-6 is not present. This is a direct effect of IL-1receptor blockade inhibiting the induction of IL-1 cytokines upon IL-1R1-activation. *Ifng* was again not regulated, but surprisingly *Il2* and *Il4* were diminished after Anakinra treatment in *wt* mice, besides IL-A-dependent blocking of IL-1R1, a further explanation for less inflammation in the *wt* mice.

This data point towards an innate immune response in *wt* mice treated with Anakinra, showing less inflammation with at the same time low level of *Il2* and *Il4* and diminished levels of *Il6*. This data also indicate that IL-6 plays a key role in therapy of inflammatory skin disease with Anakinra, as Anakinra has no effect in the absence of IL-6.

In summary the impact of ATF3 and IL-6 on inflammation was investigated in this project. The findings pointed towards a regulatory role of ATF3 and IL-6 in the regulation of pro-inflammatory cytokines. Enhanced production of IL-1 was associated with lack of ATF3 and/or IL-6 in TPA induced inflammation, with at the same time low levels of inflammation. This finding was in line with diminished IL-2 as well as IL-4 in the absence of ATF3 and/or IL-6 possible e This is also a possible explanation for the high level of IL-1 with at the same time, less tissue inflammation. This unexpected differences of key cytokines of the innate branch here such as IL-1β and IL-6, compared to cytokines involved in T cell responses such as IL-4, IL-2 or interferons led to the assumption, that the strength of the IL-1 response determines whether an inflammatory response remains innate and suppresses a delayed type hypersensitivity reaction (DTHR), or whether it progresses to a T cell mediated DTHR. This is in line with observations regarding patients with a mutated IL-36RN, an inhibitory member of the IL-1 family. These patients develop a pure innate pustular form of psoriasis while most other types of psoriasis progress from an innate response into a DTHR-like reaction (158). This provides a natural model, where a strong IL-1 signal due to hyperactivation of IL-1 signaling results in strong neutrophil-dominated pustular disease but protects from the progression into a T-cell and Type I interferon-mediated plaque type psoriasis. The generated data point towards a challenging interplay of IL-1, IL-6 and ATF3 in skin inflammation and keratinocyte proliferation that had not been noted before.

At the end the impact of ATF3 and IL-6 on cell cycle should also be investigated in a mouse model where the mice overexpress the HPV in the epidermal keratinocytes. These mice should develop spontaneously papilloma but that was not the fact in the mice with C57BL/6 background that we received from the laboratory of Prof. Pfister. It was shown that irradiation with UVA and UVB once is sufficient in the mice with C57BL/6 background to lead to the development of papillomas (159). Having a look at the clinical phenotype showed no long term effect of the irradiation in the HPV^+ mice. The mice first developed sunburn, showing the effect of the UV irradiation, but they did not develop any papillomas on the back skin. Also in the histological staining no differences between irradiated and

non-irradiated tissue could be observed. In the cytokine profile of the ears also no differences could be observed only a slight increase of *Atf3* after irradiation in three mice. Having a closer look at the *Atf3* expression in all mice showed also here no significant difference between irradiated or non-irradiated mice.

In summary the mice carry the HPV8 in the keratinocytes, which was confirmed by the presents in the genotyping, did not show any difference in the development of papilloma as compared to normal mice. Because of the loss of papilloma development the tumor promoting effects of ATF3 could not be further investigated.

7 Conclusion

The human *in vitro* data of this work showed a different carcinogenic potential of CsA and DMF targeting ATF3 in myeloid cells and in keratinocytes. Keratinocytes seem to be more sensitive to CsA induced *ATF3*, whereas the DMF mediated anti-inflammatory potential of ATF3 is more prominent in myeloid cells.

The murine results of this work showed that *in vivo* unexpectedly *Atf3*$^{-/-}$ and *Il6*$^{-/-}$ as well as *Atf3*$^{-/-}$ x *Il6*$^{-/-}$ mice had a reduced skin inflammation after TPA application, which resulted in less epidermal hyperplasia compared to *wt* controls. For the *Atf3*$^{-/-}$ mice this was despite the expected increase in *Il6* expression. Most surprisingly the *Atf3*$^{-/-}$ mice developed higher levels of Nlrp3 and IL-1β on mRNA as well as on protein level in the inflamed skin. The same pattern was found in *Il6*$^{-/-}$ as well as *Atf3*$^{-/-}$ x *Il6*$^{-/-}$ mice. Importantly, ears from *Atf3*$^{-/-}$ and *Il6*$^{-/-}$ as well as *Atf3*$^{-/-}$ x *Il6*$^{-/-}$ mice had higher levels of the IL-1 family cytokines and at the same time they showed loss of *Il2* and *Il4* mRNA and similar levels of *Ifn* and the *Ifn* induced chemokines *Cxcl9* and *Cxcl10* compared to *wt* mice. Additionally, the effects of Anakinra on acute inflammation were investigated showing that, Anakinra is able to suppress the inflammation in *wt* mice. Interestingly *Il6*$^{-/-}$ mice did not respond to Anakinra therapy, indicating that IL-6 plays a key role in therapy of inflammatory skin disease with Anakinra.

In vitro analysis of this work manifested that this strong increase in *Nlrp3* and *Il1b* mRNA, in TPA-treated mice ears, may result from keratinocytes as this effect was minor in dendritic cells. This is in agreement with published data showing that ATF3 strongly suppresses IL-6, IL-12 and TNF expression, but poorly affects the IL-1 mRNA expression in macrophages or dendritic cells (89, 160). Additionally, stimulation of keratinocytes with UV irradiation showed similar results for *Nlrp3* and *Il1b.* Unfortunately, the tumor promoting role of ATF3 with mice overexpressing HPV8 in epidermal keratinocytes could not be further investigated.

The generated data point towards a challenging interplay of IL-1, IL-6 and ATF3 in skin inflammation and keratinocyte proliferation that had not been noted before. The immune system of the skin relies on both innate and adaptive responses. The innate part of the immune system is responsible for the protection of the organism from acute danger, its fast reacting with keratinocytes assisted by infiltrating neutrophils, macrophages and monocytes (89). The subsequent adaptive immunity recruits DC, neutrophils or lymphocytes to the site of inflammation to induce memory. Key cytokines of the innate branch are IL-1, IL-6 and TNF, while the T cell response utilizes IL2, IL-4, IL-17 and interferons, depending on the differentiation of the CD4 T cells that are activated during the process of differentiation. The data suggest that the strength of the IL-1 response determines whether an inflammatory response remains innate and suppresses a delayed type hypersensitivity reaction (DTHR), or whether it progresses to a T cell mediated DTHR. This is in line with observations regarding patients with a mutated IL-36RN, a member of the IL-1 family. These patients develop a pure innate pustular form of psoriasis while all other types of psoriasis progress from an innate response into a DTHR (158). This provides a natural model, where a strong IL-1 signal due to

hyperactivation of one member of the IL-1 family results in strong neutrophil-dominated pustular disease but protects from the progression into a Th17 and later Type I interferon-mediated plaque type psoriasis.

Given that ATF3 suppresses IFN (77) and IL-1, it reduces tissue damage, especially when combined with IL-6 under many conditions. If ATF3 and IL-6 are both suppressed, local tissue damage results in very high levels of IL-1, as they are present in innate immune responses, and at the same time a loss of IL-2 and IL-4. This critical role of ATF3 in balancing the regulation between the IL-1 family and the IFN family as well as T cell responses has now to be further investigated. This gives us the chance to better understand the mechanisms of the immune system in inflammation, which may result in the discovery and development of new therapies for inflammatory skin disease.

8 Outlook

To answer the hypothesis, which results of this work, that ATF3 plays a critical role in balancing the regulation between the IL-1 and the IFN family as well as T cell responses, the mechanisms underlying acute pustular or neutrophil dominated inflammatory diseases such as pustular psoriasis or urticaria vasculitis on one side and the T cell dominated manifestation (DTHR) of plaque type psoriasis and CCLE, have to be addressed. This can be further investigated by histological and molecular profiling of lesional skin in urticaria vasculitis versus CCLE or pustular versus plaque-type psoriasis. At the same time, it is important to identify the mechanism by with ATF3 via IL-1 and interferons restrict the innate immune response on one or favor the progression of an innate response into a DTHR-like disease. This can be further investigated by using two different psoriasis models and knock-out mice targeting the IL-1, IFNR or ATF3 pathway. The new observations will clarify the impact of ATF3 either in keeping innate responses innate or in driving innate into DTHR-like reactions.

9 References

1. Sharma A, Bialynicki-Birula R, Schwartz RA, et al. Lichen planus: an update and review. *Cutis*. 2012; 90:17-23.

2. Ayala-Fontanez N, Soler DC and McCormick TS. Current knowledge on psoriasis and autoimmune diseases. *Psoriasis (Auckland, NZ)*. 2016; 6:7-32.

3. Weidinger S, Beck LA, Bieber T, et al. Atopic dermatitis. *Nature reviews Disease primers*. 2018; 4:1.

4. Papier A and Strowd LC. Atopic dermatitis: a review of topical nonsteroid therapy. *Drugs in context*. 2018; 7:212521.

5. D'Orazio J JS, Amaro-Ortiz A, Scott T. UV radiation and the skin. *Int J Mol Sci* 2013:14(16):12222–12248.

6. Pasparakis M, Haase I and Nestle FO. Mechanisms regulating skin immunity and inflammation. *Nature reviews Immunology*. 2014; 14:289-301.

7. Proksch E, Brandner JM and Jensen JM. The skin: an indispensable barrier. *Experimental dermatology*. 2008; 17:1063-1072.

8. Bieber T. Atopic dermatitis. *The New England journal of medicine*. 2008; 358:1483-1494.

9. Guttman-Yassky E, Nograles KE and Krueger JG. Contrasting pathogenesis of atopic dermatitis and psoriasis--part I: clinical and pathologic concepts. *The Journal of allergy and clinical immunology*. 2011; 127:1110-1118.

10. Weidinger S and Novak N. Atopic dermatitis. *Lancet (London, England)*. 2016; 387:1109-1122.

11. Kapur S, Watson W and Carr S. Atopic dermatitis. *Allergy Asthma Clin Immunol*. 2018; 14:52-52.

12. Hanel KH, Cornelissen C, Luscher B, et al. Cytokines and the skin barrier. *International journal of molecular sciences*. 2013; 14:6720-6745.

13. Parisi R, Symmons DP, Griffiths CE, et al. Global epidemiology of psoriasis: a systematic review of incidence and prevalence. *The Journal of investigative dermatology*. 2013; 133:377-385.

14. Guttman-Yassky E, Nograles KE and Krueger JG. Contrasting pathogenesis of atopic dermatitis and psoriasis--part II: immune cell subsets and therapeutic concepts. *The Journal of allergy and clinical immunology*. 2011; 127:1420-1432.

15. Di Meglio P, Villanova F and Nestle FO. Psoriasis. *Cold Spring Harb Perspect Med*. 2014; 4.

16. Mahmood T, Zaghi D and Menter A. Emerging oral drugs for psoriasis. *Expert Opinion on Emerging Drugs*. 2015; 20:209-220.

17. Benjegerdes KE, Hyde K, Kivelevitch D, et al. Pustular psoriasis: pathophysiology and current treatment perspectives. *Psoriasis (Auckland, NZ)*. 2016; 6:131-144.

18. Kallini JR, Hamed N and Khachemoune A. Squamous cell carcinoma of the skin: epidemiology, classification, management, and novel trends. *International journal of dermatology*. 2015; 54:130-140.

19. Rahimi S. Squamous cell carcinoma of skin: a brief review. *La Clinica terapeutica*. 2013; 164:143-147.

20. Gabay C. Interleukin-6 and chronic inflammation. *Arthritis Research & Therapy*. 2006; 8:S3.

21. Albanesi C and Pastore S. Pathobiology of chronic inflammatory skin diseases: Interplay between keratinocytes and immune cells as a target for anti-inflammatory drugs. *Current drug metabolism*. 2010; 11:210-227.

22. Pasparakis M, Haase I and Nestle FO. Mechanisms regulating skin immunity and inflammation. *Nature Reviews Immunology*. 2014; 14:289-301.

23. Elizabeth R. Mann KMS. Review: Skin and the Immune System. *J Clin Exp Dermatol Res*. 2012; S2:003. doi: 10.4172/2155-9554.S2-003.

24. Salmon JK AC, Ansel JC. . The skin as an immune organ. *Western Journal of Medicine*. 1994; 160(2):146-152.

25. Yazdi AS, Röcken M and Ghoreschi KJSiI. Cutaneous immunology: basics and new concepts. 2016; 38:3-10.

26. Yazdi AS, Röcken M and Ghoreschi K. Cutaneous immunology: basics and new concepts. *Seminars in immunopathology*. 2016; 38:3-10.

27. Quaresma JAS. Organization of the Skin Immune System and Compartmentalized Immune Responses in Infectious Diseases. *Clinical Microbiology Reviews*. 2019; 32:e00034-00018.

28. Tay SS RB, Tong PL, Tikoo S, Weninger W. . The Skin-Resident Immune Network. *Curr Dermatol Rep*. 201; ;3(1):13–22.

29. Gilliet M and Lande R. Antimicrobial peptides and self-DNA in autoimmune skin inflammation. *Current opinion in immunology*. 2008; 20:401-407.

30. Yazdi AS, Rocken M and Ghoreschi K. Cutaneous immunology: basics and new concepts. *Seminars in immunopathology*. 2016; 38:3-10.

31. Steinman RM and Hemmi H. Dendritic cells: translating innate to adaptive immunity. *Current topics in microbiology and immunology*. 2006; 311:17-58.

32. Howard CJ, Charleston B, Stephens SA, et al. The role of dendritic cells in shaping the immune response. *Animal health research reviews*. 2004; 5:191-195.

33. Banchereau J, Briere F, Caux C, et al. Immunobiology of dendritic cells. *Annual review of immunology*. 2000; 18:767-811.

34. Mellman I. Dendritic cells: master regulators of the immune response. *Cancer immunology research*. 2013; 1:145-149.

35. Akira S, Uematsu S and Takeuchi O. Pathogen recognition and innate immunity. *Cell*. 2006; 124:783-801.

36. Adachi O, Kawai T, Takeda K, et al. Targeted disruption of the MyD88 gene results in loss of IL-1- and IL-18-mediated function. *Immunity*. 1998; 9:143-150.

37. Kawai T and Akira S. The role of pattern-recognition receptors in innate immunity: update on Toll-like receptors. *Nature immunology*. 2010; 11:373-384.

38. Tattoli I, Travassos LH, Carneiro LA, et al. The Nodosome: Nod1 and Nod2 control bacterial infections and inflammation. *Seminars in immunopathology*. 2007; 29:289-301.

39. Dombrowski Y PM, Koglin S, et al. . Cytosolic DNA triggers inflammasome activation in keratinocytes in psoriatic lesions. *Sci Transl Med*. 2011; 3(82).

40. Drexler SK, Bonsignore L, Masin M, et al. Tissue-specific opposing functions of the inflammasome adaptor ASC in the regulation of epithelial skin carcinogenesis. *Proceedings*

of the National Academy of Sciences of the United States of America. 2012; 109:18384-18389.

41. Feldmeyer L, Keller M, Niklaus G, et al. The inflammasome mediates UVB-induced activation and secretion of interleukin-1beta by keratinocytes. *Current biology : CB*. 2007; 17:1140-1145.

42. Murphy K and Weaver C. *Janeway's immunobiology.* 2017.

43. Turner MD, Nedjai B, Hurst T, et al. Cytokines and chemokines: At the crossroads of cell signalling and inflammatory disease. *Biochimica et biophysica acta*. 2014; 1843:2563-2582.

44. Brennan K and Bowie AG. Activation of host pattern recognition receptors by viruses. *Current opinion in microbiology*. 2010; 13:503-507.

45. Lai Y and Gallo RL. Toll-like receptors in skin infections and inflammatory diseases. *Infectious disorders drug targets*. 2008; 8:144-155.

46. Hari A, Flach TL, Shi Y, et al. Toll-like receptors: role in dermatological disease. *Mediators Inflamm*. 2010; 2010:437246-437246.

47. Biedermann T, Zimmermann S, Himmelrich H, et al. IL-4 instructs TH1 responses and resistance to Leishmania major in susceptible BALB/c mice. *Nature immunology*. 2001; 2:1054-1060.

48. Zuo X, Sun L, Yin X, et al. Whole-exome SNP array identifies 15 new susceptibility loci for psoriasis. *Nature communications*. 2015; 6:6793.

49. Salminen A, Ojala J, Kaarniranta K, et al. Mitochondrial dysfunction and oxidative stress activate inflammasomes: impact on the aging process and age-related diseases. *Cellular and Molecular Life Sciences*. 2012; 69:2999-3013.

50. Kawai T and Akira S. Toll-like receptors and their crosstalk with other innate receptors in infection and immunity. *Immunity*. 2011; 34:637-650.

51. Latz E, Xiao TS and Stutz A. Activation and regulation of the inflammasomes. *Nature reviews Immunology*. 2013; 13:397-411.

52. Fenini G, Grossi S, Contassot E, et al. Genome Editing of Human Primary Keratinocytes by CRISPR/Cas9 Reveals an Essential Role of the NLRP1 Inflammasome in UVB Sensing. *The Journal of investigative dermatology*. 2018; 138:2644-2652.

53. Dinarello CA. Immunological and inflammatory functions of the interleukin-1 family. *Annual review of immunology*. 2009; 27:519-550.

54. Yazdi AS and Ghoreschi K. The Interleukin-1 Family. *Advances in experimental medicine and biology*. 2016; 941:21-29.

55. Casanova JL, Abel L and Quintana-Murci L. Human TLRs and IL-1Rs in host defense: natural insights from evolutionary, epidemiological, and clinical genetics. *Annual review of immunology*. 2011; 29:447-491.

56. Latz E, Xiao TS and Stutz A. Activation and regulation of the inflammasomes. *Nature Reviews Immunology*. 2013; 13:397-411.

57. Shao W, Yeretssian G, Doiron K, et al. The caspase-1 digestome identifies the glycolysis pathway as a target during infection and septic shock. *The Journal of biological chemistry*. 2007; 282:36321-36329.

58. O'Neill LA. The interleukin-1 receptor/Toll-like receptor superfamily: 10 years of progress. *Immunological reviews*. 2008; 226:10-18.

59. Gross O, Yazdi AS, Thomas CJ, et al. Inflammasome activators induce interleukin-1alpha secretion via distinct pathways with differential requirement for the protease function of caspase-1. *Immunity*. 2012; 36:388-400.

60. Barksby HE, Lea SR, Preshaw PM, et al. The expanding family of interleukin-1 cytokines and their role in destructive inflammatory disorders. *Clinical and experimental immunology*. 2007; 149:217-225.

61. Jensen LE. Targeting the IL-1 family members in skin inflammation. *Curr Opin Investig Drugs*. 2010; 11:1211-1220.

62. Wolk K, Kunz S, Witte E, et al. IL-22 increases the innate immunity of tissues. *Immunity*. 2004; 21:241-254.

63. Wood LC, Jackson SM, Elias PM, et al. Cutaneous barrier perturbation stimulates cytokine production in the epidermis of mice. *The Journal of clinical investigation*. 1992; 90:482-487.

64. Hänel KH, Cornelissen C, Lüscher B, et al. Cytokines and the skin barrier. *International journal of molecular sciences*. 2013; 14:6720-6745.

65. C. G. Interleukin-6 and chronic inflammation. *Arthritis Research & Therapy*. 2006.

66. Tanaka T NM, Kishimoto T. IL-6 in Inflammation, Immunity, and Disease. *Cold Spring Harbor Perspectives in Biology*. 2014; 6(10):a016295. doi:10.1101/cshperspect.a016295.

67. Sawamura D, Meng X, Ina S, et al. Induction of keratinocyte proliferation and lymphocytic infiltration by in vivo introduction of the IL-6 gene into keratinocytes and possibility of keratinocyte gene therapy for inflammatory skin diseases using IL-6 mutant genes. *Journal of immunology (Baltimore, Md : 1950)*. 1998; 161:5633-5639.

68. Skabytska Y, Kaesler S, Volz T, et al. How the innate immune system trains immunity: lessons from studying atopic dermatitis and cutaneous bacteria. *J Dtsch Dermatol Ges*. 2016; 14:153-156.

69. Gabay C. Interleukin-6 and chronic inflammation. *Arthritis Res Ther*. 2006; 8 Suppl 2:S3.

70. Bonifati C, Carducci M, Cordiali Fei P, et al. Correlated increases of tumour necrosis factor-alpha, interleukin-6 and granulocyte monocyte-colony stimulating factor levels in suction blister fluids and sera of psoriatic patients--relationships with disease severity. *Clinical and experimental dermatology*. 1994; 19:383-387.

71. Kang YM, Lee KY and An HJ. Inhibitory Effects of Helianthus tuberosus Ethanol Extract on Dermatophagoides farina body-induced Atopic Dermatitis Mouse Model and Human Keratinocytes. *Nutrients*. 2018; 10.

72. Thompson MR, Xu D and Williams BR. ATF3 transcription factor and its emerging roles in immunity and cancer. *Journal of molecular medicine (Berlin, Germany)*. 2009; 87:1053-1060.

73. Jiang X, Kim KJ, Ha T, et al. Potential Dual Role of Activating Transcription Factor 3 in Colorectal Cancer. *Anticancer research*. 2016; 36:509-516.

74. Jadhav K and Zhang Y. Activating transcription factor 3 in immune response and metabolic regulation. *Liver research*. 2017; 1:96-102.

75. Mueller S, Smatlik N, Burian M, et al. Differential induction of ATF3 and HO-1 in myeloid cells and keratinocytes via Dimethylfumarate or Cyclosporine A. *Journal of dermatological science*. 2017; 87:246-251.

76. Hoetzenecker W, Echtenacher B, Guenova E, et al. ROS-induced ATF3 causes susceptibility to secondary infections during sepsis-associated immunosuppression. *Nature medicine*. 2011; 18:128-134.

77. Labzin LI, Schmidt SV, Masters SL, et al. ATF3 Is a Key Regulator of Macrophage IFN Responses. *Journal of immunology (Baltimore, Md : 1950)*. 2015; 195:4446-4455.

78. Park SH, Kim J, Do KH, et al. Activating transcription factor 3-mediated chemo-intervention with cancer chemokines in a noncanonical pathway under endoplasmic reticulum stress. *The Journal of biological chemistry*. 2014; 289:27118-27133.

79. Wu X, Nguyen BC, Dziunycz P, et al. Opposing roles for calcineurin and ATF3 in squamous skin cancer. *Nature*. 2010; 465:368-372.

80. Giacomelli R, Cipriani P, Matucci Cerinic M, et al. Combination therapy with cyclosporine and methotrexate in patients with early rheumatoid arthritis soon inhibits TNFalpha production without decreasing TNFalpha mRNA levels. An in vivo and in vitro study. *Clinical and experimental rheumatology*. 2002; 20:365-372.

81. Hernandez-Martin A, Noguera-Morel L, Bernardino-Cuesta B, et al. Cyclosporine A for severe atopic dermatitis in children. efficacy and safety in a retrospective study of 63 patients. *Journal of the European Academy of Dermatology and Venereology : JEADV*. 2017; 31:837-842.

82. Markham T, Watson A and Rogers S. Adverse effects with long-term cyclosporin for severe psoriasis. *Clinical and experimental dermatology*. 2002; 27:111-114.

83. Goumenos DS, Kalliakmani P, Tsakas S, et al. Cyclosporin-A in the treatment of nephrotic syndrome: the importance of monitoring C0 (trough) and C2 (two hours after its administration) blood levels. *Medicinal chemistry (Shariqah (United Arab Emirates))*. 2006; 2:391-393.

84. Yamaguchi R, Hosaka M, Torii S, et al. Cyclophilin C-associated protein regulation of phagocytic functions via NFAT activation in macrophages. *Brain research*. 2011; 1397:55-65.

85. Euvrard S, Kanitakis J and Claudy A. Skin cancers after organ transplantation. *The New England journal of medicine*. 2003; 348:1681-1691.

86. Gilchrist M, Thorsson V, Li B, et al. Systems biology approaches identify ATF3 as a negative regulator of Toll-like receptor 4. *Nature*. 2006; 441:173-178.

87. Wu YP, Cao C, Wu YF, et al. Activating transcription factor 3 represses cigarette smoke-induced IL6 and IL8 expression via suppressing NF-kappaB activation. *Toxicology letters*. 2017; 270:17-24.

88. Zhu Q, Wang H, Jiang B, et al. Loss of ATF3 exacerbates liver damage through the activation of mTOR/p70S6K/ HIF-1α signaling pathway in liver inflammatory injury. *Cell Death & Disease*. 2018; 9:910.

89. Hoetzenecker W, Echtenacher B, Guenova E, et al. ROS-induced ATF3 causes susceptibility to secondary infections during sepsis-associated immunosuppression. *Nature medicine*. 2011; 18:128-134.

90. Ghoreschi K, Bruck J, Kellerer C, et al. Fumarates improve psoriasis and multiple sclerosis by inducing type II dendritic cells. *The Journal of experimental medicine*. 2011; 208:2291-2303.

91. Muller S, Smatlik N, Burian M, et al. Differential induction of ATF3 and HO-1 in myeloid cells and keratinocytes via Dimethylfumarate or Cyclosporine A. *Journal of dermatological science*. 2017; 87:246-251.

92. Nakamura Y, Feng Q, Kumagai T, et al. Ebselen, a glutathione peroxidase mimetic seleno-organic compound, as a multifunctional antioxidant. Implication for inflammation-associated carcinogenesis. *The Journal of biological chemistry*. 2002; 277:2687-2694.

93. Dziunycz PJ, Lefort K, Wu X, et al. The oncogene ATF3 is potentiated by cyclosporine A and ultraviolet light A. *The Journal of investigative dermatology*. 2014; 134:1998-2004.

94. Gerosa F, Baldani-Guerra B, Lyakh LA, et al. Differential regulation of interleukin 12 and interleukin 23 production in human dendritic cells. *The Journal of experimental medicine*. 2008; 205:1447-1461.

95. Calton CM, Wade LK and So M. Upregulation of ATF3 inhibits expression of the pro-inflammatory cytokine IL-6 during Neisseria gonorrhoeae infection. *Cellular microbiology*. 2013; 15:1837-1850.

96. Paulos C. Clinical and basic immunodermatology, 2nd ed. *Journal of the American Academy of Dermatology*. 2018; 78:e133.

97. Madsen M, Hansen PR, Nielsen LB, et al. Effect of 12-O-tetradecanoylphorbol-13-acetate-induced psoriasis-like skin lesions on systemic inflammation and atherosclerosis in hypercholesterolaemic apolipoprotein E deficient mice. *BMC Dermatol*. 2016; 16:9-9.

98. Kulkarni NM, Muley MM, Jaji MS, et al. Topical atorvastatin ameliorates 12-O-tetradecanoylphorbol-13-acetate induced skin inflammation by reducing cutaneous cytokine levels and NF-kappaB activation. *Archives of pharmacal research*. 2015; 38:1238-1247.

99. Madsen M, Hansen PR, Nielsen LB, et al. Effect of 12-O-tetradecanoylphorbol-13-acetate-induced psoriasis-like skin lesions on systemic inflammation and atherosclerosis in hypercholesterolaemic apolipoprotein E deficient mice. *BMC Dermatol*. 2016; 16:9.

100. Stanley PL, Steiner S, Havens M, et al. Mouse skin inflammation induced by multiple topical applications of 12-O-tetradecanoylphorbol-13-acetate. *Skin pharmacology : the official journal of the Skin Pharmacology Society*. 1991; 4:262-271.

101. Mueller MM. Inflammation in epithelial skin tumours: old stories and new ideas. *European journal of cancer (Oxford, England : 1990)*. 2006; 42:735-744.

102. Iversen OH. TPA (12-O-tetradecanoyl-phorbol-13-acetate) as a carcinogen for mouse skin. A positive dose-response relationship. *Virchows Archiv B, Cell pathology including molecular pathology*. 1985; 49:129-135.

103. Rountree RB, Willis CR, Dinh H, et al. RIP4 regulates epidermal differentiation and cutaneous inflammation. *The Journal of investigative dermatology*. 2010; 130:102-112.

104. Marcuzzi GP, Hufbauer M, Kasper HU, et al. Spontaneous tumour development in human papillomavirus type 8 E6 transgenic mice and rapid induction by UV-light exposure and wounding. *The Journal of general virology*. 2009; 90:2855-2864.

105. Marcuzzi GP, Hufbauer M, Kasper HU, et al. Spontaneous tumour development in human papillomavirus type 8 E6 transgenic mice and rapid induction by UV-light exposure and wounding. *The Journal of general virology*. 2009; 90:2855-2864.

106. Orth G. Human papillomaviruses associated with epidermodysplasia verruciformis in non-melanoma skin cancers: guilty or innocent? *The Journal of investigative dermatology*. 2005; 125:xii-xiii.

107. Orth G. Genetics of epidermodysplasia verruciformis: Insights into host defense against papillomaviruses. *Seminars in immunology*. 2006; 18:362-374.

108. Schaper ID, Marcuzzi GP, Weissenborn SJ, et al. Development of skin tumors in mice transgenic for early genes of human papillomavirus type 8. *Cancer research*. 2005; 65:1394-1400.

109. Nazir R, Rehman S, Nisa M, et al. Chapter 7 - Exploring bacterial diversity: from cell to sequence. In: S. A. Bandh, S. Shafi and N. Shameem, eds. *Freshwater Microbiology*. Academic Press; 2019:263-306.

110. Pyrak E, Krajczewski J, Kowalik A, et al. Surface Enhanced Raman Spectroscopy for DNA Biosensors-How Far Are We? *Molecules*. 2019; 24:4423.

111. Deshmukh J PR, Pfister H, Haase I. . Deletion of epidermal Rac1 inhibits HPV-8 induced skin papilloma formation and facilitates HPV-8- and UV-light induced skin carcinogenesis. *Oncotarget*. 2016; 7(36).

112. Müller-Hermelink N, Braumüller H, Pichler B, et al. TNFR1 signaling and IFN-gamma signaling determine whether T cells induce tumor dormancy or promote multistage carcinogenesis. *Cancer Cell*. 2008; 13:507-518.

113. Yemelyanova A, Vang R, Kshirsagar M, et al. Immunohistochemical staining patterns of p53 can serve as a surrogate marker for TP53 mutations in ovarian carcinoma: an immunohistochemical and nucleotide sequencing analysis. *Modern pathology : an official journal of the United States and Canadian Academy of Pathology, Inc*. 2011; 24:1248-1253.

114. Billiau A. Interferons and inflammation. *Journal of interferon research*. 1987; 7:559-567.

115. Deshmukh J PR, Pfister H, Haase I. Deletion of epidermal Rac1 inhibits HPV-8 induced skin papilloma formation and facilitates HPV-8- and UV-light induced skin carcinogenesis. *Oncotarget*. 7(36):57841–57850.

116. S. Euvrard JK, A. Claudy,. Skin cancers after organ transplantation. *Engl J Med* 2003; 348 (17):1681–1691.

117. Hoefnagel JJ, Thio HB, Willemze R, et al. Long-term safety aspects of systemic therapy with fumaric acid esters in severe psoriasis. *The British journal of dermatology*. 2003; 149:363-369.

118. Nicolay JP, Muller-Decker K, Schroeder A, et al. Dimethyl fumarate restores apoptosis sensitivity and inhibits tumor growth and metastasis in CTCL by targeting NF-kappaB. *Blood*. 2016; 128:805-815.

119. Loewe R, Valero T, Kremling S, et al. Dimethylfumarate impairs melanoma growth and metastasis. *Cancer research*. 2006; 66:11888-11896.

120. Cui H, Guo M, Xu D, et al. The stress-responsive gene ATF3 regulates the histone acetyltransferase Tip60. *Nature communications*. 2015; 6:6752-6752.

121. Meier K, Drexler SK, Eberle FC, et al. Silencing of ASC in Cutaneous Squamous Cell Carcinoma. *PloS one*. 2016; 11:e0164742.

122. T. Hai CDW, D.K. Marsee, A.E. Allen, U. Sivaprasad. ATF3 and stress

responses. *Gene Expr 7*. 1999; (4–6) 321–335.

123. Niedel JE, Kuhn LJ and Vandenbark GR. Phorbol diester receptor copurifies with protein kinase C. *Proceedings of the National Academy of Sciences of the United States of America*. 1983; 80:36-40.

124. Gebhardt C, Riehl A, Durchdewald M, et al. RAGE signaling sustains inflammation and promotes tumor development. *The Journal of experimental medicine*. 2008; 205:275-285.

125. Inouye S, Fujimoto M, Nakamura T, et al. Heat shock transcription factor 1 opens chromatin structure of interleukin-6 promoter to facilitate binding of an activator or a repressor. *The Journal of biological chemistry*. 2007; 282:33210-33217.

126. Gillard GO, Collette B, Anderson J, et al. DMF, but not other fumarates, inhibits NF-kappaB activity in vitro in an Nrf2-independent manner. *Journal of neuroimmunology*. 2015; 283:74-85.

127. Park BS and Lee J-O. Recognition of lipopolysaccharide pattern by TLR4 complexes. *Experimental &Amp; Molecular Medicine*. 2013; 45:e66.

128. Ma F, Zhang J, Zhang J, et al. The TLR7 agonists imiquimod and gardiquimod improve DC-based immunotherapy for melanoma in mice. *Cell Mol Immunol*. 2010; 7:381-388.

129. Melisi D, Frizziero M, Tamburrino A, et al. Toll-Like Receptor 9 Agonists for Cancer Therapy. *Biomedicines*. 2014; 2:211-228.

130. Calton CM, Wade LK and So M. Upregulation of ATF3 inhibits expression of the pro-inflammatory cytokine IL-6 during Neisseria gonorrhoeae infection. *Cellular microbiology*. 2013; 15:1837-1850.

131. Jansky L, Reymanova P and Kopecky J. Dynamics of cytokine production in human peripheral blood mononuclear cells stimulated by LPS or infected by Borrelia. *Physiological research*. 2003; 52:593-598.

132. Wan Y, Freeswick PD, Khemlani LS, et al. Role of lipopolysaccharide (LPS), interleukin-1, interleukin-6, tumor necrosis factor, and dexamethasone in regulation of LPS-binding protein expression in normal hepatocytes and hepatocytes from LPS-treated rats. *Infection and immunity*. 1995; 63:2435-2442.

133. Gomez CR, Karavitis J, Palmer JL, et al. Interleukin-6 contributes to age-related alteration of cytokine production by macrophages. *Mediators Inflamm*. 2010; 2010:475139-475139.

134. Cohen SB. The use of anakinra, an interleukin-1 receptor antagonist, in the treatment of rheumatoid arthritis. *Rheum Dis Clin North Am*. 2004; 30:365-380, vii.

135. Launay D, Dutoit-Lefevre V, Faure E, et al. Effect of in vitro and in vivo anakinra on cytokines production in Schnitzler syndrome. *PloS one*. 2013; 8:e59327-e59327.

136. Cavalli G and Dinarello CA. Anakinra Therapy for Non-cancer Inflammatory Diseases. *Front Pharmacol*. 2018; 9:1157-1157.

137. Steinhoff M, Brzoska T and Luger TA. Keratinocytes in epidermal immune responses. *Current opinion in allergy and clinical immunology*. 2001; 1:469-476.

138. Tahara E, Kadara H, Lacroix L, et al. Activation of protein kinase C by phorbol 12-myristate 13-acetate suppresses the growth of lung cancer cells through KLF6 induction. *Cancer biology & therapy*. 2009; 8:801-807.

139. Stowell NC, Seideman J, Raymond HA, et al. Long-term activation of TLR3 by poly(I:C) induces inflammation and impairs lung function in mice. *Respiratory research*. 2009; 10:43.

140. Schwarz T and Luger TA. Effect of UV irradiation on epidermal cell cytokine production. *Journal of photochemistry and photobiology B, Biology*. 1989; 4:1-13.

141. Boespflug ND, Kumar S, McAlees JW, et al. ATF3 is a novel regulator of mouse neutrophil migration. *Blood*. 2014; 123:2084-2093.

142. Xu YZ, Thuraisingam T, Marino R, et al. Recruitment of SWI/SNF complex is required for transcriptional activation of the SLC11A1 gene during macrophage differentiation of HL-60 cells. *The Journal of biological chemistry*. 2011; 286:12839-12849.

143. Xing Z, Gauldie J, Cox G, et al. IL-6 is an antiinflammatory cytokine required for controlling local or systemic acute inflammatory responses. *The Journal of clinical investigation*. 1998; 101:311-320.

144. Nasti TH and Timares L. Inflammasome activation of IL-1 family mediators in response to cutaneous photodamage. *Photochem Photobiol*. 2012; 88:1111-1125.

145. Yoshizumi M, Nakamura T, Kato M, et al. Release of cytokines/chemokines and cell death in UVB-irradiated human keratinocytes, HaCaT. *Cell biology international*. 2008; 32:1405-1411.

146. Gabay C. Interleukin-6 and chronic inflammation. *Arthritis research & therapy*. 2006; 8 Suppl 2:S3-S3.

147. Huang M, Yang D, Xiang M, et al. Role of interleukin-6 in regulation of immune responses to remodeling after myocardial infarction. *Heart Failure Reviews*. 2015; 20:25-38.

148. Xing Z, Gauldie J, Cox G, et al. IL-6 is an antiinflammatory cytokine required for controlling local or systemic acute inflammatory responses. *The Journal of clinical investigation*. 1998; 101:311-320.

149. Scheller J, Chalaris A, Schmidt-Arras D, et al. The pro- and anti-inflammatory properties of the cytokine interleukin-6. *Biochimica et biophysica acta*. 2011; 1813:878-888.

150. Kong L, Zhou Y, Bu H, et al. Deletion of interleukin-6 in monocytes/macrophages suppresses the initiation of hepatocellular carcinoma in mice. *J Exp Clin Cancer Res*. 2016; 35:131-131.

151. Sun X and Kaufman PD. Ki-67: more than a proliferation marker. *Chromosoma*. 2018; 127:175-186.

152. Boyd MT and Vlatkovic N. p53: a molecular marker for the detection of cancer. *Expert Opin Med Diagn*. 2008; 2:1013-1024.

153. Kopitar-Jerala N. The Role of Interferons in Inflammation and Inflammasome Activation. *Frontiers in immunology*. 2017; 8:873.

154. Woodward EA, Prêle CM, Nicholson SE, et al. The anti-inflammatory effects of interleukin-4 are not mediated by suppressor of cytokine signalling-1 (SOCS1). *Immunology*. 2010; 131:118-127.

155. Woodward EA, Prele CM, Nicholson SE, et al. The anti-inflammatory effects of interleukin-4 are not mediated by suppressor of cytokine signalling-1 (SOCS1). *Immunology*. 2010; 131:118-127.

156. Hoyer KK, Dooms H, Barron L, et al. Interleukin-2 in the development and control of inflammatory disease. *Immunological reviews*. 2008; 226:19-28.

157. Sevcikova S, Kubiczkova L, Sedlarikova L, et al. Impact of anakinra treatment on cytokine and lymphocytes/ monocytes profile of an Erdheim-Chester patient. *Klinicka onkologie : casopis Ceske a Slovenske onkologicke spolecnosti*. 2014; 27:276-282.

158. Capon F. IL36RN mutations in generalized pustular psoriasis: just the tip of the iceberg? *The Journal of investigative dermatology*. 2013; 133:2503-2504.

159. Deshmukh J, Pofahl R, Pfister H, et al. Deletion of epidermal Rac1 inhibits HPV-8 induced skin papilloma formation and facilitates HPV-8- and UV-light induced skin carcinogenesis. *Oncotarget*. 2016; 7:57841-57850.

160. De Nardo D, Labzin LI, Kono H, et al. High-density lipoprotein mediates anti-inflammatory reprogramming of macrophages via the transcriptional regulator ATF3. *Nature immunology*. 2014; 15:152-160.